ABSTRACT

Title of Document: CHARACTERIZATION OF PHYSICOCHEMICAL PROPERTIES OF XANTHAN/CURDLAN HYDROGEL COMPLEX FOR APPLICATIONS IN FROZEN FOOD PRODUCTS

Patrick D. Williams, Doctor of Philosophy, 2011

Directed By: Associate Professor, Y. Martin Lo, Department of Nutrition and Food Science

Syneresis, expulsion of moisture from food, remains a major challenge in frozen products due to post-production temperature fluctuation during distribution, transportation, and storage. Curdlan, a FDA approved microbial polysaccharide, produces a hydrogel under certain conditions exhibiting good gel strength during freeze-thaw abuse, better than similar polysaccharides. However, curdlan alone cannot effectively suppress syneresis in aqueous solutions. The present study aims at developing an effective hydrogel complex containing curdlan and a secondary biopolymer to reduce or eliminate syneresis. Polysaccharides, κ-carrageenan, guar, locust bean, and xanthan gums were investigated. Xanthan gum, when added to curdlan, was found capable of eliminating syneresis for up to five freeze-thaw cycles (FTCs) while exhibiting stability in several rheological experiments. The xanthan curdlan hydrogel complex (XCHC) was further investigated to elucidate its structure

in relation to its high elasticity and moisture holding capacity. A gel and indications of syneresis was clearly seen in magnetic resonance images of curdlan alone, whereas XCHC was homogeneous. The three dimensional network, indicated by frequency sweeps, of curdlan was responsible for its gel structure. Though not three dimensional, elasticity and angular frequency dependency for XCHC were significantly closer to curdlan than xanthan alone. Addition of xanthan to curdlan restricted spin-spin relaxation times of XCHC to intermediate and slower exchange regimes, promoting the polymer's interaction with water while inhibiting intermolecular interactions found in curdlan. Furthermore, the effects of pH and NaCl concentration on the rheology of XCHC were examined. Though both pH and NaCl were found to reduce the hydrogel's moduli, XCHC remained stable over the pH range 4 to 8 through FTCs and were not significantly different. Statistically, the modulus measurements of samples treated with 5-200 mM NaCl were slightly different and fluctuated throughout the FTCs. Nonetheless, the slope of the storage modulus over all NaCl-treated samples averaged ~9% different from untreated XCHC, indicative of similar gel behavior despite lower elasticity. Finally, the hydrogel was incorporated into a simulated pumpkin pie filling. Treating the filling with XCHC delayed moisture migration by one FTC, yielded a brighter color, reduced variability and minimized surface cracking that could lead to decreased quality and microbial growth.

CHARACTERIZATION OF PHYSICOCHEMICAL PROPERTIES OF XANTHAN/CURDLAN HYDROGEL COMPLEX FOR APPLICATIONS IN FROZEN FOOD PRODUCTS

By

Patrick Daniel Williams

Dissertation submitted to the Faculty of the Graduate School of the
University of Maryland, College Park, in partial fulfillment
of the requirements for the degree of
Doctor of Philosophy
2011

Advisory Committee:
Professor Y. Martin Lo, Chair
Professor Thomas Castonguay
Professor Mark Kantor
Professor Srinivasa Raghavan
Professor Qin Wang

To my wife and family.

Acknowledgements

I would like to thank my advisor, Dr. Y. Martin Lo, for his continual support, guidance and support throughout my graduate career. In addition, his thoughtfulness and care for his students, abundance in leadership, and just a pleasure to work under has made him an excellent role model for me. I am also very thankful for the advice and direction from my committee members, Dr. Srinivasa Raghavan, Dr. Qin Wang, Dr., Mark Kantor, and Dr. Thomas Castonguay and for their considerable support, guidance, and knowledge. I would also like to thank Drs. Kathryn and Mike McCarthy and Mecit Oztop at the University of California – Davis, they played a pivotal role in moving my project forward.

I want to thank all my labmates for being patient with me, their unwavering support, and laughs; Dr. Pavan Kumar Soma [SPK], Peter Machado, Dr. Sanem Argin, Ansu Cherian, Dr. Meryl Lubran, Dr. Marla Luther, Daniel Reese, Avani Sanghvi, Karen Silagyi, Dr. Margaret Slavin, Ana Aguado, Yuting Zhou, Tong Liu, Michael Wiederoder, Melody Ge, Eric Thornber, I-Chang Yang. I want to especially thank my wife, Cintia, for her patience, encouragement, and support. Finally, I would like to thank my entire family for their unconditional love and support that they have given me my entire life.

Table of Contents

List of Tables

List of Figures

Chapter 1: Introduction

1.1 Introduction

According to a 2011 IBIS World industry report, frozen foods are expected to be a $28 billion industry by 2012 and during the economic downturn, revenue has increased by 3.1% and 2.0% in 2008 and 2009, respectively, due to consumer recognizing the affordability and durability of frozen foods (IBIS 2011). Mintel reports a growth of more than 16% in frozen desserts and novelties in the U.S. market from 2003 to 2008 (Mintel 2009) and it was also reported that the frozen food growth rate has risen from 3.1% to 5.8% in one year beginning in January of 2008 in the U.K. (TNS 2008). However, the frozen desserts and novelties market has been stagnant due to the lack of innovation and the economic downturn (Mintel 2009). It is evident that frozen foods and desserts are an important sector in the food industry, but needs innovation. Despite this, the demand for high quality products is always an importance aspect in the market, where the texture and stability of the products are undoubtedly of the utmost importance for existing as well as new frozen products to elevate their quality standards, gain consumer acceptance, and spur innovation.

To date, various hydrocolloidal polysaccharides such as guar gum or locust bean gum have been employed as stabilizing, thickening, emulsifying, or suspending agents in the development of texture and/or sustaining texture in frozen specialty foods and desserts such as ice cream, sauces, and whip toppings. In most cases, individual hydrocolloids are capable of improving the quality of food products if the characteristic rheological attributes of the hydrocolloid were able to give the products

the desired textural properties. However, increasing reports have shown that, when combining different gums, some synergistic effects can occur that increase the functionality and/or enhance viscous properties of the gum combination (Westra 1989; Towle 1996; Imeson 1997; Wang et al 2002a,b; Richter et al. 2005; Higiro et al. 2006; Kim et al. 2006; Makri et al. 2006; Fernandez et al. 2007).

Moreover, while the emulsifying, thickening, and suspending properties of hydrocolloids might work well in conventional foods, their applicability in frozen foods is often challenged, especially with loss of moisture in the form of dripping during freezing-thawing or temperature fluctuations during distribution/storage remains the most significant issue in retaining product quality and nutrients. A number of hydrocolloids, including carrageenan, xanthan gum, locust bean gum, guar gum, MCC, and CMC, are used as texture modifiers to protect the products from heat shock deteriorations and bodying agent (Towle 1996; Marshall et al 2003), help stabilize frozen foods (Sworn 2000), and reduce recrystallization (Goff 2006). Specifically, locust bean and guar gum are used to give and improve the texture of ice cream (Towle 1996; Marshall et al. 2003); MCC can be used to reduce ice crystals in frozen desserts (Marshall et al 2003) or a low-fat texture modifier (Champion et al. 1982); and when used as an emulsifier, stabilizer or thickener, xanthan gum has the ability to keep its viscosity after being defrosted (Imeson 1997; Sworn 2000). Nevertheless, there are limited studies in the literature characterizing the textural effects of different gum combinations under freeze-thaw conditions.

Xanthan in combination with curdlan has been demonstrated by our research group to reduce syneresis, water loss, to a point where it is not detected and yields

stable rheological and physical properties over freeze-thaw cycles when compared to curdlan combined with guar, locust bean, or k-carrageenan gums. Therefore, the ultimate goal of the following research is to characterize the physicochemical properties of the xanthan/curdlan system and investigate its efficacy in pumpkin pie.

1.2 Research Objectives

The ultimate goal of the proposed research is to screen and identify possible hydrocolloids that could possibly reduce or eliminate syneresis, water loss, when added to curdlan, while maintaining elastic behavior and improving freeze-thaw stability and characterize the complex. Combining xanthan with curdlan proved the most viable candidate for further study, therefore possible reasons for the combinations ability to be resilient under temperature abuse using advanced techniques was explored. Characterization was achieved by utilizing rheological, microscopy, and resonance techniques over freeze-thaw abuse. Moreover, the effects of NaCl and pH on rheological properties of the complex were investigated for the optimal range in which the hydrogel is least affected. Finally, the efficacy of the system was applied to pumpkin pie, where the impact of the xanthan curdlan hydrogel on the moisture migration, observable physical changes, color, gel strength and adhesiveness of the pies was investigated. In order to achieve this goal, there were four specific objectives, where the subsequent chapters following the literature review are presented as separate manuscripts:

Objective #1: Screen curdlan with xanthan, locust bean, guar, and κ-carrageenan to increase its freeze-thaw stability through their physical and rheological properties.

Objective #2: Utilize magnetic resonance imaging (MRI), nuclear magnetic resonance (NMR) relaxometry, scanning electron microscopy (SEM), and rheometry to investigate structure and water distribution of the most stable system, further characterizing the combination.

Objective #3: Build a foundation for the combinations optimal range, by studying the effects of pH and sodium chloride as major food components.

Objective #4: Explore efficacy of the complex in pumpkin pie, investigating quality aspects, including moisture migration, color, and texture.

Chapter 2: Literature Review

Adapted from: Soma PK, Williams PD, Lo YM. 2009. *Front Chem Eng China* 3(4): 413-426.

2.1 Introduction

Hydrocolloids are polysaccharides and proteins (Ockerman, 1978; Williams and Phillips, 2000) with hydrophilic and colloidal properties (Graham 1977; Hoefler 2004) that could be used to provide certain textural properties such as thickening or stabilizing. Fixed length polypeptide chains of 50 or more amino acid residues with possibly 20 different amino acids make up the protein structure, where as polysaccharides colloids vary in length and consist of heteropolysaccharides and homopolysaccharides (Graham 1977). Hydrocolloids stem from several sources, including, botanical, algal, microbial, and animal sources (Glicksman 1982; Williams and Phillips 2000; Hoefler 2004). They are used in sauces and dressings (Mandala et al. 2003; Sikora et al. 2008), as emulsion stabilizers (Garti et al. 2001; Dickenson 2008; Mikkonen 2009), and for their freeze-thaw stability (Freeland 2002).

In frozen foods, gums help maintain or control textural aspects including reducing ice re-crystallization, minimize water distribution, and viscosity enhancement (Goff 2006). Hydrocolloids that provide these functions in frozen foods and desserts are included in Table 2.1, where the bold hydrocolloids are most often used in the frozen food industry. Due to their frequent use in frozen foods and desserts, several of the gums in bold will be further examined as relevant hydrocolloids in frozen foods.

Table 2.1. Hydrocolloids in use as stabilizers in frozen foods and desserts, bold indicates most often used (Towle 1996; Marshal et al. 2003).

Sources	Hydrocolloids
Proteins	Gelatin, Microparticulated Milk and Egg Proteins
Plant Exudates	Arabic, Ghatti, Karaya, and Tragacanth
Seed Gums	**Locust Bean**, **Guar**, Psyllium, Tara, Konjac Glucomannan, Starch and Modified Starches
Microbial Gums	Xanthan, Gellan
Seaweed Extracts	Agar, **Alginates, Carrageenan**
Pectins	Low and High Methoxyl
Cellulose	**Microcrystalline Cellulose**, **Sodium Carboxymethylcellulose**, Methyl and Methylethyl Celluloses, hydroxypropyl and Hydroxypropylmethyl Celluloses

2.2 Seed Hydrocolloids

2.2.1 Guar Gum

Native to India and Pakistan, guar gum is obtained from the guar plant, *Cyamposis tetragonolobus* of the *Leguminosae* family (Glicksman 1986; Wielinga et al. 2000). Currently, the plant is commercially grown annually in Texas, Oklahoma, Arizona, and the southern hemisphere in response to the fluctuations in availability of obtaining guar bean gum from foreign sources (Glicksman 1986; Wielinga et al. 2000). Made up of nearly all galactomannan, the nonionic structure of guar gum consists of a backbone with (1→4)-linked β-D6 mannopyranosyl unit with a side chain unit consisting of (1→6)-linked α-D-galactopyranosyl at a ratio of 1.8:1, respectively (Fig. 2.1). The large amount of galactose substitutions prevents strong cohesion of the main backbone and therefore extensive crystalline regions cannot be

formed allowing hydration at and above room temperature (Wielinga et al. 2000). Hydration of guar gum can be correlated to the inter- and intramolecular hydrogen bonding through the unsubstituted regions of the backbone (Goycoolea et al. 1995; Sandolo et al. 2008) and thus makes guar gum soluble in cold, highly agitated water while exhibiting pseudoplastic behavior. It is used as a formulation aid, stabilizer, firming agent, and thickener (Towle 1996) with a classification of Generally Recognized As Safe (GRAS) by the U.S. Food and Drug Administration (FDA).

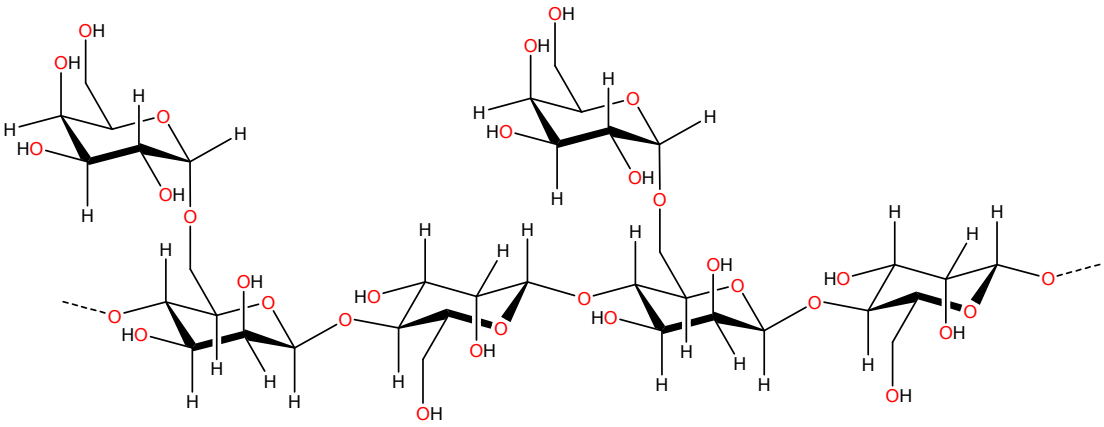

Figure 2.1. Structure of guar gum.

Wielinga et al. (2000) first reported that guar gum can help enhance the freeze-thaw stability of solutions. It was found that guar gum can be stable over two freeze-thaw cycles in aqueous, NaCl, CaCl2, citric acid, acetic acid and milk serum solutions at a concentration of 1.0%. Another study found that when added to curdlan gum in the same amount totaling 2.0% (w/v), syneresis was undetectable over five freeze-thaw cycles (Williams et al. 2009). Galactomannans such as guar gum and locust bean gum are amongst the most frequently used ingredients for the stabilization of ice cream (Marshall et al. 2006). Among fresh and frozen vegetable puree, guar

gum was found effective in reducing drip loss in potatoes, carrots, and turnips (Downey 2002). Moreover, when added to frozen dough, guar gum has shown improvements in bread texture, volume and crumb structure (Ribotta et al. 2004).

2.2.2 Locust Bean Gum

Locust bean gum (LBG), a.k.a. carob bean or St. John's gum, is obtained from the seeds of the carob tree, *Ceratonia siliqua*, grown in Mediterranean countries (Glicksman 1986; Wielinga et al. 2000). The galactomannan structure of LBG (Fig. 2.2), similar to guar gum, consists of a backbone with (1→4)-linked β-D-mannopyranosyl units and a side chain consisting of a single (1→6)-linked α-D-galactopyranosyl unit with a ratio of 3.9:1. Contrary to the structure of guar gum, LBG side chains are very unevenly substituted with sections of the backbone concentrated with substitutions and sections with no substitutions. Slightly soluble in water at room temperature, LBG must be heated to approximately 60 - 85 °C to achieve complete hydration. LBG solution exhibits pseudoplasticity (shear-thinning behavior), which shows reduced viscosity at increased shear rate, and can form a weak gel network with concentrations as low as 0.5% (Dea et al. 1977). Classified as GRAS by the FDA, LBG is used for its stabilizing, thickening, and fat-replacing properties.

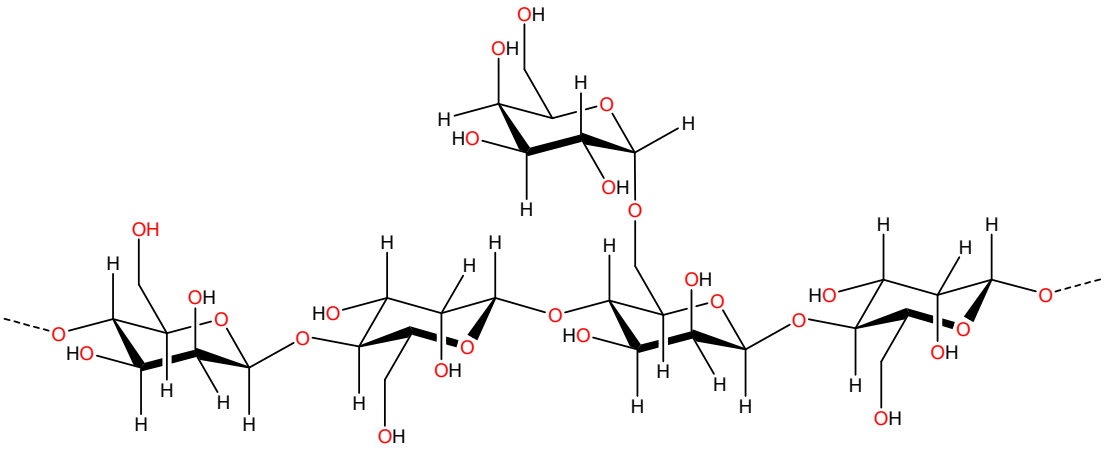

Figure 2.2. Structure of locust bean gum.

Unlike guar gum, there was little stability in a system containing LBG. For instance, LBG forms a gel after the first freeze-thaw cycle in the presence of NaCl, acetic acid, and milk serum, and syneresis occurs in both aqueous and $CaCl_2$ solutions (Wielinga et al. 2000). This could be attributed to the unevenly substituted sections of the backbone that create junction zones and thus a gel or gel-like network. It has been shown that freeze-thaw cycles and rate of freezing and/or thawing affect its gel strength (Tanaka et al. 1998; Lozinsky et al. 2000, 2001; Zeira et al. 2004). Therefore, LBG alone could not provide the freeze-thaw stability over multiple cycles.

Several studies with LBG and xanthan gum have been performed because of their unique synergistic gelling behavior that is not formed with the other galactomannan, guar gum (Rocks 1971; Goycoolea et al. 1995; Wang et al. 2002b). Conformational studies via parameters such as intrinsic viscosity that depicts molecular occupancy in highly dilute solutions have been used to better understand this interaction. It was reported that the intrinsic viscosity exhibited lower values than

weighted averages, suggesting that there is some flexibility in the structure of xanthan that may allow LBG to bond to the backbone (Wang et al. 2002b; Higiro et al. 2006). Even so, LBG is best known for its use in ice cream to prevent iciness during heat shock (Glicksman 1986; Towle 1996; Marshall et al. 2003) and many times combined with guar and carrageenan. However, little to no studies have been conducted to examine any potential synergistic effects provided by LBG and xanthan under freeze-thaw abuse. On the other hand, frozen dough containing LBG showed better gluten quality through dough extensibility analysis and lower proof times compared to control samples and exhibited increased specific loaf volume along with improved external and internal bread characteristics compared to the control along with high moisture content (Sharadanant and Khan 2003a;2003b; Mandala et al. 2008).

2.3 Seaweed Extract Hydrocolloids

2.3.1 Alginate

The extraction and processing of brown algae from host of species including *Laminaria hyperborean, Macrocystis pyrifera, Laminaria giditata, Ascophyllum nodosum, Laminaria japonica, Eclonia maxima* and others can produce the intermediate product, alginic acid. After the process of neutralization with sodium carbonate or sodium hydroxide, alginic acid forms the more stable water-soluble product called sodium alginate (Onsoyen 1997; Draget 2000). The linear structure of alginate consists of either the homopolymeric blocks β-D-mannuric acid (M) and α-L-guluronic acid (G) or the heteropolymeric blocks of alternating M and G linked by (1→4)-glycosidic linkages, making it a polyanionic hydrocolloid (Fig. 2.3). The amount of homo- and heteropolymeric blocks present in alginate is dependent upon

the sources previously mentioned. Thermo-irreversible gels can be formed by controlling the amount of calcium and acidity. On the other hand, low acid solutions below pH 4.0, form thermo-reversible gels when combined with high-methoxyl pectin. There are a variety of different viscosity grades of alginates due to the amount of G-blocks available for Ca^{2+} to from an "egg-box" structure at junction zones creating a strong gel. Due to its ability to form strong gels, they are used to control the shape of foods such as onion rings, pimiento and anchovy olive fillings, apple pieces for pie fillings, cocktail berries, meat chunks for pet food, shrimp-like fish products, and fish patties (Onsoyen 1997).

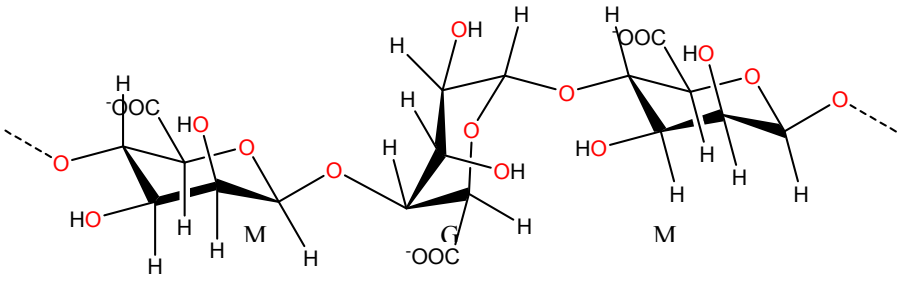

Figure 2.3. Structure of alginate gum.

Although temperature does not hinder gelation of sodium alginate, it affects the final gel properties; however, once a gel it is heat and freeze-thaw stable (Onsoyen 1997; Draget 2000). Sodium alginate has been seen to improve frozen dough stability along with whey by increase the specific loaf volume (Shon et al. 2009). Following each of seven freeze-thaw cycles, alginate increased dough development, water adsorption, and reduced syneresis, however, yielded different texture aspects as indicated by tensile strength and exhibiting a firmer dough when compared to control samples (Lee et al. 2008).

2.3.2 Carrageenan

Three varieties of carrageenan, kappa (κ), lambda (λ), and iota (ι), can be extracted from the red seaweeds. They are primarily extracted from the *Gigartina* species and *Chondrus crispus* which produce kappa and lambda types, and *Eucheuma cottonii* and *spinosum* species which produce kappa and iota types, respectively (Imeson 2000; Hoefler 2004). The general structure of carrageenan contains repeating galactose units and 3,6-anhydrogalactose both with 15-40% (w/w) ester sulfate content and side chain consisting of alternating α-(1→3)- and β-(1→4)-glycosidic linkages. The three types of carrageenan do not exist singly, but as a combination of two types and available with one predominating type or molecules containing structural components of more than one type. Each type of carrageenan has a unique set of characteristics, including gel strength, viscosity, temperature stability, synergism, and solubility. The solubility of each type of carrageenan depends on the number of sulfate groups, which increases water solubility, compared to anhydro bridges, which is hydrophobic. Having the least water solubility, κ- carrageenan has one sulfate group for every two galactose units and one anhydro bridge, ι-carrageenan has two sulfate groups for every two galactose units along with one anhydro bridge, and with the highest solubility, λ-carrageenan has three sulfate groups for every two galactose units and no anhydro bridges (Imeson 2000; Hoefler 2004).

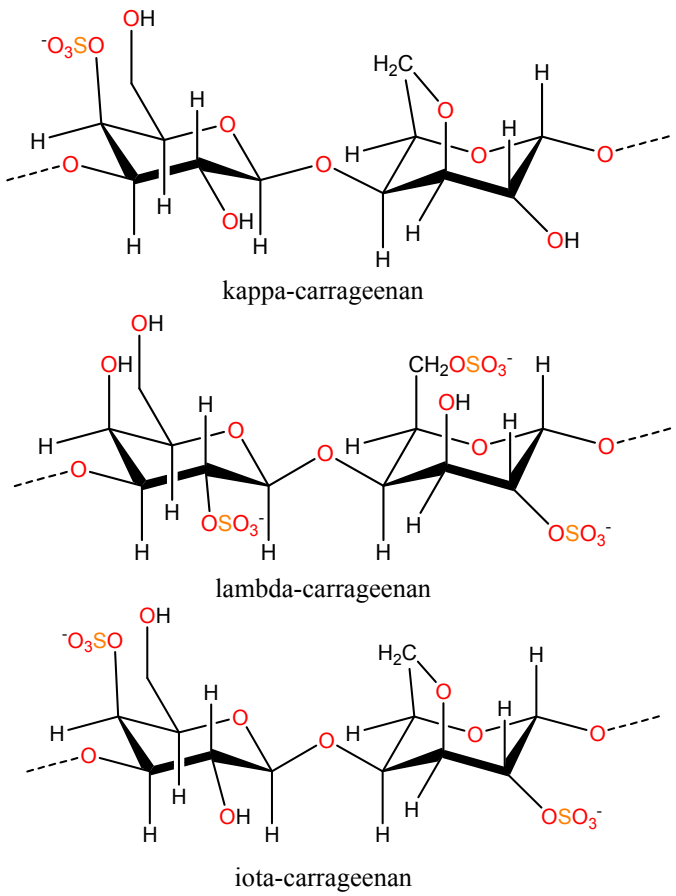

Figure 2.4. Structures of kappa-, lambda-, and iota-carrageenan.

There are distinct differences between each type of carrageenan, but all types are soluble at high temperatures and are stable above pH 4.5. Though the least soluble, κ-carrageenan provides the strongest, yet brittle, gel that allows for some syneresis. The ι-carrageenan type is more elastic and is freeze-thaw stable allowing for no syneresis and λ-carrageenan thickens without gelling. Moreover, due to syneresis, κ-carrageenan has poor freeze-thaw stability; however, by the right combination of κ- and ι-carrageenan intermediate freeze-thaw stability can be acquired along with a range of gel textures without syneresis (Imeson 2000). In ice cream and other frozen milk-based products, a small amount of κ-carrageenan (0.01-

0.3%) is used to prevent phase separation of casein (Fox 1997; Marshall et al. 2003). κ-Carrageenan alone and along with whey has exhibited higher specific volume in bread after the dough was frozen storage (Sharadanant and Khan 2003b; Shon et al. 2009).

Table 2.2. Summary of carrageenan properties.

	Kappa	**Iota**	**Lambda**
Sulfate Group	1	2	3
Anhydro Bridge	1	1	0
Texture	Firm, brittle, syneresis, strong gels with K^+	Elastic, cohesive, no syneresis , strong gels with Ca^{++}	No gelling, thickening, provides "body"

2.4 Microbial Hydrocolloid

2.4.1 Xanthan

Produced by fermentation of *Xanthomonas campestris*, xanthan gum is an anionic microbial polysaccharide with a disaccharide backbone and a trisaccharide side chain. The backbone consists of two repeating (1→4)-β-D-glucose units, the same as cellulose, and located on C3 of every other glucose, α-D-mannose, β-D-glucuronic acid, and β-D-mannose trisaccharide is attached. Various terminal mannose residues are pyruvated depending on the *X. campestris* strain.

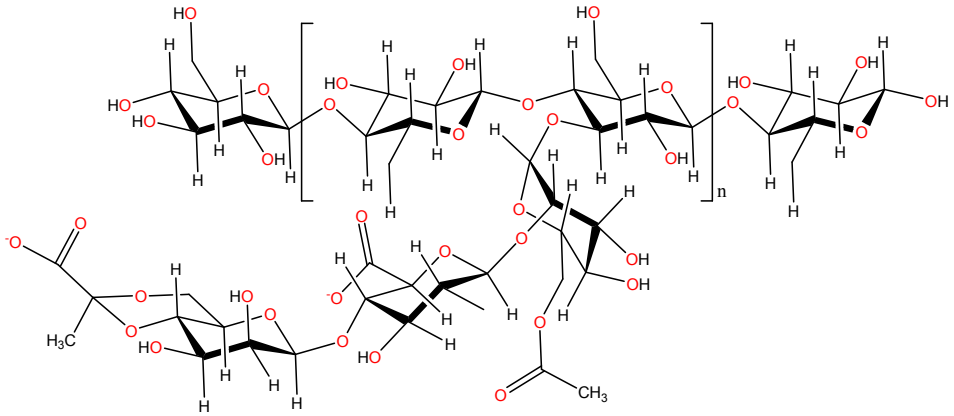

Figure 2.5. Structure of xanthan gum.

Xanthan is soluble in water with the ability to hydrate in cold water, exhibiting pseudoplastic behavior. The viscosity of xanthan is stable over a range of pH values, salt concentrations, and temperatures (Moorhouse et al. 1977a; Whitcomb et al. 1978; Sworn, 2000). Thickening, stabilizing, and emulsifying are some of the well recognized characteristics of xanthan gum. As a thickening agent, low shear rates show stiff, aggregated, highly ordered molecules and, as shear is increased, the stiff molecules separate and align in the direction of shear force. As a consequence, pseudoplasticity is exhibited (Wilkes 1999). While 1.0% xanthan solution produces gel-like consistency, as little as 0.1% xanthan gum can increase viscosity and shows similar rheological properties. Giannouli and Morris (2003) suggested that xanthan can from stronger more cohesive networks, similar to how Ca^{2+} enhances xanthan's weak gel network, when frozen and thawed.

Because of its resilience to pH and temperature fluctuations, xanthan gum has been extensively studied for its own properties and synergistic effects with other gums, starches, and food ingredients. The interactions between xanthan and galactomannans have been examined to identify their synergy that alter viscous and

gelation properties (Rocks 1971; Sworn 2000; Pai et al. 2002; Wang 2002(a,b); Richter et al. 2004; Higiro 2006). Synergy of xanthan has also been explored with xyloglucan (Kim et al., 2006), glucomannan (Paradossi et al. 2002), and its positive effects with arabic and LBG in emulsions (Makri 2006), as well as its effect on starch when combined with other gums (Chaisawang et al. 2006).

Furthermore, the stability of frozen entrees and sauces was improved by xanthan gum with respect to syneresis and viscosity control over freeze-thaw cycles (Sworn 2000). The presence of xanthan gum in starch gels has significantly increased its freeze-thaw stability, according to Lo and Ramsden (2000), indicating an excellent compatibility with major food components. Xanthan gum has also had a positive impact with frozen dough by increasing the specific volume of the bread after one week of frozen dough storage and heating via a microwave (Mandala 2005), with better efficiency in combating crust deterioration than LBG and guar (Mandala et al. 2008). Improved dough quality by the addition of xanthan could be due to the reduction of free water as indicated by a reduction in fusion enthalpy (Matuda 2008).

2.5 Cellulose Derivative Hydrocolloids

2.5.1 Sodium Carboxymethyl Cellulose

Sodium carboxymethyl cellulose (CMC), or cellulose gum, is produced by treating cellulose with sodium hydroxide and reacted with sodium monochloroacetate and finally washed (Ganz 1977). CMC is water soluble with the ability to increase viscosity to 5 Pa s in a 1% aqueous solutions, which is considerably lower than that of xanthan gum. CMC solutions exhibit shear-thinning (Murray 2000) and sometimes Newtonian behavior or shear-thickening (Yaşar et al. 2007). It is currently used as a

thickener or bodying agent for instant products, sauces, dressings, and soft drinks; however, high viscosity forms of CMC can cause a "gummy" mouth feel (Murray 2000). Similar to carrageenan and locust bean gum, CMC is used to stabilize frozen products like ice cream by inhibiting ice crystal formation (Murray 2000; Marshall 2003).

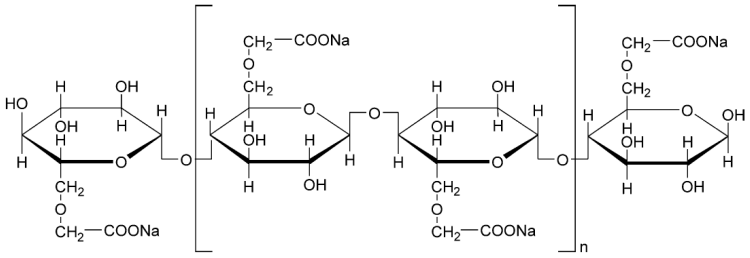

Figure 2.6. Sodium Carboxymethyl Cellulose.

Similar to LBG, CMC was found to reduce proof times and more resistant to extension in previously frozen dough and improve external and internal characteristics of bread, but also increased a desired yellow color in the crust compared to control samples (Sharadanant and Khan 2003a,b).

2.5.2 Microcrystalline Cellulose

Microcrystalline cellulose (MCC) is a linear structure consisting of anhydroglucose units linked by a (1→4) β-glycosidic bond. Acid hydrolysis is performed on to depolymerize wood cellulose under high shear conditions to liberate small crystalline structures. MCC is water-insoluble and thus needs sufficient shear or copolymer network to properly disperse in water (Iijima and Takeo 2000). Temperature has little to no effect on the functionality or apparent viscosity of the networks and remains stable during high temperature processing such as baking or

retort. Not only can MCC be applied to high temperature processes, it can be used as a texture modifier for low-fat desserts (Marshall et al. 2003) and prevents growth of ice crystals in frozen foods during freeze-thaw cycles (Champion et al. 1982). Synergy is important to create and improve texture properties, however, it is more difficult to achieve with other material or gums due to its highly linear structure. In many cases, co-processing under specific conditions is required to form hydrogen bonds between MCC and the material (Glicksman 1986).

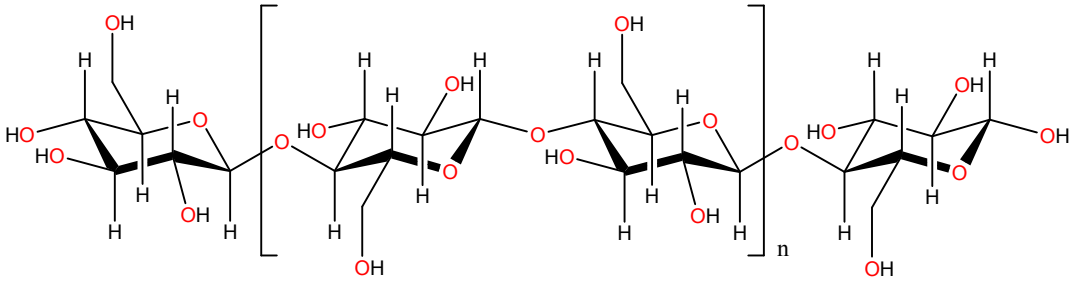

Figure 2.7. Structure of cellulose.

2.6 Curdlan

Alcaligenes faecalis var. *myxogenes*, now classified as *Agrobacterium* biovar. 1, produces the neutral, linear polysaccharide curdlan. Curdlan is the third microbial extracellular polysaccharide following xanthan gum and gellan gum to be approved for food uses in the United States (FDA 1996). Improved production continues to be explored (West 2009; Puliga et al., 2010; Seviour et al., 2011; Yu et al., 2011). Repeating units of (1→3)-β-glucan can form a low-set thermo-reversible gel when heated between ~55 °C and 80 °C or a high-set, triple helix, thermo-irreversible gel when heated above ~80 °C and then cooled (Harada 1994; Hirashima et al. 1997; Nakao 1997; McIntosh et al. 2005; Gagnon et al. 2007). The gelation mechanism of the low- and high-set gels continues to be studied (Tada et al. 1999; Hatakeyama et

al. 2006; Gagnon et al. 2007). Curdlan has a lack of water solubility, alcohols, and most organic solvents but shows solubility in alkaline solutions (Pederson 1979; McIntosh 2005). It is known to be able to hold moisture in meat processing and flour products, stable over a pH range of 2-12 and freeze-thaw conditions, except as an aqueous solution there is syneresis (Nakao 1997).

Composed of a three dimensional structure stabilized by crosslinks that connect junction zones between molecules (Harada et al. 1966; Saito et al. 1978; Marchessault and Deslandes 1978; Nakao et al. 1991; Jezequel 1998), curdlan gum was once the focus of extensive research efforts to expand its applications to improve the texture of various food products (Kanzawa et al. 1987; Nakao et al. 1991; Sanderson 1996; Wang et al., 2010) as well as the delivery of medicinal ingredients (Harada and Harada 1996; Na et al. 2000) and in combination with chitosan as an antibacterial gel (Sun et al., 2011). To date, unfortunately, despite curdlan's ability to form viscous aqueous suspensions with shear-thinning flow behavior (Hirashima et al. 1997; Lopes da Silva et al. 1998; Funami et al. 1999), the applicability of curdlan in the U.S. market remains scarce and limited, due mainly to its less profound viscosity than xanthan gum in solution and inferior gel formation capacity when compared with gellan (Sadar 2004).

Nevertheless, curdlan continues to be used as a texture modifier in Chinese and Japanese noodles and surimi-based products (Nakao et al. 1991; Nishinari 2000) as well as in processed meats such as pork, fried battered chicken, hamburger patties, duck and meatballs to yield juicier and softer products (Nakao, 1997; Hsu and Chung 2000; Chen et al., 2010). Though insoluble in water (Pederson 1979), curdlan is

known to form thermo-reversible or irreversible aqueous gels via heating (Maeda et al. 1967; McCleary 1979; Fulton and Atkins 1980; Harada et al. 1994) or addition of Ca^{2+} or Mg^{2+} (Kanzawa et al. 1987, 1989; Konno and Harada 1994). Furthermore, curdlan is also capable of forming tasteless, odorless, and colorless hydrogel complexes with other polysaccharides (Lo and Ramsden 2000; Lee et al. 2002). This unique gelling mechanism could be used to increase retention or absorption of moisture and other ingredients (Lo et al. 2003) while withstand the temperature extremes of freezing and retorting processes (Wielinga and Maehall 2000; McIntosh et al. 2005). However, the stability of such complexes when subjected to temperature abuse remains uncharacterized.

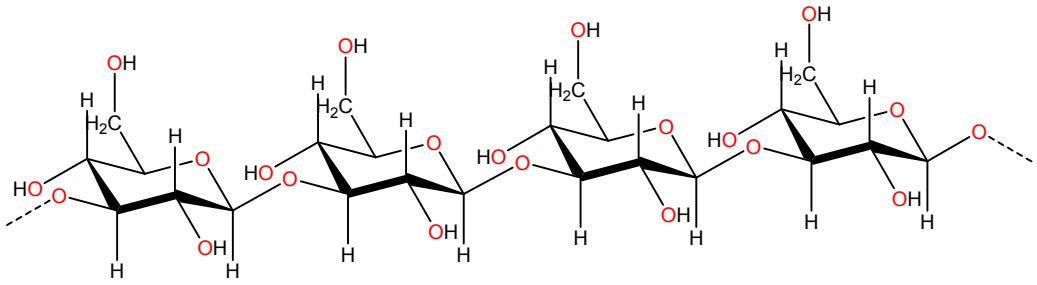

Figure 2.8. Structure of curdlan.

2.7 Characterization Tools

Several tools, listed in Table 2.3, have been reported in the literature capable of characterizing different gums to aid in understanding any positive effects that could exist when more than one polymer are present in a system. Rheological properties, including viscosity and dynamic modulus (Appendix A), are often used to characterize the behavior of gum, starch, and gum/starch combinations (Whitcomb et al. 1978; Williams and Langdon 1996; Wang 2002(a,b); Giannouli et al. 2003; Ikeda

et al. 2004; Higiro et al. 2006; Khouryieh et al. 2006; Kim et al. 2006; Nishinari 2007; Pongsawatmanit et al. 2007; Choi et al. 2008). Other rheological properties such as gel strength and adhesiveness could also provide a broader view of the behavior and stability of the gum system. Utilizing a variety of rheological experiments assists in a well-formed characterization of the structural and textural information of hydrogels.

In order to further depict structural characteristics and water-polymer interactions, methods such as microscopy and magnetic resonance are useful (Table 2.3). Surface morphology can be investigated using scanning electron microscopy (SEM) to elucidate the network properties and microstructure of the combination. It has been successfully employed for investigating skim milk with xanthan and locust bean gum (Sanchez 2000), tapioca starch modified by guar and xanthan gum (Chaisawang 2006), effects of xanthan, locust bean gum, and guar on sucrose (Fernández et al. 2007), chitosan and methylcellulose (Pinotti et al. 2007), and carrageenan/*O. ficus indica* (Medina-Torres et al. 2006).

To delve further in to the nature and adjustments in the molecular structure of polysaccharides in water, nuclear magnetic resonance (NMR) relaxometry and magnetic resonance imaging (MRI) has been used for molecular analysis in carbohydrates (Lüsse and Arnold, 1998; Vittadini et al., 2002), including xanthan and xyloglucan (Kim et al. 2006), xanthan and locust bean gum (Gil et al., 1996) and pectin molecules (Kerr and Wicker, 2000). In these studies the spin-spin relaxation time, T_2, was monitored to identify inter- and intramolecular interactions, along with

their interactions with water, indicating syneresis, water distribution, and structural behavior that can be related to rheology.

Table 2.3. Investigative methodology of hydrocolloidal systems.

Investigative Methodology	Test Properties	Reference
Rheological	Flow characteristics, elasticity classification	Whitcomb 1978; Steffe 1992; Williams and Langdon 1996; Tada et al. 1999; Wang et al. 2002; Giannouli et al. 2003; Ikeda et al. 2004; Jin et al. 2006; Khouryieh et al. 2006; Kim et al. 2006;
Differential Scanning Calorimetry	Thermal analysis, gelation mechanisms explored	Annable et al. 1994; Williams and Langdon 1996; Ikeda et al. 2004; Hatakeyama et al. 2006; Jin et al. 2006; Kim et al. 2006;
Nuclear Magnetic Resonance	Molecular structure and structural changes	Lüsse and Arnold, 1998; Vittadini, 2002; Kim et al. 2006;
Electron Spin Resonance	Molecular structure and structural changes	Shimada et al. 1993; Annable et al. 1994; Williams and Langdon 1996
Dynamic Light Scattering	Particle Size	Coviello and Burchard 1992; Rodd et al. 2001; Richter et al. 2004,2005;
Atomic Force Microscopy	Surface morphology	Ikeda et al. 2004; Jin et al. 2006
Scanning Electron Microscopy	Surface morphology	Kanzawa et al. 1989; Sanchez et al. 2000

Chapter 3: Texture stability of hydrogel complex containing curdlan gum over multiple freeze-thaw cycles

Williams et al., 2009. *J Food Process Pres* 33: 126–139.

3.1 Introduction

A neutral, linear, polysaccharide produced by the microorganism *Alcaligenes faecalis* var. *myxogenes*, curdlan is the third microbial extracellular polysaccharide following xanthan gum and gellan gum to be approved for food use in the United States (FDA 1996). Composed of a three dimensional structure stabilized by crosslinks that connect junction zones between molecules (Harada et al. 1966; Saito et al. 1978; Marchessault and Deslandes 1978; Nakao et al. 1991; Jezequel 1998), curdlan gum was once the focus of extensive research efforts to expand its applications to improve the texture of various food products (Kanzawa et al. 1987; Nakao et al. 1991; Sanderson 1996), as well as the delivery of medicinal ingredients (Harada and Harada 1996; Na et al. 2000). To date, unfortunately, despite curdlan's ability to form viscous aqueous suspensions with shear-thinning flow behavior (Hirashima et al. 1997; Lopes da Silva et al. 1998; Funami et al. 1999), the applicability of curdlan in the U.S. market remains scarce and limited, due mainly to its less profound viscosity than xanthan gum in solution and inferior gel formation capacity when compared with gellan (Sadar 2004).

Nevertheless, curdlan continues to be used as a texture modifier in Chinese and Japanese noodles and surimi-based products (Nakao et al. 1991; Nishinari 2000)

as well as in processed meats such as pork, fried battered chicken, hamburger patties, and meatballs to yield juicier and softer products (Nakao, 1997; Hsu and Chung 2000). Insoluble in water, alcohol, and most organic solvents (Pederson 1979), curdlan is known to form thermo-reversible or irreversible gels via heating (Maeda et al. 1967; McCleary 1979; Fulton and Atkins 1980; Harada et al. 1994) or addition of Ca^{2+} or Mg^{2+} (Kanzawa et al. 1987, 1989; Konno and Harada 1994). Furthermore, curdlan is also capable of forming tasteless, odorless, and colorless hydrogel complexes with other polysaccharides (Lo and Ramsden 2000; Lee et al. 2002). This unique gelling mechanism could be used to increase retention or absorption of moisture and other ingredients (Lo et al. 2003) while withstand the temperature extremes of freezing and retorting processes (Wielinga and Maehall 2000; McIntosh et al. 2005). However, the stability of such complexes when subjected to temperature abuse remains uncharacterized.

The present study investigates the feasibility of using curdlan gum to form stable hydrogel complexes that could improve texture stability over multiple freeze-thaw cycles (FTCs). Hydrogel complexes formed by curdlan and a secondary biopolymer, namely κ-carrageenan, xanthan, guar, and locust bean gum, were subjected to discrete temperature fluctuations. Five FTCs were conducted to resemble the possible temperature abuses of a frozen product (1) from processing plant to warehouse, (2) from warehouse to distributor, (3) from distributor to retail, (4) from retail to consumer, and (5) thawing and refreezing by consumer at home. The extent of syneresis, or water loss, and a spectrum of textural attributes of the gel complexes after each FTC were characterized and compared.

3.2 Materials and Methods

3.2.1 Materials and Sample Preparation

Odorless, fine, free-flowing white powder curdlan containing a minimum of 90% β-D-glucan and with a maximum of 10% water was used (Takeda Vitamin & Food USA, Orangeburg, NY). Samples of κ-carrageenan (Colloid F-390), xanthan (Ticaxan®), guar (Guar Gum 8/22A), and locust bean gum (Pre-Hydrated LBG) were kindly supplied by TIC Gums (Belcamp, MD). A predetermined amount of each of the biopolymer powders was weighed and dry blended at ambient temperature before introduced to deionized (DI) water under constant stirring to achieve an aqueous biopolymer solution containing 1.0% (w/v) curdlan and 1.0% (w/v) of κ-carrageenan, xanthan, guar, or locust bean gum.

3.2.2 Hydrogel Complexes and Freeze-Thaw Cycles

Each of the biopolymer solutions continued to be magnetically stirred while gradually heated to reach 90°C on a heat plate. Once the temperature was met, the biopolymer solutions were removed from the heat and poured into 50 mL test tubes. The solutions were allowed to cool to room temperature to form the hydrogel complexes, which were covered and refrigerated for 24 h at 4°C before subjected to FTCs. Five FTCs were employed where each of the hydrogel complexes was stored at -16°C for 18 h, followed by thawing at 25 °C for 6 h. The thawed samples were collected and tested for syneresis, viscosity, heat stability, storage and loss moduli, gel strength, and adhesiveness.

3.2.3 Syneresis and Textural Measurements

Syneresis of the hydrogel complexes after each FTC was determined by centrifuging the samples at 2200 rpm (707 × *g*) for 20 min in a Beckman Model TJ-6 centrifuge (Beckman Coulter, Palo Alto, CA). The volume of exuded water was determined using a laboratory graduated cylinder (Fisher Scientific, Fairlawn, NJ). A TA.XT2i texture analyzer (Texture Technologies, Inc., Scarsdale, NY) was employed to determine the gel strength and adhesiveness profiles using a P/0.5R probe with a 5-kg load cell (Fiszman and Damasio 2000). Hydrogel complexes (50 mL) formed in cylindrical centrifuge tubes (1-in diameter; Fisher Scientific) were gently transferred onto the texture analyzer platform. For this analysis, when 5 g of force was detected by the probe, it continued to descend into the sample for 10 s before returning to the starting position.

General and dynamic rheological measurements of the hydrogel complexes were conducted using an AR2000 Rheometer (TA Instruments, New Castle DE) with a 60-mm aluminum truncated cone before and after each of the FTCs. The apparent viscosity of the hydrogel complexes was measured at 20°C under a shear rate of 0.15 to 100 s^{-1}. The heat stability of the complexes was assessed by ramping the temperature of the samples after each FTC from 20°C to 80°C and measuring their viscosity at a shear rate of 2 s^{-1}. The storage (*G'*) and loss (*G"*) moduli of samples before and after each FTC were investigated using a frequency sweep over a range of angular frequency (6.283−150 rad/s) while controlling respectively the strain at 10^{-2}, 2.5×10^{-3}, 4×10^{-3}, and 10^{-2} for samples containing κ-carrageenan, xanthan, guar, and locust bean gum.

3.3 Results and Discussion

3.3.1 Syneresis

Syneresis, or loss of water, is an important parameter critical to the stability of a gel system (Xu et al. 1992; Hoover et al. 1997). Prior to freezing-thawing treatments, no syneresis was detected in the hydrogel complexes investigated (Table 3.1), indicating good water holding capacity of the hydrogels upon formation. After the first FTC, apparent syneresis averaging 18% and 32% were detected in the curdlan complexes formed with κ-carrageenan (κ-Ca/C) and locust beam gum (LBG/C), respectively. Loss of moisture in the gel complexes after additional FTCs in the curdlan/locust bean system (approaching 60% after the fifth cycle) was more profound than the curdlan/κ-carrageenan complex where an average of 15-20% syneresis was observed after each FTC. No syneresis was detected in curdlan hydrogel complexes formed with guar gum (G/C) and xanthan gum (X/C) up to five FTCs, indicating strong and stable water holding capacity in these two hydrogel systems.

Table 3.1. Syneresis[*] of 2.0% aqueous curdlan solutions alone and with equal fractions of curdlan with xanthan (X/C), guar (G/C), κ-carrageenan (κ-Ca/C), and locust bean gum (LBG/C).

	Syneresis (%)				
FTC	Curdlan	X/C	G/C	κ-Ca/C	LBG/C
0	46.7 ± 0.9	ND[‡]	ND	ND	ND
1	54.1 ± 4.3	ND	ND	18.56 ± 1.21	31.63 ± 3.84
2	56.5 ± 4.5	ND	ND	15.75 ± 1.46	43.95 ± 2.44
3	58.1 ± 5.1	ND	ND	17.74 ± 1.02	46.78 ± 2.57
4	59.8 ± 3.9	ND	ND	18.31 ± 0.60	57.01 ± 1.60
5	61 ± 3.9	ND	ND	15.55 ± 0.54	59.61 ± 2.28

[*]Data were expressed as mean ± SD (n=3).
[‡]ND = Not Detected.

The ability of the hydrogel complexes to hold moisture is dependent upon the conformation of curdlan and the secondary biopolymer in the system, since curdlan is a linear polysaccharide that forms complex tertiary structures resulting from intramolecular and intermolecular hydrogen bonding (Nishinari 2000; Lo et al. 2003). Before FTCs, the heating (up to 90 °C) involved in the hydrogel formation process could be responsible for the strong initial water-holding capacity, since temperature is known to influence the conformation of curdlan molecules. It has been shown that curdlan swells at around 55ºC, resulting in partial rupture of intramolecular hydrogen bonding (Jezequal 1998). When the temperature is reduced, new hydrogen bonds then crosslink the single-helix curdlan micelles to form a low-set gel (Maeda et al. 1967; Kimura et al. 1973). A high-set, thermal-irreversible gel could be formed if the aqueous solution is heated to above 80ºC (Pszczola 1997; Jezequal 1998).

Furthermore, the conformation of curdlan is also known to vary with the concentration of alkaline in a solution (Ogawa et al. 1972). At low NaOH concentrations, curdlan shows an ordered (helical) conformation. A significant change occurs once the concentration of NaOH is increased to between 0.19 and 0.24 N. Curdlan becomes fully soluble with a random structure once the NaOH exceeds 0.24 N. The random structure returns to an ordered state once the solution is neutralized. Therefore, the stability of the intramolecular and intermolecular hydrogen bonding was also dependent on the chemical compatibility of curdlan with the secondary biopolymer in the system. Although the β-1,3 glucosidic linkages that connect curdlan's repeating D-glucose subunits (Harada and Harada 1996; Jezequal 1998; Funami et al. 1999; Imeson 2000) are also found in κ-carrageenan, the neutral

nature of the D-glucose that makes up curdlan might have hindered the interactions between curdlan and κ-carrageenan, consequently losing its water-holding capacity, as evidenced by the 15-20% syneresis after freeze-thaw treatments (Table 3.1).

Locust bean gum is a neutral galactomannan with linear chains of 1,4-linked beta-D-mannan backbone with 1,6-linked alpha-D-galactose side units (Meer 1977; Wielinga and Maehall 2000). The galactose side units are the only portion responsible for hydration and hydrogen-bonding activity; however, at a 4:1 mannose:galactose ratio the galactose units could easily become unavailable if they are trapped intramolecularly (Dea et al. 1977). Contrarily, both xanthan and guar gum are highly substituted. Xanthan gum is an anionic linear hydrocolloid with a (1→4) linked β-D-glucose backbone, and has a large side unit on every other glucose unit at location C-3 (Kovac and Kang 1977; Sworn 2000; Giannouli and Morris 2003). Guar gum, a neutral hydrocolloid with linear chains of D-mannopyranosyl units with D-galactopyranose substituents protruding by (1→6) linkages, contains approximately two mannose residues per galactose (Maier et al. 1992). The highly substituted nature of these two polymers allows for excellent hydration and hydrogen-bonding activity (Hoyt 1966; Argin-Soysal et al. 2009), which could attribute to the zero syneresis achieved when xanthan or guar was incorporated in the curdlan hydrogel complexes (Table 3.1).

3.3.2 Apparent Viscosity and Heat Stability

Xanthan/curdlan and guar/curdlan hydrogel complexes conducted in the present study were found to exhibit pseudoplastic behavior, as indicated by the Cross model below, representing the curve better than the simpler power law model.

$$\eta = \eta_\infty + \frac{\eta_0 - \eta_\infty}{1 + k_C \dot{\gamma}^m} \quad [1]$$

Where η is the viscosity, η_∞ is the infinite shear viscosity, η_0 is the zero shear viscosity, k_C is the consistency coefficient of the Cross model, m is the flow behavior index and $\dot{\gamma}$ is the shear rate. There was variation in the values over the FTCs, however, a trend can be elucidated from Table 3.2. As expected from gels, the viscosity of κ-Ca/C and LBG/C at zero shear viscosity was significantly higher than G/C and X/C complexes. The zero shear viscosity of X/C was greater than G/C, signifying a texture that is possibly more 'gel like.' Conversely, the G/C and X/C samples showed higher consistency coefficients than other complexes tested.

More consistent with gel behavior, the consistency coefficient was lower for κ-Ca/C and LBG/C. Interestingly the latter also exhibited shear thickening behavior, where the flow behavior index is greater than 1. Complexes G/C and X/C had a rate index below 1, indicating shear thinning behavior. Finally, the quick ramp (30 °C/min) in temperature yielded a significant increase in apparent viscosity at 80 °C, η_{80}, and 2 s^{-1}. As shown in Table 3.2, κ-Ca/C and LBG/C exhibited the least stability through FTCs, where LBG/C increased through FTCs until decreasing after the fifth FTC and κ-Ca/C decreased over the FTCs. With the exception of the third FTCs, the heat ramping had the same affect throughout FTCs on G/C and X/C. The lack of heat stability between all samples may be due to some water evaporation though a solvent trap was utilized.

Table 3.2. Apparent viscosity modeling at 20 °C* exhibiting the Cross model over a shear rate range from 0.15 to 100 s^{-1} and apparent viscosity at 80 °C*, η_{80}, a shear rate of 2 s^{-1}.

	Apparent viscosity parameters at 20 °C and apparent viscosity at 80 °C and for curdlan copolymers					
	FTC	η_0 (Pa s)	η_∞ (Pa s)	k_C (Pa s^m)	m	η_{80} (Pa s)
X/C	0	$6.18 \times 10^4 \pm 4.37 \times 10^3$	0.02 ± 0.01	$1.22 \times 10^5 \pm 1.73 \times 10^5$	0.81 ± 0.02	85.6 ± 15.7
	1	206 ± 19	0.03 ± 0.00	62.75 ± 9.53	0.85 ± 0.01	77.9 ± 1.4
	2	122 ± 69	0.04 ± 0.00	27.16 ± 15.92	0.87 ± 0.01	105.1 ± 15.7
	3	135 ± 13	0.04 ± 0.00	26.83 ± 3.59	0.88 ± 0.02	57.6 ± 4.6
	4	289 ± 273	0.04 ± 0.00	67.89 ± 73.98	0.88 ± 0.00	85.4 ± 5.6
	5	135 ± 43	0.03 ± 0.01	20.99 ± 5.47	0.88 ± 0.00	81.3 ± 16.4
G/C	0	75 ± 0	$2.41 \times 10^{-6} \pm 2.37 \times 10^{-7}$	7.71 ± 3.41	0.72 ± 0.04	30.2 ± 7.7
	1	75 ± 15	$9.59 \times 10^{-7} \pm 1.64 \times 10^{-7}$	30.01 ± 12.82	0.63 ± 0.01	39.6 ± 17.4
	2	88 ± 10	0.08 ± 0.12	102.8 ± 125.87	0.74 ± 0.24	26.2 ± 9.6
	3	204 ± 140	$8.61 \times 10^{-7} \pm 6.95 \times 10^{-7}$	577.41 ± 811.18	0.69 ± 0.15	54.1 ± 7.8
	4	42 ± 55	$4.85 \times 10^{-7} \pm 6.75 \times 10^{-7}$	21.63 ± 30.07	0.65 ± 0.04	39.1 ± 27.8
	5	47 ± 7	1.46 ± 2.07	20.14 ± 19.92	0.64 ± 0.07	39.3 ± 2
LBG/C	0	53 ± 6	$1.79 \times 10^{-6} \pm 8.5 \times 10^{-7}$	8.84 ± 3.06	0.59 ± 0.01	78.8 ± 1.4
	1	533 ± 93	$4.39 \times 10^{-8} \pm 3.36 \times 10^{-8}$	4.71 ± 5.1	1.24 ± 0.47	191 ± 29.9
	2	387 ± 145	$1.91 \times 10^{-8} \pm 1.35 \times 10^{-8}$	0.4 ± 0.14	2 ± 0.12	167.4 ± 38.7
	3	543 ± 5	$2.02 \times 10^{-5} \pm 2.18 \times 10^{-5}$	0.7 ± 0.03	1.6 ± 0.02	345.3 ± 33.3
	4	1123 ± 313	$6.76 \times 10^{-8} \pm 1.92 \times 10^{-8}$	1.45 ± 1.2	1.41 ± 0.49	357 ± 5.9
	5†	1239 ± 1359	$3.42 \times 10^{-5} \pm 3.09 \times 10^{-5}$	10.22 ± 13.85	0.76 ± 0.21	271.4 ± 34.4
	5‡	154 ± 137	0.15 ± 0.21	0.1 ± 0.04	2.1 ± 0.37	
k-Ca/C	0	424 ± 230	0.03 ± 0.04	3.67 ± 1.62	1.23 ± 0.19	69.6 ± 1.7
	1	740 ± 297	$8.16 \times 10^{-7} \pm 4.33 \times 10^{-7}$	10.31 ± 6.42	1.08 ± 0.04	64 ± 2.9
	2	525 ± 374	$4.65 \times 10^{-3} \pm 6.57 \times 10^{-3}$	10.33 ± 6.89	0.98 ± 0.08	48.9 ± 33.9
	3	437 ± 275	0.06 ± 0.06	5.01 ± 2.37	1.16 ± 0.04	38.4 ± 13.2
	4	879 ± 740	0.05 ± 0.07	9.51 ± 9.28	1.20 ± 0.07	43 ± 5
	5	438 ± 380	$5.8 \times 10^{-8} \pm 5.8 \times 10^{-8}$	3.42 ± 2.21	1.24 ± 0.01	29.2 ± 22.1

*Values are the mean ± standard deviation (n=2).

†Shear rate range for 0.15 to 18 s^{-1}, following the Cross model; ‡Shear rate range for 18 to 100 s^{-1}, following the Casson model.

3.3.3 Storage and Loss Moduli

Frequency sweep testing was conducted within the linear viscoelastic range determined from strain sweep measurements. With the exception of locust bean gum, all hydrogel complexes exhibited a greater elastic (or solid-like) portion, as indicated by the storage modulus, *G'*, predominating the loss modulus (viscous portion), *G"*, throughout the five FTCs in Figure 3.1. The differences between *G'* and *G"* in the curdlan/guar and curdlan/xanthan combinations were significantly lower than the other two combinations, suggesting the formation of polymer entanglements when curdlan was mixed with guar or xanthan (Lo et al. 2003). This is in agreement with the low apparent viscosity of G/C and X/C at 20 °C (Table 3.2). The values of *G'*, a measurement of energy stored during deformation and related to the solid-like portion of the system, were significantly higher when curdlan was mixed with κ-carrageenan or locust bean gum. The greatest *G'* values were observed with the locust bean/ curdlan combination, which also showed two distinct crossover points between *G'* and *G"* before the hydrogels were subjected to FTCs—first at angular frequency of 0.15 rad/s and modulus of 2.21 Pa and second at 17.37 rad/s and 46.03 Pa.

The crossover points, the overlap frequency that represents the point at which the characteristic behavior of the gels shifted from elastic to viscous, in the curdlan/locust bean combination were indicative of its weak gel structure. The hydrogel complexes continued to behave like viscous solutions where the two polymers formed typical entanglement solutions between the two crossover points. Although the significance of the second crossover point at high angular frequency on the structure of curdlan/locust bean hydrogels remained unclear, this unique

phenomenon could also attribute to the dramatic changes of viscosity and heat stability (Table 3.2) observed in the system after multiple FTCs.

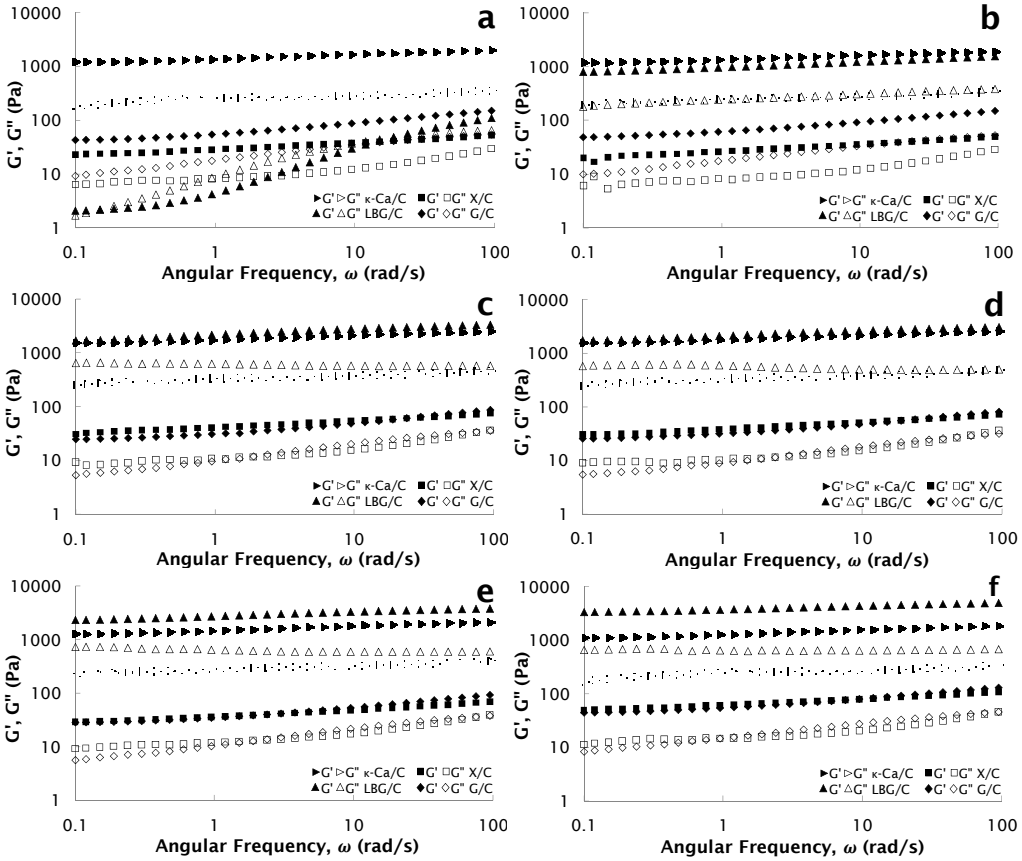

Figure 3.1. Frequency sweeps of 2.0% aqueous curdlan solutions alone and with equal fractions of curdlan with xanthan (X/C), guar (G/C), κ-carrageenan (κ-Ca/C), or locust bean gum (LBG/C). Storage, G', and loss modulus, G", prior to (a), and after the first (b), second (c), third (d), fourth (e), and fifth (f) freeze-thaw cycles.

It has been postulated that, at higher frequencies, the polymer chain entanglements are retained throughout the short period of oscillation and they act as temporary cross-links, causing the material to exhibit pronounced elasticity (Dea 1979; Imeson 2000; Lo et al. 2003). However, after freeze-thaw treatments, the curdlan/locust bean

combination showed distinct gel-like properties where *G'* predominated *G"* over the entire frequency range.

3.3.4 Gel Strength and Adhesiveness

The gel strength data were in support of the moduli measurements where the curdlan/κ-carrageenan complexes were found to have the highest gel strength prior to FTCs (Table 3.3). The gel strength of curdlan/κ-carrageenan continued to decline after each FTC, suggesting the inability of the system to withstand temperature fluctuations. At the end of the fifth FTC, the gel structure was completely destructed. Conversely, the gel strength of curdlan hydrogels formed with xanthan or guar gum both stayed extremely low throughout the five FTCs, reflective of the pudding-like texture of both hydrogel complexes. The gel strength of curdlan/locust bean complexes was significantly increased after the first FTC, and remained relatively stable over the next three cycles before declining again after the fifth FTC. Such high gel strength even after multiple FTCs could be attributed to the considerable smooth mannose backbone regions that give locust bean gum the ability to form strong gels with other polymers such as xanthan, carrageenan, and agarose (Meer 1977; McCleary 1979; Launay and Cuvelier 1986).

Adhesiveness, the work required to separate a surface from food materials, is an important attribute that could have both positive and negative ramifications depending on the applications (Meiron and Saguy 2007). The adhesiveness of curdlan/locust bean hydrogels was the highest amongst all combinations prior to FTCs, followed by guar, κ-carrageenan, and xanthan (Table 3.3). Except for xanthan,

Table 3.3. Gel Strength and adhesiveness* of 2.0% aqueous solutions with equal fractions of curdlan with xanthan, guar, k-carrageenan, or locust bean gum over five freeze-thaw cycles (FTCs).

Gel Strength and Adhesiveness of Curdlan Combinations				
FTC	X/C	G/C	k-Ca/C	LBG/C
Gel Strength (N)				
0	0.075±0.001	0.089±0.013	0.205±0.019	0.079±0.002
1	0.080±0.001	0.091±0.015	0.164±0.005	0.494±0.117
2	0.082±0.002	0.077±0.001	0.156±0.020	0.301±0.025
3	0.084±0.001	0.089±0.014	0.146±0.017	0.262±0.025
4	0.086±0.001	0.075±0.001	0.114±0.004	0.268±0.009
5	0.085±0.001	0.076±0.001	0.090±0.002	0.202±0.039
Adhesiveness (|N s|)				
0	0.044±0.003	0.186±0.019	0.104±0.011	0.262±0.044
1	0.048±0.012	0.097±0.001	0.019±0.002	0.004±0.006
2	0.060±0.015	0.106±0.000	0.005±0.003	0.005±0.004
3	0.060±0.005	0.165±0.044	0.001±0.014	0.004±0.004
4	0.063±0.003	0.050±0.011	0.007±0.001	0.005±0.001
5	0.060±0.000	0.047±0.002	0.007±0.001	0.005±0.001

*Data were expressed as mean ± SD (n=3).

the adhesiveness of the complexes quickly declined after the first FTC, with curdlan/locust bean being the most drastic. However, it was drastically reduced after the first FTC and the hydrogels remained almost non-adhesive after subsequent FTCs. Unlike locust bean gum or κ-carrageenan, guar gum in combination with curdlan formed hydrogels that showed an unusual spike in adhesiveness after the third FTC yet continued to decline in following cycles.

The tendency of a food to adhere and possibly interact with its packaging material could have significant ramifications that may affect its overall quality, appearance, and shelf life (Meiron and Saguy 2007). It could also affect the barrier characteristics of the package, which could have significant ramifications (e.g., flavor, color, and nutrients deterioration) (Hwang et al., 2000; Ayhan et al., 2001).

With regard to product quality, especially concerning the product's shelf life and shelf stability, it is highly desirable to employ a hydrogel complex that could remain stable over multiple FTCs. Therefore, the most consistent adhesiveness observed in the curdlan/xanthan hydrogel complexes up to five FTCs suggests that curdlan in combination with xanthan could serve as an excellent candidate to prevent syneresis in frozen products over temperature fluctuations, either intentionally or unintentionally, without altering the textural quality of the product.

3.4 Conclusion

Over the five FTCs investigated, the curdlan/xanthan hydrogel complexes proved to be the most resilient, showing zero syneresis with superior consistency storage and loss moduli, gel strength, and adhesiveness compared to curdlan complexes formed with guar, κ-carrageenan, or locust bean gum. Guar and curdlan combination also showed good stability with no syneresis, but yielded lower zero shear viscosity, fluctuations in both the dynamic modulus and adhesiveness. Conversely, locust bean gum, when incorporated into curdlan hydrogels, was found the most unstable due mainly to the formation of a weak gel network that quickly broke down, leading to increased syneresis as FTCs progressed. The curdlan/κ-carrageenan formulation gave high gel strength; however, besides noticeable syneresis (15-20%) the drastic changes in viscosity and adhesiveness after FTCs were undesirable for food applications. Further investigations are warranted in order to optimize the formulation that fulfills product-specific requirements.

Chapter 4: Characterization of Water Distribution in Xanthan-Curdlan Hydrogel Complex Using Magnetic Resonance Imaging, Nuclear Magnetic Resonance Relaxometry, Rheology, and Scanning Electron Microscopy

Williams et al., 2011. *J Food Sci: Food Engineering and Physical Sciences*

4.1 Introduction

Syneresis, the spontaneous expulsion of liquid from a gel (Parker, 1984), remains a challenge in processed foods, especially frozen products, since product quality could be drastically reduced by uncontrolled moisture loss or migration, which consequently creates ice crystals that could lead to microbial growth and texture deterioration in food (Goff et al., 1993; Lund 2000). In our previous study (Williams et al., 2009), we successfully demonstrated that a hydrogel complex formed by xanthan and curdlan gum significantly reduced syneresis over five freeze-thaw cycles (FTCs) to an undetectable level, while retaining stable rheological and textural properties. The viscosity, heat stability, loss and storage moduli, gel strength, and adhesiveness remained relatively consistent throughout the FTCs investigated. However, the distribution of water and its interactions with the xanthan curdlan hydrogel complex (XCHC) remains uncharacterized.

Xanthan gum, an anionic microbial polysaccharide widely used as a thickening, stabilizing, and emulsifying agent in the food, chemical, and pharmaceutical industries due to its desirable pseudoplastic behavior in water (Whitcomb and Macosko, 1978), is produced by *Xanthomonas campestris* fermentation and consists of repeating (1→4)-β-D-glucose units in the backbone with a trisaccharide side chain, namely α-D-mannose, β-D-glucuronic acid, and β-D-

mannose, located on C3 of every other glucose. Besides having excellent compatibility with major food components, xanthan, when combined with other gums or starches, showed synergistic effects in viscosity and moisture control (Lo and Ramsden 2000; Sworn 2000). Curdlan, on the other hand, is a neutral linear microbial polysaccharide made of (1→3)-β-glucan repeating units, making it insoluble in water, alcohols, and most organic solvents, except for alkaline solutions (Pederson, 1979; McIntosh et al., 2005). It can form a low-set thermo-reversible gel when heated between ~55°C and 80°C, or a high-set, triple helix, thermo-irreversible gel when heated above ~80°C and then cooled (Harada et al., 1994; Hirashima et al., 1997; Nakao, 1997; McIntosh et al., 2006; Gagnon and Lafleur, 2007). Capable of holding moisture in processed meat and flour products, curdlan is stable over a pH range of 2 to 12 and freeze-thaw conditions, except as an aqueous solution wherein syneresis occurs (Nakao, 1997). The gelation mechanism of the low- and high-set gels continues to be of interest in the literature (Tada et al., 1999; Hatakeyama et al., 2006; Gagnon et al., 2007). Nevertheless, no information is yet available on the interaction of xanthan and curdlan undergone freezing-thawing treatments.

Nuclear magnetic resonance (NMR) relaxometry and magnetic resonance imaging (MRI) techniques have allowed identification of water distribution and molecular interactions of gums without destruction of the sample. These non-invasive techniques have been used to study the gelation process of combined hydrocolloids and their interactions with water. For instance, NMR was employed to characterize molecular mobility for the combination of several polysaccharides, including xanthan gum (Lüsse and Arnold, 1998; Vittadini et al., 2002), as well as structural interactions

(Whitney et al., 1998; Lazaridou et al., 2000; Tojo and Prado, 2003; Kim et al., 2006). With the assistance of NMR, the effect of water on pectin molecules was elucidated (Kerr and Wicker, 2000), whereas the molecular interactions between locust bean gum and cellulose was specified to involve mannosyl residues and not galactosyl residues as first thought (Newman and Hemmingson, 1998). Capable of measuring the proton density of water throughout a sample, MRI, when used in conjunction with NMR, could relate the homogeneity of a hydrogel to its textural behavior (Gil et al., 1996). Oztop and others (2010) recently quantified the effect of water uptake on whey protein hydrogels by using MRI and NMR relaxometry. They showed that the spin-spin relaxation time (T_2) distributions were highly correlated with the water uptake and were able to explain the interactions of the gel with water at different pH values. Integration of MRI and NMR relaxometry with conventional rheological measurements widely used to investigate textural behavior of polysaccharides (Whitcomb and Macosko, 1978; Wang et al., 2002a,b; Giannouli and Morris, 2003; Ikeda et al., 2004; Higiro et al., 2006; Khouryieh et al., 2006; Kim et al., 2006; Nishinari 2007; Pongsawatmanit et al., 2007; Choi and Yoo, 2008), should provide a powerful approach in attaining a more complete understanding of how the water distribution is affected by the structure of polymers in a hydrogel complex.

In the present study, the moisture distribution in xanthan, curdlan, and XCHC was investigated using MRI and NMR relaxometry, and the results were correlated with respective rheological measurements. The surface morphology, as well as the microstructure of the polysaccharides in question, was visualized by scanning electron microscopy (SEM).

4.2 Materials and Methods

4.2.1 Sample Preparation

Xanthan and curdlan were provided by TIC Gums (Belcamp, Md., U.S.A.) and Takeda USA (Orangeburg, N.Y., U.S.A.), respectively. Each of the sample solutions containing xanthan or curdlan alone as well as equal fractions of both were prepared to reach a final concentration of 2% (w/v) in de-ionized water. The polysaccharides were gradually added to continuously stirred water until well hydrated, then heated to 90 °C under reflux using a water bath. Samples were then allowed to cool to room temperature and finally placed in the appropriate testing vessel at 4 °C for 24 hrs. To complete a freeze-thaw cycle (FTC), the samples were placed at -20 °C for 18 hrs, followed by 6 hrs of thawing at room temperature.

4.2.2 Magnetic Resonance imaging and nuclear magnetic resonance relaxometry

MRI and NMR relaxometry experiments were carried out using a 1.03T NMR spectrometer with 43.8 MHz for ^{1}H-resonance frequency (Aspect Imaging, Hevel Modi'in Industrial Area, Israel). A T_1 weighted spin echo sequence was used for MR acquisition. The echo time (*TE*) was 7.6 ms and the repetition time (*TR*) was 500 ms. Four saggital slices with a thickness of 3 mm were acquired. The 3rd slice was used for data analysis. The field of view (FOV) was 50 mm by 50 mm which yields an in-plane spatial resolution of 391 μm/pixel. All imaging experiments were performed with a time invariant reference vial of distilled water in the image. The image files were analyzed by using MATLAB® v. 7.8.0 (The MathWorks Inc., Natick, Mass., U.S.A.).

For the NMR relaxometry, the spin-spin relaxation (T_2) measurements were performed on the same samples with the same MRI spectrometer. A Carr-Purcell-Meiboom-Gill (CPMG) pulse sequence was used with echo time (*TE*) of 1 ms, 16 acquisition points, 12000 echoes for curdlan, 1024 echoes for xanthan, and 2048 echoes for XCHC. T_2 measurements were acquired four times for each sample. Multi-exponential decay fitting of the CPMG curves (T_2 distributions) were performed using the Nonnegative-Least-Square (NNLS) macro of the software PROSPA (Magritek, New Zealand).

The spin-lattice relaxation (T_1) measurements were performed by using a saturation recovery pulse sequence with delay time ranging from 1 ms to 20000 ms, with 1024 acquisition points and 4 scans. The T_1 values were analyzed by fitting the recovery data to a monoexponential fit by using MATLAB®.

4.2.3 Rheology

Frequency sweeps, i.e. angular frequency vs. storage and loss moduli, were performed with controlled strain AR2000 rheometer (TA Instruments, New Castle, Del., U.S.A.) prior to and after each FTC. A 60-mm aluminum truncated cone (1°) geometry with a gap of 30 μm was implemented. The frequency sweep was performed from 100 to 0.1 rad/s at 20 °C within the linear viscoelastic region, with % strain being 1.6, 0.16, and 0.02 for curdlan, xanthan, and the xanthan curdlan hydrogel complex, respectively. Three replications were conducted for each sample.

4.2.4 Scanning Electron Microscopy

Samples undergoing SEM were first freeze dried after the 24 hr refrigeration period. SEM was performed using a SU-70 Ultra-High Resolution Analytical SEM (Hitachi, Tokyo, Japan). Freeze dried samples were gold sputtered for analysis by the microscope.

4.2.5 Statistical Analysis

For statistical analysis, Minitab® v. 15 (Minitab, Inc., State College, Penn., U.S.A.) was used. Analysis of variance was performed to evaluate the effect of gel type and processing (control and freeze-thaw cycle) on T_1 and T_2. Tukey's test at 5% significance level was used as the comparison test. For rheological samples, Tukey's HSD test at 5% significance level was employed as the comparison test using SAS® v. 9.2 (SAS Institute Inc., Cary, N.C., U.S.A) (see Appendix C).

4.3 Results and Discussion

4.3.1 Spin-lattice relaxation time, T_1, measurements

The spin-lattice relaxation time, T_1, a time constant characterizing the exchange of energy between the nuclear spins and their molecular surrounding, are shown in Table 4.1. As expected, the proton spin-lattice relaxation times for each type of curdlan and/or xanthan hydrogel were shorter than water (Table 4.1). Additionally, the values were significantly different from one another ($p<0.05$). The xanthan hydrogel exhibited the longest T_1 and the curdlan hydrogel exhibited the shortest. The combination of xanthan and curdlan (XCHC) had spin-lattice relaxation

times between those of the pure gums. There was no significant difference in T_1 values between different days, indicating that FTC did not have an effect on T_1.

Table 4.1. – Spin-lattice relaxation times[a], T_1, of 2.0% xanthan, curdlan and xanthan curdlan hydrogel complex (XCHC) subjected to freeze-thaw cycles (FTCs).

	Spin-lattice relaxation times, T_1 (ms)		
FTCs	Xanthan	XCHC	Curdlan
0	2067 ± 34	1934 ± 4	1537 ± 58
1	2171 ± 110	1946 ± 11	1714 ± 42
5	2210 ± 101	1918 ± 21	1671 ± 59

[a]Each value is the mean ± SD, n = 3.

T_1 values were characteristic of each hydrogel and were used to optimize the image acquisition. The T_1 spectra have been used to quantify the porous microstructure of hydrogels (Chiu et al., 1995).

Although T_1 measurements were not used in this case to provide information about the interaction of water with the biopolymers and the water distribution in the hydrogels directly, differences in T_1 values are reflected in MR signal intensities for the hydrogels. Since the MR images were T_1 weighted, lower signal intensity was observed in the hydrogels with the longer T_1 values, this is described in detail in the next section.

4.3.2 Magnetic resonance imaging

The MR signal intensity equation for a spin-echo sequence is given by (Bernstein et al., 2004):

$$S = M_0(1 - 2e^{-(TR-TE/2)/T_1} + e^{-TR/T_1})e^{-TE/T_2} \quad [1]$$

where M_0 is the initial magnetization, TR is the repetition time, and TE is the echo time; T_1 and T_2 are spin-lattice and spin-spin relaxation times, respectively. When the repetition time, TR, is set such that it is lower than T_1, and TE is small compared to the T_2 of the sample, the image becomes T_1 weighted. The TR value used in this study was 500 ms, which was lower than the T_1 of all hydrogels (Table 4.1). Therefore, the low signal indicates long T_1 component and a high signal indicates shorter T_1.

Representative images of curdlan hydrogel are given in Figure 4.1. The first image illustrates the sample prior to a FTC. The second and third images illustrate the sample after 1 and 5 FTCs respectively. Each image has a reference vial of water on the left. The reference water vial has lower signal intensity due to the longer T_1 of water than that of the hydrogels. The curdlan hydrogel was less homogeneous than other hydrogels in this study, as seen in the images by regions of higher and lower signal intensity within the sample. These images are characteristic of samples that exhibit phase separation, e.g., syneresis. The mean signal intensity and the standard deviation of the signal intensities were calculated in the sample region for each image. The decrease in signal intensities for curdlan hydrogels was about 8% (Figure 4.1). Other hydrogels also decreased in signal intensity after one FTC but did not change after multiple FTCs.

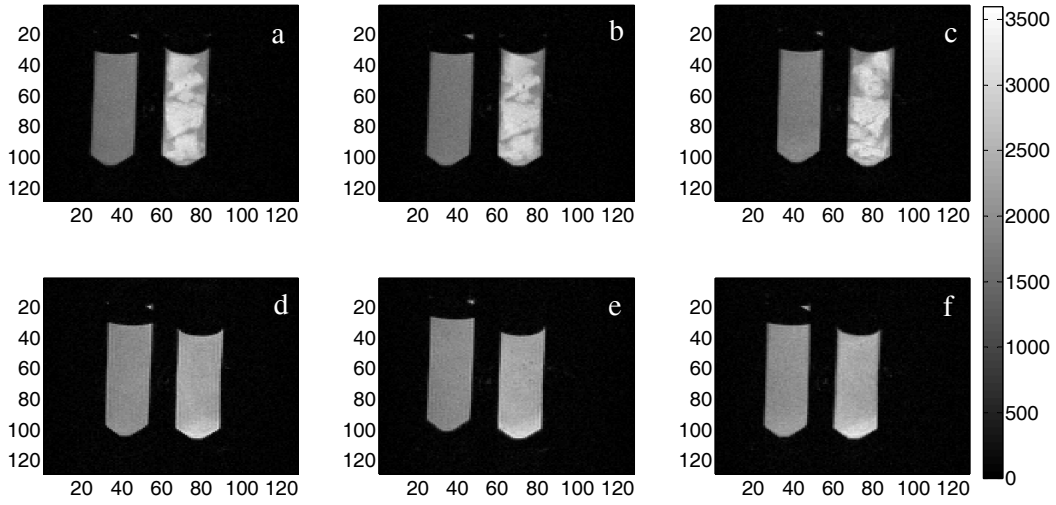

Figure 4.1. Representative magnetic resonance images (MRI) of curdlan (top row) and the xanthan curdlan complex hydrogels (bottom row) prior to freezing (a, d) after one freeze thaw cycle (b, e) and after the fifth freeze thaw cycle (c, f). The scale on the right gives the relationship between signal intensity and grayscale for the images. Axes in the images denote the voxel numbers.

Coefficient of variation (COV) values were calculated as the ratio of the standard deviation of the signal intensity in an image to the mean signal intensity (Table 4.2). Larger *COV* values were observed for curdlan hydrogels and increased with additional FTCs, while other hydrogels' *COV* values did not change significantly. The lower decrease in signal intensity and no change in *COV* values compared to the curdlan hydrogels could be explained by the stabilizing effect of xanthan. Syneresis was not visually observable in these gels and the signal intensity in the MR images was homogeneous indicating no syneresis.

Table 4.2. Coefficient of variation[a] (*COV*) values given as percentages for signal intensities acquired by the spin-echo sequence in relation to magnetic resonance images of 2.0% xanthan, curdlan and xanthan curdlan hydrogel complex (XCHC) subjected to freeze-thaw cycles (FTCs).

	Coefficient of Variation (%)		
FTCs	Xanthan	XCHC	Curdlan
0	5.37 ± 0.36	10.33 ± 0.90	12.37 ± 3.19
1	6.56 ± 0.08	8.76 ± 0.63	13.60 ± 1.39
5	6.56 ± 0.12	9.44 ± 0.54	14.48 ± 0.56

[a]Each value is the mean ± SD, n = 3.

4.3.3 Spin-spin relaxation time, T_2, measurements

T_2 distributions of the hydrogel samples were obtained from the CPMG decay curves by using the Non-Negative Least Square Algorithm in PROPSA. T_2 characterizes the rate at which the M_{xy} component of the magnetization vector decays in the transverse plane and characterizes the interactions between neighboring nuclear spins. In gels, this relaxation rate is affected by the exchangeable hydroxyl protons resulting in a multi-exponential behavior that is quantified by a T_2 distribution. The conformation and mobility of the biopolymer chains resulting from FTC is reflected in the T_2 distributions. The T_2 distributions for the hydrogel samples are given in Table 4.3. The distributions include the peak T_2 values and the areas associated with the peak.

Initially, there were two proton pools (or compartments) for the curdlan: one associated with the gel structure and one associated with water not entrapped by the gel structure. With one FTC, a third compartment was observed. The T_2 of all the proton pools increased with respect to FTC which was consistent with curdlan's unstable behavior after a freeze-thaw treatment. The first two compartments associated with gel structures had different amounts of water. These were related to

the exchangeable protons of the biopolymer, such as hydroxyl and hydroxymethyl groups (-OH, -CH_2OH) corresponding to the intermolecular interaction of the biopolymer. The first proton pool was in an intermediate exchange regime whereas the second pool was in a slower exchange regime.

The third compartment with the longest T_2 was associated with the water not entrapped in the gel structure but the water moving between the gel particulates. These protons were also associated with protons that were not interacting strongly (Kerr and Wicker 2000) with the polymer molecules, which might be indicative of the hydrophobic effect that causes curdlan's insolubility in water.

All compartments experienced a change in the relative areas of the proton pools after the FTCs (Table 4.3). The first compartment's contribution increased, whereas a decrease in the relative area of the second proton pool was observed. The increase in the area of the first compartment could be attributed to an increasing development of a three-dimensional network observed with high-set curdlan gels. The decrease in the area of the second compartment was compensated by the increase in the first area. The third compartment's area also showed a 25% increase which was consistent with images and the syneresis occurring in the hydrogel.

Due to its high water solubility, only one compartment with a T_2 value of 186 ms was observed for the xanthan hydrogels. Unlike curdlan, the T_2 values in xanthan did not change nor did the relative proton pool areas change upon freeze-thaw. These results were also consistent with the imaging experiments.

Two compartments were observed with the XCHC. The relative areas of the proton pools were different compared to that of the curdlan only hydrogels, where the

lower T_2 value (~110 ms) was very small (4%) versus the relative area of the second pool at 342 ms. In XCHC, curdlan hydrogels may be suspended in the xanthan solution. In that regard the first peak could be attributed to the protons coming from the suspended curdlan hydrogels. There was no significant difference (p>0.05) in the T_2 values or relative areas of the compartments due to FTCs (Table 4.3). A third compartment was not found with XCHC as it was in curdlan, indicating XCHC was more resistant to syneresis than curdlan.

In this study, T_2 distributions were used to characterize changes in hydrogels that were subjected to severe treatments. T_2 relaxation spectrums were sensitive to composition for all hydrogels. For the hydrogel that exhibited increasing syneresis after FTCs, the relaxation spectrums also changed and hence were sensitive to process induced structural changes.

Table 4.3. Spin-spin relaxation time[a], T_2, and relative area of 2.0% xanthan, curdlan and xanthan curdlan hydrogel complex (XCHC) subjected to freeze-thaw cycles (FTCs) from nuclear magnetic resonance relaxometry.

		1st Proton Pool		**2nd Proton Pool**		**3rd Proton Pool**	
	FTCs	T_2 (ms)	Relative Area (%)	T_2 (ms)	Relative Area (%)	T_2 (ms)	Relative Area (%)
Curdlan							
	0	-	-	230.25 ± 0.00	60.06% ± 6.68	1411.26 ± 0.00	37.03 ± 6.36
	1	77.58 ± 0.00	9.91 ± 0.08	238.91 ± 12.25	54.18% ± 0.36	1631.54 ± 0.00	35.03 ± 0.01
	5	131.82 ± 13.55	25.53 ± 5.95	292.70 ± 30.09	26.74% ± 4.12	1723.58 ± 61.36	46.54 ± 4.32
Xanthan							
	0	186.99 ± 0.00	98.76 ± 0.53	-	-	-	-
	1	183.96 ± 6.06	99.88 ± 0.17	-	-	-	-
	5	186.99 ± 0.00	99.96 ± 0.05	-	-	-	-
XCHC							
	0	110.58 ± 19.09	4.00 ± 0.50	341.93 ± 0.00	95.43 ±1.07	-	-
	1	133.92 ± 8.98	5.29 ± 0.35	341.93 ± 0.00	94.29 ± 0.13	-	-
	5	104.14 ± 30.59	4.67 ± 0.92	341.93 ± 0.00	94.71 ± 1.12	-	-

[a]Each value is the mean ± SD, n=3.

4.3.4 Rheology and Morphology

Frequency sweeps of curdlan samples, prior to and following the five FTCs, showed greater storage modulus, G', than the loss modulus, G", over the entire frequency range, indicating gel behavior (Figure 4.2). A fully cured three-dimensional gel network is indicated when G' predominates G" with their slopes being independent of the angular frequency.

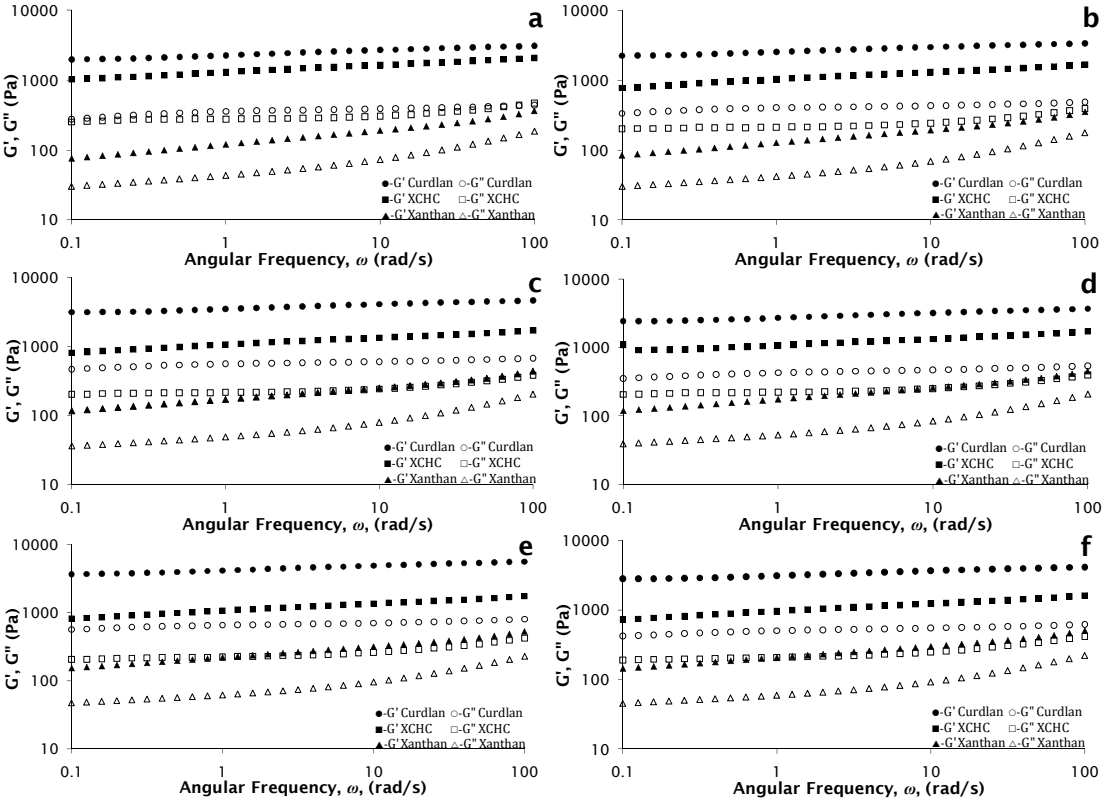

Figure 4.2. Frequency sweeps of 2.0% xanthan, curdlan, and xanthan curdlan hydrogel complex (XCHC). Storage, G', and loss modulus, G", prior to (a), and after the first (b), second (c), third (d), fourth (e), and fifth (f) freeze-thaw cycles.

The slope can be quantified by modeling the storage modulus with the power law,

$$G' = a\omega^b \quad [2]$$

where a is the intercept, b is the slope and ω is the angular frequency. Curdlan exhibited a positive, but slight, dependency upon the angular frequency and therefore did not definitively exhibit a three-dimensional gel structure from rheological data. As seen in Table 4.4, the slope of curdlan prior to FTCs was 0.069, whereas the slope of 1% agar, a known fully cured gel, was 0.037 (Ross-Murphy, 1988; Steffe, 1996).

Table 4.4. Linear regression of storage modulus (G' = $a\omega^b$) and syneresis over five freeze-thaw cycles (FTCs) for 2.0% xanthan, xanthan curdlan hydrogel complex (XCHC), and curdlan. The intercept, *a*, and slope, *b*, of the storage modulus are presented.

	Xanthan			**XCHC**			**Curdlan**		
FTC	*a* (Pa s^b)	*b*	Syneresis (%)	*a* (Pa s^b)	*b*	Syneresis (%)	*a* (Pa s^b)	*b*	Syneresis‡ (%)
0	120	0.211	-	1298	0.102	-	2280	0.069	46.7 ± 0.9
1	128	0.198	-	1028	0.107	-	2570	0.065	54.1 ± 4.3
2	170	0.190	-	1054	0.103	-	3515	0.062	56.5 ± 4.5
3	177	0.183	-	1091	0.093	-	2738	0.066	58.0 ± 5.1
4	221	0.169	-	1062	0.106	-	4190	0.064	59.8 ± 3.9
5	208	0.173	-	954	0.111	-	3141	0.063	61.0 ± 3.9

‡Each value is the mean ± standard deviation, n = 3.

The fluctuation of the dynamic modulus was due in part to the difficulty in handling the sample. The syneresis of curdlan caused the water-to-gel ratio to become inconsistent for each FTC when placed on the plate for rheological tests. Nonetheless, the SEM image of curdlan confirmed the three dimensional network (Figure 4.3), showing the concentrated polymers in a 'honeycomb' like orientation that could be responsible for curdlan's elastic behavior, where free water could be

moving between and around the gel matrix. This potentially trapped water could be represented by the longest T_2 relaxation time, which is subsequently released over FTCs as seen in the MR images (Figure 4.1).

Frequency sweeps of xanthan showed G' predominating G" over the entire frequency range with a significant positive slope. The modulus values were at least one order of magnitude lower than that of curdlan solution, indicating low elasticity. Though there was no detectable syneresis in xanthan samples, the modulus for the second through fifth FTCs was noticeably higher than the modulus of previous cycles. Xanthan is known to exhibit 'gel-like' behavior, which is indicated by its frequency sweep; however, the SEM photos did not reveal a three-dimensional network. SEM images in Figure 4.3 showed two-dimensional layers closely packed. The lack of a three-dimensional network in the SEM micrographs was expected due to xanthan's dynamic modulus dependency upon angular frequency and low modulus values.

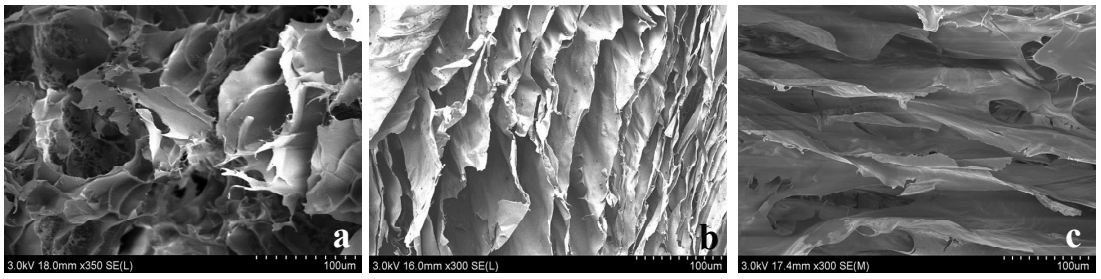

Figure 4.3. Scanning electron microscope micrographs of the 2.0% curdlan (a), 2.0% xanthan (b), and 2.0% xanthan curdlan hydrogel complex (c) freeze dried samples.

The storage modulus was greater than the loss modulus for XCHC over the entire frequency range with a lesser positive slope than that of xanthan but a greater slope when compared to curdlan. Furthermore, the elasticity of XCHC was significantly closer to curdlan than xanthan. The elasticity did decrease after the first FTC remaining constant until a slight increase was observed after the fifth FTC. Table 4.4 shows a 33-56% difference in the slope of the storage modulus, *b*, of XCHC from curdlan, whereas xanthan exhibited 89-100% difference from curdlan. However, no syneresis was detected. While the rheological behavior of XCHC was found relatively close to curdlan than xanthan, the surface morphology exhibited layers. Unlike xanthan, these wavy layers were not closely packed, the layers bend or curve towards each other mimicking a three-dimensional structure, however there was no evidence of a connection between the layers. The structure could explain the positive slope found in the frequency sweeps of XCHC but relatively high elasticity when compared to the xanthan solution. Hence, the tightly packed layers may contribute to the frequency dependency of XCHC.

4.4 Conclusion

A comprehensive view of curdlan, xanthan and XCHCs structural behavior in water was achieved by combining NMR relaxometry, MRI, rheology, and SEM. The fully cured gel of curdlan, interpreted from frequency sweeps, SEM, and MRI, yielded increasing amounts of syneresis under freeze-thaw abuse due to the weak interactions between the biopolymer and water as elucidated from NMR relaxometry. The addition of xanthan to curdlan (XCHC) reduced syneresis to an undetectable level and exhibited elasticity closer to that of curdlan than xanthan –

while lacking a three dimensional network. Moreover, XCHC remained unaffected after the first FTC, making XCHC an ideal candidate to simulate a stable gel without syneresis under freeze-thaw abuse.

4.5 Acknowledgement

We acknowledge the support of the Maryland NanoCenter and its NispLab. The NispLab is supported in part by the NSF as a MRSEC Shared Experimental Facility.

Chapter 5: Effect of pH and salt concentration on the xanthan curdlan hydrogel complex utilizing rheological techniques

5.1 Introduction

Curdlan is well known to be insoluble in water, but can produce an aqueous gel under the proper conditions. However, syneresis occurs and increases under freeze-thaw abuse. Syneresis remains a challenge in processed foods, especially frozen products, since product quality could be drastically reduced by uncontrolled moisture loss or migration, which consequently creates ice crystals that could lead to microbial growth and texture deterioration in food (Goff et al., 1993; Lund 2000). In our previous study (Williams et al., 2009), we successfully demonstrated that a hydrogel complex formed by xanthan, a negatively-charged hydrocolloid, and curdlan gum, a neutral, linear microbial polysaccharide, significantly reduced syneresis over five freeze-thaw cycles (FTCs) to an undetectable level, while retaining rheological and textural properties. Though the usage of xanthan and curdlan alone in food matrices has been studied, the fundamental effects of basic food components such as sodium chloride and pH has yet to be explored in regards to this combination.

The uncommon microbial gum produced by *Agrobacterium biovar 1*, curdlan, is one of three microbial polysaccharides approved by the FDA (21CFR 172.809). The linear (1→3) β-glucan is insoluble in water, alcohols and most organic solvents, however, solubility has been shown in alkaline solutions (Pederson 1979; McIntosh 2005). Curdlan has been used as a texture modifier for Chinese and Japanese noodles and processed meats for juicier texture (Nakao et al. 1991; Nakao, 1997; Hsu and Chung 2000; Nishinari 2000). Despite its insolubility in water, curdlan can produce

both a low-set thermo-reversible and high-set thermo-irreversible gel in aqueous solutions (Harada 1994; Hirashima et al. 1997; Nakao 1997; McIntosh et al. 2005; Gagnon et al. 2007). The high-set thermo-irreversible aqueous gel is created when curdlan is heated above 80 °C, where its gel strength is consistent after one freeze-thaw cycle, unlike agar, carrageenan, and konjac (Nakao 1997). Over the pH range of 2-10, curdlan can gel in the presence of sugars, starches, salt and the incorporation of fats and oils (Nakao 1997; McIntosh et al., 2005).

Xanthan gum is another microbial polysaccharide approved by the FDA (21CFR 172.695) produced by *Xanthomonas campestris*. The structure consists of two repeating (1→4)-β-D-glucose units making up the backbone with a trisaccharide side chain consisting of α-D-mannose, β-D-glucuronic acid, and β-D-mannose. It is known that xanthan gum is unaffected by salt concentrations above approximately 10^{-2} M in the dilute and semi-dilute regime (Rochefort and Middleman 1987; Dolz et. al, 2002) and is stable over a pH range of 1 to 9 (Rao et al., 1998; Hoefler 2004).

In the present study, the combination of frequency sweeps, temperature ramps, gel strength, and adhesiveness will yield an optimal range of texture stability for the xanthan curdlan hydrogel complex (XCHC) over a range of pH values and sodium chloride concentrations. By investigating the effects of salt and pH under temperature abuse utilizing rheological properties, a foundation for further applications involving the combination can be established.

5.2 Methods and Materials

5.2.1 Sample Preparation

Odorless, fine, free-flowing white powder curdlan containing a minimum of 90% β-D-glucan and with a maximum of 10% water was used (Takeda Vitamin & Food USA, Orangeburg, NY). Xanthan (Ticaxan®) was kindly supplied by TIC Gums (Belcamp, MD). The biopolymer powders were weighed and dry blended at ambient temperature before introduced to deionized (DI) water under constant stirring to achieve an aqueous solution containing 1.0% (w/v) curdlan and 1.0% (w/v) xanthan gum.

The pH was adjusted after the gums were well hydrated. Values of pH were evaluated from 2 to 8 by 1. Solutions of 1.0N HCl and 1.0 N NaOH were added once the gum solution was well hydrated using a RW 20 Digital overhead stirrer (IKA, Germany) to achieve the desired pH values below six and six and above, respectively. Sodium chloride was blended and introduced to water along with the biopolymer powders until well hydrated using the overhead stirrer, yielding 5, 20, 75, 100, and 200 mM of NaCl. Either the pH or NaCl solutions were then immersed in a water bath to reach a temperature of 90 °C under reflux. The biopolymer solutions were removed from the heat and allowed to cool to room temperature and subsequently poured into 50 mL centrifuge tubes. The solutions were refrigerated for 24 h at 4 °C before subjected to freeze-thaw cycles (FTCs). Five FTCs were employed where each solution was stored at -18°C for 18 h, followed by thawing at 25 °C for 6 h. The thawed samples were collected for rheological experimentation. Each sample and their two replications were averaged and presented.

5.2.2 Rheological Measurements

Frequency sweeps and temperature ramps were performed with controlled strain AR2000 Rheometer (TA Instruments, Delaware) prior to and after each FTC. A 60-mm aluminum truncated cone (1°) geometry with a gap of 30 μm was implemented. The frequency sweep was performed from 100 to 0.1 rad/s. Temperature ramping was performed at an angular frequency of 6.283 rad/s, first with a heat ramp step from 18 °C to 80 °C, immediately followed by a cooling step returning the sample to 18 °C at a rate of 2 °C /min. A TA-XT2i texture analyzer (Texture Technologies, Inc., Scarsdale, NY) was used to measure the gel strength and adhesiveness with a 0.5" dia. acrylic probe attachment.

5.2.3 Statistical analysis

For statistical analysis, SAS (v. 9.2) was used. Tukey's HSD test at 5 % significance level was employed as the comparison test (see Appendix C).

5.3 Results and Discussion

5.3.1 Effect of pH

A fully cured three-dimensional network is indicated when the storage modulus, G', predominates the loss modulus, G", and both are independent of the angular frequency (Steffe 1996). Curdlan, 2% aqueous solution, closely resembles this behavior. Xanthan alone exhibits 'gel-like' behavior where G' predominates G" over the entire angular frequency range, however, the moduli are directly proportional to the angular frequency and exhibits low modulus values. The dynamic modulus of

the untreated xanthan curdlan hydrogel complex (XCHC), or control, falls in between curdlan and xanthan solutions, with values closer to that of curdlan.

It was evident that adjusting the pH, above or below its original pH of approximately 5.83, causes a reduction in dynamic modulus values during frequency sweeps (Figure 5.1). However, the moduli of XCHC with pH of 2 began to increase after the second FTC and continued to increase through the fifth FTC above control values. Furthermore, its modulus was significantly larger than solutions with pH of 3 through 8 over all FTCs.

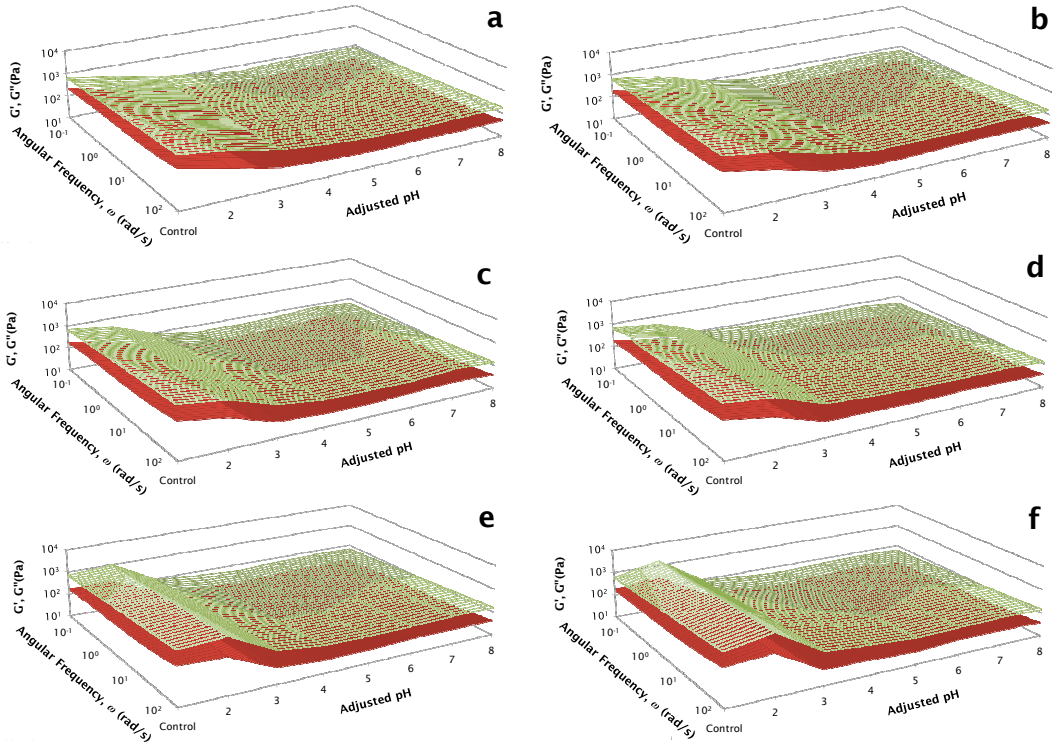

Figure 5.1. Frequency sweeps of 2.0% xanthan curdlan hydrogel complex (XCHC) with pH values of 2, 3, 4, 5, 6, 7, and 8. Storage, G'(10^1 - 10^2 10^2 - 10^3 10^3 - 10^4), and loss modulus, G" (10^1 - 10^2 10^2 - 10^3 10^3 - 10^4), prior to (a), and after the first (b), second (c), third (d), fourth (e), and fifth (f) freeze-thaw cycles.

XCHC with a pH of 3 was also larger than samples with pH values of 4 to 8 prior to FTCs, but consistent over the five FTCs. Subsequent FTCs showed modulus values for pH equal to 3 were higher than other treated samples near or above angular frequencies of 1 rad/s after the first FTC and above 10 rad/s for the following FTCs. Though there were fluctuations at high frequencies (above 10 rad/s) over the five FTCs for samples at pH = 4, the samples were not different from samples with pH values from 5 through 8. FTCs did not affect XCHC samples with pH values of 5 through 8, nor were they significantly different from each other (Figure 5.1).

The storage modulus of these samples held in the range of approximately 50-180 Pa over the frequency range. Whereas, the storage modulus values of the control was an order of magnitude larger ranging from 600 to 2100 Pa. The slope of the dynamic modulus over the frequency range indicates the possibility of gel or gel-like properties. The slope, *b*, of the storage modulus for the curdlan gel ranged from 0.062 to 0.069 over five freeze-thaw cycles. Though storage modulus values were reduced due to pH adjustment, the difference in the slope of the storage modulus from curdlan was 44-84%, with slopes ranging from 0.109-0.152 in Table 5.1, and only averaged 15% different from the control. This implied less dependency upon the angular frequency than xanthan alone, where an 89-100% difference from curdlan was exhibited. Electrostatic interaction between the adjusted pH and negatively charged xanthan may be the cause for the reduction in modulus by an order of magnitude. Nonetheless, XCHC frequency sweeps were relatively stable over a pH range of 4 to 8 during freeze-thaw abuse.

Table 5.1. Linear regression of the storage modulus, G' = $a\omega^b$, for pH treated xanthan curdlan hydrogel complex (XCHC) samples. The intercept, *a*, and slope, *b*, of the storage modulus are presented.

	Freeze-Thaw Cycles					
	0	1	2	3	4	5
Modulus slope, b						
pH						
2	0.124±0.004	0.123±0.005	0.119±0.001	0.115±0.002	0.113±0.003	0.110±0.001
3	0.116±0.005	0.11 ±0.003	0.124±0.003	0.121±0.002	0.121±0.004	0.121±0.003
4	0.136±0.013	0.147±0.005	0.152±0.012	0.143±0.008	0.144±0.008	0.142±0.003
5	0.141±0.007	0.134±0.006	0.138±0.009	0.128±0.007	0.136±0.010	0.132±0.005
6	0.116±0.003	0.113±0.004	0.117±0.004	0.112 0.001	0.113±0.003	0.115±0.005
7	0.114±0.001	0.109±0.003	0.111±0.004	0.116±0.001	0.113±0.001	0.112±0.002
8	0.109±0.003	0.114±0.003	0.116±0.008	0.122±0.004	0.112±0.006	0.111±0.005
Modulus intercept, a (Pa s^b)						
pH						
2	506±67.3	525±87.1	584±144.5	650±23.2	1375±218.8	2211±750.9
3	213±59.9	168±30	141±26.5	140±8.5	145±39.6	142±17.8
4	130±62	74±3	74±19.7	99±20.1	78±21.9	93±14.4
5	95±30	78±12	75±10.4	92±11.4	77±18.7	74±8.5
6	98±21	86±4.9	79±7.6	92±3.3	88±6.1	85±6.2
7	112±17.4	103±8.6	110±12.5	96±3.8	98 ±10.6	95±14.4
8	116±8.8	96±11.8	83±18.2	73±7.7	95±19.4	84±10.6

Similar to the frequency sweep results, the adhesiveness and gel strength of XCHC samples with pH values from 4 to 8 were the same and were not affected by freeze-thaw abuse (Table 5.2). Adhesiveness for samples with pH equal to 2 was highest and decreased until after the third FTC remaining the same until after the fifth freeze-thaw cycles. A 2.9% water loss, syneresis, was yielded after the second freeze-thaw cycle and noticeably increased to 24.6% after the third FTC (Table B.2).

Table 5.2. Adhesiveness and gel strength of the xanthan curdlan complex solutions with the pH adjusted from 2 to 8 over five freeze thaw cycles (FTCs).

	Freeze Thaw Cycles					
	0	1	2	3	4	5
Adhesiveness (|N s|)						
pH						
2	0.940±0.043	0.579±0.059	0.252±0.058	0.131±0.080	0.081±0.025	0.074±0.012
3	0.960±0.328	1.003±0.311	0.901±0.456	0.950±0.280	0.956±0.289	1.026±0.396
4	0.438±0.101	0.438±0.210	0.479±0.209	0.426±0.167	0.414±0.081	0.454±0.178
5	0.371±0.012	0.377±0.005	0.418±0.051	0.405±0.024	0.439±0.042	0.473±0.030
6	0.329±0.053	0.341±0.019	0.356±0.019	0.378±0.022	0.408±0.029	0.440±0.087
7	0.332±0.036	0.358±0.036	0.395±0.040	0.498±0.123	0.445±0.012	0.535±0.156
8	0.348±0.020	0.361±0.032	0.391±0.038	0.407±0.024	0.444±0.059	0.467±0.047
Gel Strength (N)						
pH						
2	0.106±0.004	0.094±0.003	0.085±0.006	0.099±0.015	0.094±0.013	0.113±0.022
3	0.108±0.009	0.109±0.011	0.111±0.018	0.112±0.011	0.110±0.011	0.112±0.012
4	0.086±0.005	0.085±0.008	0.085±0.006	0.084±0.006	0.085±0.006	0.088±0.010
5	0.084±0.000	0.085±0.000	0.086±0.001	0.086±0.000	0.086±0.001	0.087±0.001
6	0.079±0.001	0.083±0.000	0.084±0.001	0.085±0.000	0.086±0.001	0.087±0.003
7	0.079±0.001	0.082±0.001	0.083±0.000	0.087±0.002	0.086±0.000	0.091±0.005
8	0.083±0.001	0.086±0.000	0.088±0.001	0.089±0.001	0.091±0.001	0.092±0.002

This amount of syneresis coincides with reduction in adhesiveness and increased dynamic modulus. The gel strength for pH of 2 was also the highest of the treated samples, but decreasing slightly after the first FTC remaining stable during the following FTCs. Contradicting the behavior of pH = 2, a pH of 3 exhibited greater values of adhesiveness and gel strength and was not affected by freeze-thaw abuse. The increased modulus and gel strength of XCHC at pH 2 and 3 could be due the fact that xanthan is negatively charged and electrostatic interactions caused by the introduction of positive charges created a stronger gel.

In order to further investigate the stability of the pH adjusted samples, the ability to withstand temperature ramps at an angular frequency of 6.283 rad/s was explored. Generally, the storage modulus, presented in Figure 5.2, increased during

both the heating and cooling cycles, displaying hysteresis. The storage modulus was lower at pH = 5, 6, 7, and 8, where samples at pH = 5 yielded the most hysteresis.

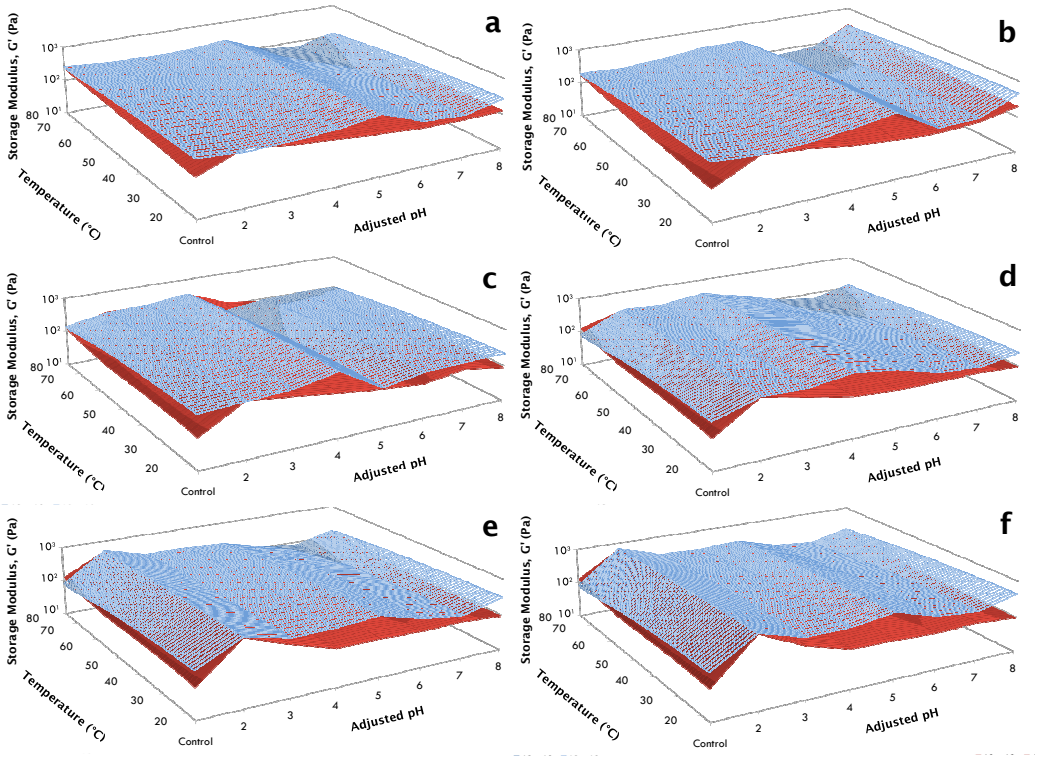

Figure 5.2. Temperature ramps of the storage modulus, G', of 2.0% xanthan curdlan hydrogel complex (XCHC) with pH values of 2, 3, 4, 5, 6, 7, and 8. Heating ramp, G' (10^1 - 10^2 10^2 - 10^3), and cooling ramp, G'(10^1 - 10^2 10^2 - 10^3), prior to (a), and after the first (b), second (c), third (d), fourth (e), and fifth (f) freeze-thaw cycles.

Conversely, there was minimal hysteresis with XCHC at pH = 2. Reduction in the sample pH (Table B.1) following refrigeration could be an indication of electrostatic interactions creating sensitivity to temperature allowing for fluctuations in elasticity during temperature ramps. However, this does not explain the reduction in modulus for the control and hysteresis with the control. Hysteresis under temperature ramps

may be impart due to slow temperature ramping and the geometry gap of 30 μm (Figure A.1) allowing the sample enough surface area permitting curdlan to form a network that was hindered by xanthan in solution.

5.3.2 Effect of Salt Concentration

Similar to the effects of pH, but to a lesser extent, sodium chloride reduced the dynamic moduli of the hydrogel complex prior to FTCs (Figure 5.3). Treatments of 5, 20, 75,100, and 200 mM NaCl were different from each other and fluctuated throughout FTCs with no discerning patterns. However, this disparity regarding significant differences for pH and NaCl treated samples could be explained by the coefficient of variance (COV). The COV was 17 for NaCl treated samples, whereas COV was 57 for pH treated samples exhibiting more variability between samples. Furthermore, the slope of G' in Table 5.3 averaged 9 % difference from the control, yielding similar gel behavior at lower modulus values.

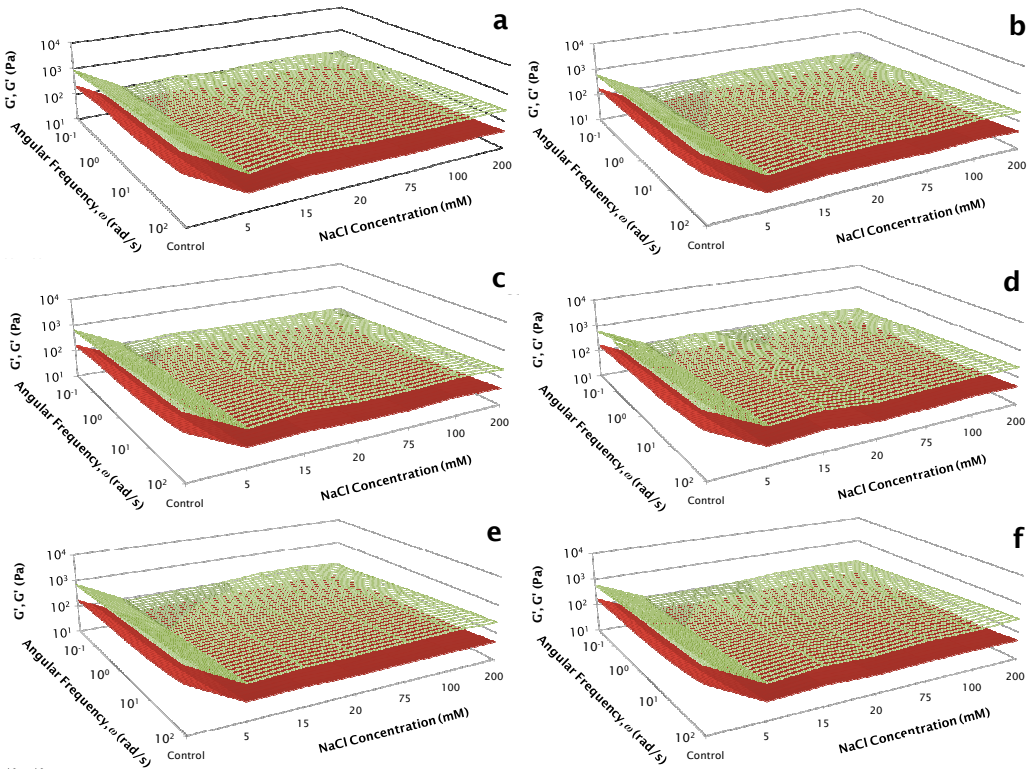

Figure 5.3. Frequency sweeps of 2.0% xanthan curdlan hydrogel complex (XCHC) treated with 5, 15, 20, 75, 100, and 200 mM NaCl. Storage, G'(10^1 - 10^2 10^2 - 10^3 10^3 - 10^4), and loss modulus, G" (10^1 - 10^2 10^2 - 10^3 10^3 - 10^4), prior to (a), and after the first (b), second (c), third (d), fourth (e), and fifth (f) freeze-thaw cycles.

Similar to dynamic modulus, variation was displayed with adhesiveness in Table 5.4. Analogous to dilute and semi-dilute xanthan solutions (Rochefort and Middleman 1987; Dolz et. al, 2002), the low sodium chloride concentrations affected adhesiveness. Samples treated with 5 and 15 mM NaCl were significantly lower than subsequent treatments and increased over FTCs. Increased molecular mobility of the system could be responsible for increased adhesiveness (Adhikari et al., 2001).

Table 5.3. Modeling of the storage modulus, $G' = a\omega^b$, for NaCl treated xanthan curdlan hydrogel complex (XCHC) samples.

	Modeling of Storage Modulus for NaCl (mM) Treated Samples					
FTC	5	15	20	75	100	200
Modulus slope, b						
0	0.113 ± 0.003	0.107 ± 0.004	0.107 ± 0.002	0.098 ± 0.005	0.099 ± 0.001	0.114 ± 0.03
1	0.117 ± 0.005	0.112 ± 0.001	0.098 ± 0.009	0.096 ± 0.005	0.102 ± 0.003	0.112 ± 0.004
2	0.111 ± 0.014	0.111 ± 0.008	0.099 ± 0.001	0.098± 0.001	0.100± 0.002	0.108 ± 0.002
3	0.111 ± 0.002	0.111 ± 0.001	0.104 ± 0.002	0.099 ± 0.002	0.084 ± 0.026	0.107 ± 0.004
4	0.111 ± 0.002	0.118 ± 0.001	0.102 ± 0.004	0.093 ± 0.003	0.094 ± 0.006	0.106 ± 0.010
5	0.100 ± 0.021	0.116 ± 0.006	0.105 ± 0.010	0.094 ± 0.006	0.096 ± 0.002	0.096 ± 0.002
Modulus intercept, a (Pa s^b)						
0	106 ± 19	167.4 ± 52.3	145.6 ± 28	153.1 ± 15	158.3 ± 12.1	146.3 ± 7.2
1	89.5 ± 3.8	137.5 ± 31.1	163.1 ± 31.2	147.6 ± 21.6	171.5 ± 15.8	135.9 ± 12.5
2	116.7 ± 14.1	166 ± 67.1	139.1 ± 7	140.6 ± 6.5	165.3 ± 15.9	129.5 ± 18.5
3	126.8 ± 39.3	149.5 ± 38.1	123.8 ± 9.8	151 ± 7.4	176.6 ± 23.1	151.1 ± 0.9
4	104.1 ± 10.4	131.2 ± 34.8	140.6 ± 17.7	164 ± 6.2	182.2 ± 39.2	149.8 ± 17.2
5	107.2 ± 31.9	142.6 ± 22.7	133.7 ± 5.1	179.2 ± 17.8	172.3 ±23.8	172.3 ± 23.8

With decreased adhesiveness, higher gel strength was expected for 5, 15, and 20 mM NaCl compared to higher NaCl concentrations, however, both adhesiveness and gel strength were lower. This behavior could be explained by the fact that xanthan and curdlan are not oppositely charged and are unlikely to bond, thus being separate solutions while keeping its structure.

Table 5.4. Adhesiveness and gel strength of the xanthan curdlan complex solutions with 5 to 200 mM NaCl over five freeze thaw cycles (FTCs).

	Freeze Thaw Cycles					
	0	1	2	3	4	5
Adhesiveness (|N s|)						
5	0.563±0.006	0.681±0.058	0.755±0.022	0.763±0.023	0.921±0.123	0.916±0.029
15	0.436±0.053	0.434±0.049	0.755±0.048	0.763±0.028	0.921±0.306	0.916±0.053
20	1.285±0.026	1.263±0.183	1.401±0.093	1.508±0.101	1.571±0.095	1.556±0.046
75	1.770±0.155	1.533±0.106	1.750±0.162	1.687±0.049	1.561±0.017	1.677±0.025
100	1.588±0.046	1.520±0.070	1.449±0.034	1.554±0.171	1.507±0.224	1.585±0.060
200	1.619±0.062	1.275±0.037	1.314±0.095	1.265±0.122	1.513±0.104	1.418±0.050
Gel Strength (N)						
5	0.095±0.001	0.098±0.001	0.102±0.002	0.104±0.001	0.107±0.003	0.107±0.001
15	0.104±0.004	0.107±0.005	0.110±0.007	0.110±0.004	0.112±0.002	0.108±0.002
20	0.116±0.001	0.118±0.006	0.122±0.003	0.123±0.001	0.126±0.002	0.127±0.002
75	0.136±0.004	0.132±0.004	0.133±0.004	0.130±0.003	0.128±0.002	0.132±0.002
100	0.132±0.001	0.129±0.003	0.127±0.002	0.130±0.007	0.124±0.002	0.130±0.001
200	0.132±0.001	0.124±0.001	0.123±0.002	0.121±0.003	0.127±0.004	0.124±0.006

The changes in stability of sodium chloride treated samples during temperature ramping were similar to its behavior during frequency sweeps. Temperature ramps of the storage modulus in Figure 5.4 showed some hysteresis upon cooling and minor fluctuations throughout FTCs for all treated samples, exhibiting better heat stability than pH treated samples.

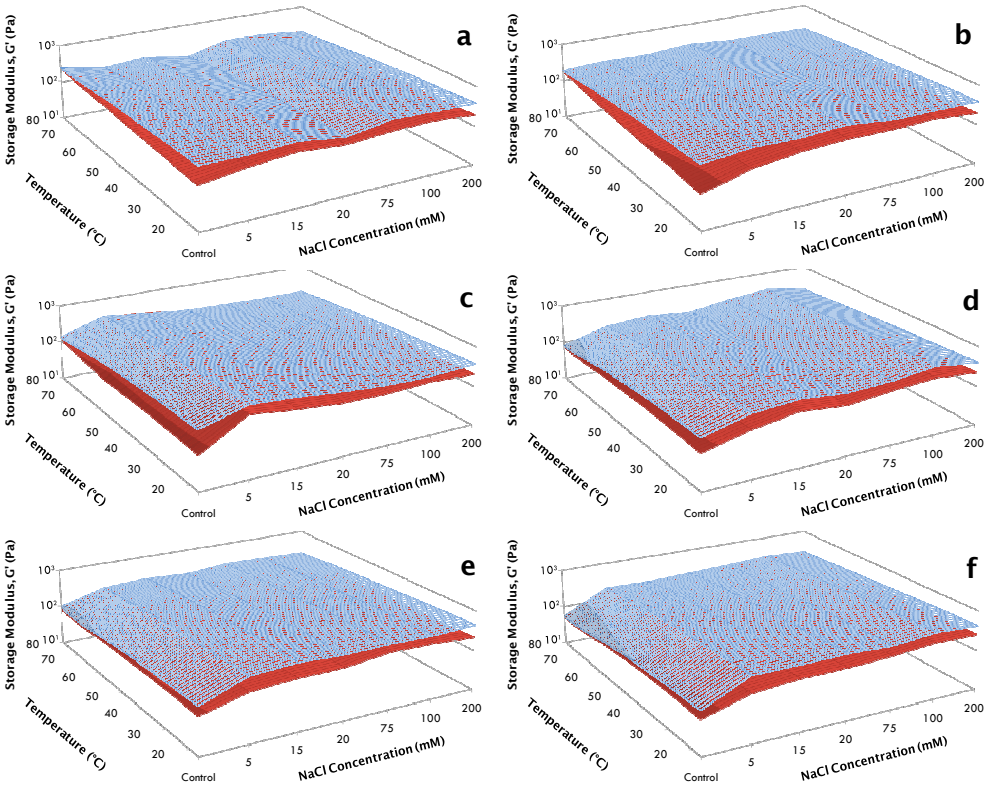

Figure 5.4. Temperature ramps of the storage modulus, G', of 2.0% xanthan curdlan hydrogel complex (XCHC) treated with 5, 15, 20, 75,100, and 200 mM NaCl. Heating ramp, G' (10^1 - 10^2 10^2 - 10^3), and cooling ramp, G'(10^1 - 10^2 10^2 - 10^3), prior to (a), and after the first (b), second (c), third (d), fourth (e), and fifth (f) freeze-thaw cycles.

5.4 Conclusion

Electrostatic interactions between xanthan and respective treatments may have resulted in reduced modulus values during frequency sweeps. Nonetheless, the effects of pH values of 4, 5, 6, 7, and 8 or 75,100, or 200 mM NaCl were similar to each other, where freeze-thaw cycles had little effect on the dynamic modulus, gel strength, and adhesiveness of the samples. Sodium chloride samples were more resistant to temperature ramping over the five FTCs. Despite the reduction in dynamic modulus, the aforementioned treatments show XCHC as a viable candidate in food matrices with like food components due its stability and strong gel behavior.

Chapter 6: Efficacy of the xanthan curdlan hydrogel complex in pumpkin pie

6.1 Introduction

Previous studies have shown how the xanthan curdlan complex is a potential candidate for food matrices through its ability to maintain texture qualities throughout freeze-thaw abuse, while not allowing water to release in an aqueous solution. Furthermore, it has been shown that the complex continues to be resistant to water loss and stable after freeze-thaw abuse when adjusted to pH values from 4 to 8 and sodium chloride concentrations of 75 to 200 mM. However, its efficacy in a food product has yet to be investigated. Thus, pumpkin pie filling was found to be a possible food product to improve, where not only moisture migration from the filling to the crust can occur, but also there is the common problem of the filling cracking once backed which could potentially be a reservoir for bacteria (Kane et al., 1971).

One of three microbial polysaccharides approved by the FDA (21CFR 172.809), curdlan is produced fermentatively by *Agrobacterium biovar 1*. The linear (1→3) β-glucan is insoluble in water, alcohols and most organic solvents, however, show solubility in alkaline solutions (Pederson 1979; McIntosh 2005). Curdlan has been used as a texture modifier for Chinese and Japanese noodles and processed meats for juicier texture (Nakao et al. 1991; Nakao, 1997; Hsu and Chung 2000; Nishinari 2000). Despite its insolubility in water, curdlan can produce both a low-set thermo-reversible and high-set thermo-irreversible gel in aqueous solutions (Harada 1994; Hirashima et al. 1997; Nakao 1997; McIntosh et al. 2005; Gagnon et al. 2007). The high-set thermo-irreversible aqueous gel is created when curdlan heated above 80

°C, where its gel strength is consistent after one freeze-thaw cycle, unlike agar, carrageenan, and konjac (Nakao 1997). Over the pH range of 2-10, curdlan can gel in the presence of sugars, starches, salt and the incorporation of fats and oils (Nakao 1997; McIntosh et al., 2005).

Xanthan gum is another microbial polysaccharide approved by the FDA (21CFR 172.695) produced by *Xanthomonas campestris*. The structure consists of two repeating (1→4)-β-D-glucose units making up the backbone with a trisaccharide side chain consisting of α-D-mannose, β-D-glucuronic acid, and β-D-mannose. It is known that at xanthan gum is unaffected by salt concentrations above approximately 10^{-2} M in the dilute and semi-dilute regime (Rochefort and Middleman 1987; Dolz et. al, 2002) and is stable over a pH range of 1 to 9 (Rao et al., 1998; Hoefler 2004).

By combining curdlan with xanthan, high elasticity is retained, resilience is increased and syneresis is prevented. Moreover, xanthan is known to be an excellent stabilizer of dairy products (Sworn 2000). Therefore, introducing the complex to pumpkin pie could better maintain its quality during freeze-thaw abuse.

6.2 Methods and Materials

Odorless, fine, free-flowing white powder curdlan containing a minimum of 90% β-D-glucan and with a maximum of 10% water was used (Takeda Vitamin & Food USA, Orangeburg, N.Y.). Xanthan (Ticaxan®) was kindly supplied by TIC Gums (Belcamp, Md.). The biopolymer powders were weighed and dry blended before introduced to pumpkin filling.

The pumpkin filling procedure was adapted from Beranbaum (1998) substituting milk for a combination of water, milk solids non-fat, and heavy cream

resulting in the composition of whole milk. Well hydrated, 2.0% aqueous solution of equal amounts of xanthan and curdlan (XCHC) was added in substation for two-thirds portion of the water added in the standard. Pumpkin puree, brown sugar, spices, and salt (Table B.3) where mixed together. Over medium heat, the mixture was brought to a sputtering simmer (~90 °C), stirring constantly. The heat was reduced to low, stirring constantly, for 9 minutes until thick and shiny. The puree mixture was scraped out of the pot and placed into a food processor and processed for 1 minute. The non-fat milk solids (4.84 g) were dissolved in 14.3 g of water then added to the pumpkin puree mixture along with 28.8 g water (control) or XCHC and cream, processing until incorporated. The eggs (50 g) were whisked to achieve the appropriate amount and added slowly, finally adding the vanilla extract.

The mixture, 90 g of pumpkin filling, was then poured into ~45 g pie shells that were pre-baked at 350 °F for 24 minutes with a 40 g weight in 4-3/4" by 3/4" deep circular aluminum baking pans. Pies were baked for 35 min at 350 °F and allowed to cool to room temperature, before refrigerating at 4 °C for 24 hrs and subjecting them to five FTCs.

A TA-XT2i texture analyzer (Texture Technologies, Inc., Scarsdale, NY) was used to measure the gel strength and adhesiveness with a 0.5” dia. acrylic probe attachment. An IC-500 AW-LAB (Novasina, Switzerland) water activity meter was used to measure the water activity of both the crust and pumpkin pie filling prior to FTCs and then after each subsequent FTC. The ColorFlex colorimeter with CIELAB color space (HunterLab, Reston, Va.) was implemented to compare the color of the

original pie filling recipe to the pie filling with the xanthan/curdlan complex before and after baking the filling.

6.3 Results and Discussion

6.3.1 Adhesiveness and Gel Strength

Besides cracking of the filling, adhesiveness can often be a problem in manufacturing operations along with lack of adherence of pie filling to the crust (Kane et al., 1971; Adhikari et al., 2001). Therefore, the adhesiveness of the baked filling was investigated. Adhesiveness results in Table 6.1 showed that the xanthan curdlan hydrogel complex (XCHC) did not contribute additional adhesiveness to the filling, thus, no different than that of the control. Nevertheless, it is clear that there was less deviation between samples for XCHC treated filling. Similarly, the gel strength for the XCHC treated pie filling was not significantly different from the control. The XCHC may not contribute to either adhesiveness or gel strength due the relatively small amount added compared to other texture contributing components such as the pumpkin puree and coagulated milk proteins.

Table 6.1. Adhesiveness and gel strength* of pumpkin pie filling and treated with the xanthan curdlan hydrogel complex (XCHC) over five freeze-thaw cycles (FTCs).

	Adhesiveness (|N s|)		**Gel Strength (N)**	
FTC	Control	XCHC	Control	XCHC
0	25.982 ± 8.690	23.730 ± 1.956	2.325 ± 0.296	2.009 ± 0.21
1	26.292 ± 7.641	24.047 ± 2.551	2.774 ± 0.544	2.200 ± 0.116
2	28.328 ± 10.483	28.703 ± 7.268	2.554 ± 1.11	2.120 ± 0.677
3	27.999 ± 4.053	27.689 ± 3.557	2.449 ± 0.37	2.130 ± 0.579
4	18.597 ± 6.795	26.214 ± 3.016	2.143 ± 0.435	2.325 ± 0.384
5	23.335 ± 4.058	22.561 ± 0.704	2.621 ± 0.427	1.958 ± 0.173

*Values represent the means ± standard deviations (n = 3).

6.3.2 Water Activity and Color

Though subtle, the water activity, a_w, of the pie filling was greater than the crust. The difference in water activity between the filling and crust for both the control and XCHC over FTCs, signifying moisture migration to the crust. Interestingly, the water activity of the pie filling remained the same over FTCs for both the control, Figure 6.1, and XCHC treated samples, Figure 6.2. This phenomenon could be attributed to the continual release of water throughout the filling resulting in separation, where an amount of water is transferred to the crust and an amount remains with the filling allowing its water activity to remain constant. XCHC treated samples proved better at delaying water migration to the crust until after the fourth FTC, whereas the water activity of the control crust increased after the third FTC. Furthermore, once the filling was removed, there was a noticeable difference in the surface attributes of the crusts for the control and XCHC treated pie (Figure B.1). Crust separation was exhibited in the control after three FTCs where it was not seen with the XCHC treated pie and could be attributed to an affinity of the crust to the water rather than a polysaccharide solution in the filling.

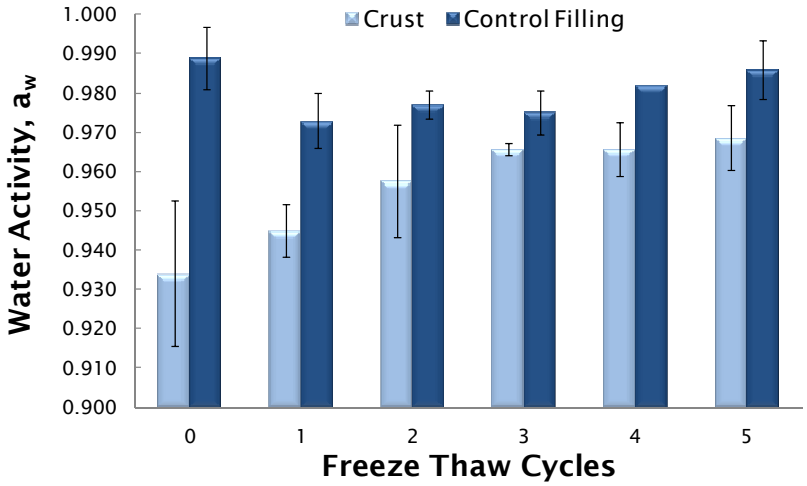

Figure 6.1. Water activity of the crust (■) and filling (■) of control samples over five freeze-thaw cycles (n=3).

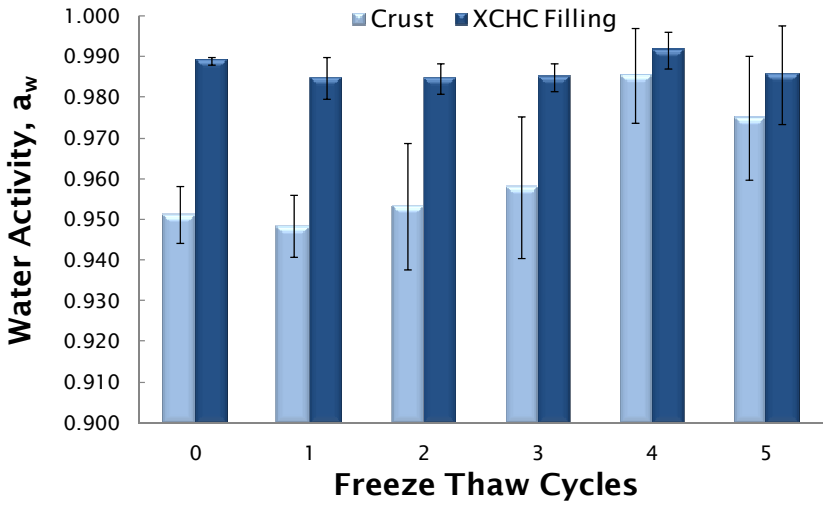

Figure 6.2. Water activity of the crust (■) and filling (■) of the xanthan curdlan hydrogel complex (XCHC) treated samples over five freeze-thaw cycles (n=3).

The color of both the surface of the pie and the filling was measured. From Table 6.2, color values a* and b* were greater for the XCHC treated samples than the control, yielding more red and yellow hues, respectively, translating into a brighter pie surface seen on the right in Figure 6.3. A sensory evaluation regarding appearance

could yield positive results for the treated pie. Generally, FTCs did not affect the surface color of either pie. Inspecting the surfaces of the pies in Figure 6.3, cracking and wrinkles are noticeable on the control pie due to upward expansion of the filling during baking and subsequent contraction upon cooling. However, a smoother surface was found with the XCHC treated pie. The limited amount of cracks and wrinkles could be due to the addition of the complex, where its elastic properties allowed the surface to stretch and contract, maintaining its structure.

Table 6.2. CIELAB values, L*, a*, and b*, for surface and filling of control and xanthan curdlan hydrogel complex (XCHC) treated pumpkin pies over five freeze-thaw cycles (FTCs).

	Surface			Filling		
FTC	L*	a*	b*	L*	a*	b*
Control						
0	40.78 ± 2.86	15.95 ± 0.67	38.41 ± 5.88	43.55 ± 0.92	14.67 ± 0.45	42.61 ± 0.24
1	42.28 ± 2.87	16.46 ± 0.17	38.83 ± 6.01	42.85 ± 1.83	15.27 ± 0.48	42.58 ± 0.87
2	43.70 ± 2.74	15.70 ± 0.33	40.36 ± 6.71	44.48 ± 2.05	14.49 ± 0.51	42.79 ± 1.69
3	43.66 ± 1.64	16.06 ± 0.63	40.39 ± 4.42	43.18 ± 2.08	14.70 ± 0.56	44.50 ± 2.07
4	43.87 ± 1.64	15.96 ± 1.14	40.79 ± 5.70	43.66 ± 1.77	14.41 ± 0.19	43.46 ± 1.03
5	43.66 ± 2.11	16.09 ± 0.80	40.66 ± 6.76	43.24 ± 0.59	14.60 ± 0.17	43.32 ± 0.45
XCHC						
0	42.41 ± 0.30	18.14 ± 0.99	46.46 ± 1.61	42.67 ± 1.34	14.84 ± 0.68	43.46 ± 0.55
1	42.67 ± 0.13	18.03 ± 0.36	45.05 ± 0.92	43.83 ± 1.74	14.76 ± 0.59	43.56 ± 0.58
2	43.01 ± 0.82	17.88 ± 0.34	43.90 ± 0.94	44.41 ± 1.94	14.22 ± 0.31	43.52 ± 0.16
3	43.64 ± 0.88	18.08 ± 0.59	47.25 ± 0.57	42.38 ± 0.87	14.71 ± 0.30	43.01 ± 0.28
4	43.57 ± 0.29	17.99 ± 0.23	45.79 ± 1.34	45.13 ± 0.82	13.91 ± 0.01	43.19 ± 0.17
5	44.37 ± 0.67	17.72 ± 0.19	47.53 ± 0.40	43.45 ± 1.95	14.45 ± 0.34	42.94 ± 1.16

Though the surface was brighter, the color of pie filling under the surface of XCHC treated sample was indistinguishable from the control (Table 6.2). This disparity between the surface and filling could explain the brighter attribute of the XCHC samples. The hydrogel complex could be hindering Maillard browning

reactions between lactose and milk proteins and/or caramelization of sucrose from the brown sugar.

Figure 6.3. Images of the control pumpkin pie surface on the left and XCHC treated pie surface on the right.

6.4 Conclusion

Gel strength, adhesiveness, and pumpkin pie filling color of the XCHC treated pumpkin pie were indistinguishable from the control. However, XCHC limited moisture migration by an additional freeze-thaw cycle compared to the control. Furthermore, the surface was brighter, exhibiting less cracks and wrinkles that could harbor bacteria. XCHC was found to improve certain aspects of pumpkin pie, thus further studies with an increased amount of XCHC could further limit moisture migration from the filling to the crust throughout all freeze-thaw cycles are warranted.

Chapter 7: Conclusions and Recommendations

Curdlan has been shown to yield a gel under specific conditions and retain its gel strength after a freeze-thaw cycle, however, syneresis occurs—an undesirable trait for frozen foods. By combining curdlan with xanthan, syneresis was eliminated while maintaining good texture properties and excellent stability throughout five freeze-thaw cycles. Coupling rheology with non-invasive techniques such as relaxometry, imaging, and microscopy provided clear understanding of the combinations' behavior that leads to its reliance under freeze-thaw abuse. Through NMR relaxometry it was confirmed that water was interacting relatively strongly with the polysaccharides. Wavy layers seen in microscopy explained the ability of the hydrogel complex to achieve higher elasticity than xanthan alone.

Furthermore, the combination was found to be stable when pH values were altered from 4 to 8 and sodium chloride concentrations from 75 to 200 mM, demonstrating the potential to impart its resilience on a range of frozen food products. Due its elasticity and consistent behavior, introduction of the xanthan curdlan hydrogel complex to pumpkin pie has resolved the issue of surface cracking and wrinkling that may harbor bacteria. Moreover, addition of the complex produced a brighter pie surface that could be appealing in sensory evaluations. Finally, products such as ice cream, dough, sauces, and other types of pies could benefit from the texture enhancing and stabilizing ability of the xanthan curdlan hydrogel complex.

To narrow an optimum range of usage for this complex, it is recommended that further studies on the effects of major food components such as whey and casein protein, divalent ions, higher sodium chloride concentrations and pH values should be investigated.

Appendix A: Supplemental Information

A.1 Rheometer Operation and Understanding

Rheology is the science of the deformation and flow of matter referring to the manner which materials respond to stress and strain (Seffe 1996). Rheological properties are an integral part in understanding the effects of food polysaccharides in a food system. The ability to thicken or modify the texture of a food system can be related to the viscosity of the food system and thus rheology can serve as tool in ensure consistency of some stage of food production involving gums. More importantly, rheology can indicate structural behavior. Through small angle oscillatory rheology, gel behavior can be determined. First, the proper rheological geometry must be determined. Curdlan is known to form a high-set gel and therefore a parallel plate can be utilized. However, to reduce slippage a truncated cone and plate apparatus was used for the experiments in this work (Figure A.1). The sample is placed on the plate where a particular geometry is positioned atop the sample creating fixed gap specific to that geometry.

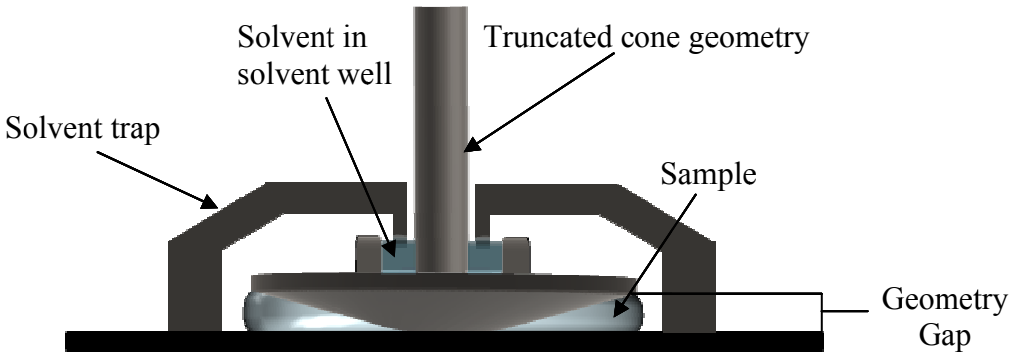

Figure A.1. Cross sectional view of cone and plate rheological apparatus.

The geometry, here a truncated cone, oscillates about an angle specified for that geometry and applies a strain, in turn, yielding a stress, Figure A.2. The difference in the stress and strain curves at their amplitudes, σ_o and γ_o, respectively, yields the phase lag (δ).

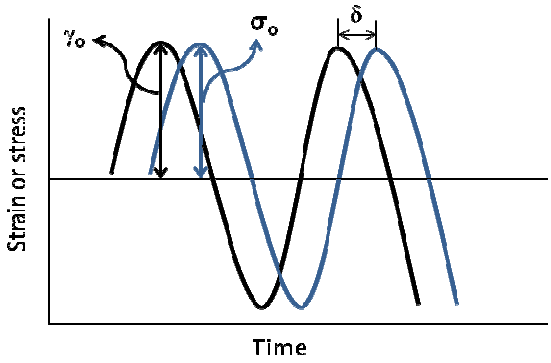

Figure A.2. Strain input (—) and stress output (—) as a function of time, where the difference in the stress and strain curves is the phase lag, δ. Where the strain amplitude is γ_o, and the stress amplitude is σ_o.

These three parameters are used to acquire the dynamic moduli, storage (G') and loss (G") modulus, and assists in determining the structural behavior of the sample in the following manner:

$$G' = \left(\frac{\sigma_o}{\gamma_o}\right)\cos(\delta) \quad [1]$$

$$G'' = \left(\frac{\sigma_o}{\gamma_o}\right)\sin(\delta) \quad [2]$$

The storage modulus, G', represents the elastic or solid like behavior and the loss modulus, G", represents the viscous or more liquid like behavior. Viscoelastic materials consist of both viscous and elastic behavior. In order to yield meaningful information, the amount of strain applied to the sample should be determined by a strain sweep and must be within the linear viscoelastic range (LNR). The sweep is

increased from 0.01% strain to 50% strain, depending on the geometry, where the dynamic modulus exhibits independence of strain at low strains and abruptly declines quickly at some % strain. The percent strain approximately 75% of the strain value immediately prior to the modulus decline is used.

Once the % strain is found, oscillatory experiments, including a frequency sweep and temperature ramps, can be performed. Depending upon the response of the moduli, texture properties can be interpreted. A frequency sweep entails decreasing the angular frequency and measuring the corresponding moduli. Viscous behavior is exhibited when G" values are greater than G' values with an increasing slope over the entire frequency range, Figure A.3a. Figure A.3b shows elastic behavior, exhibiting greater values of G' than G" with angular frequency independence indicating a fully cured three-dimensional network. When G' is predominating G" the entire angular frequency range with positive slopes, a 'gel-like' behavior is exhibited.

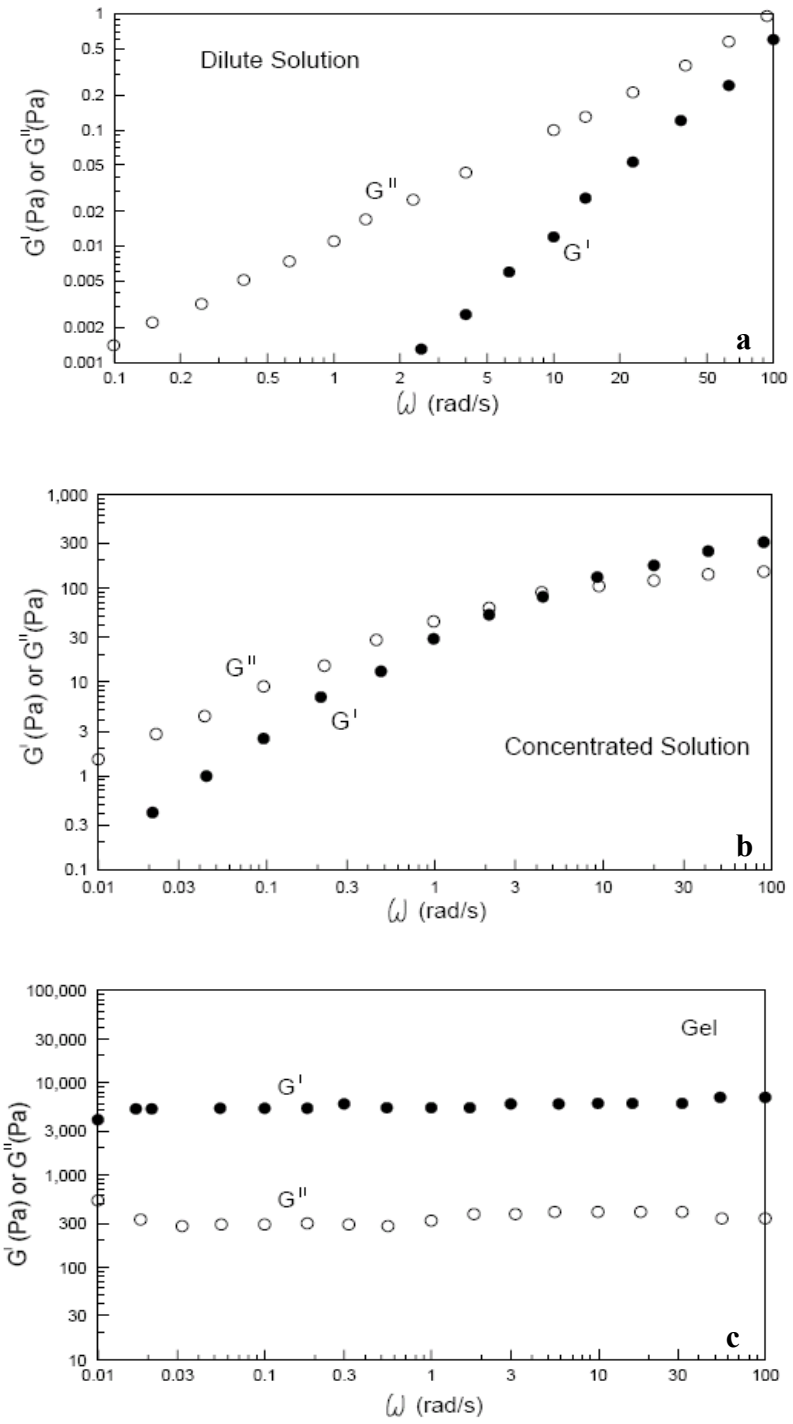

Figure A.3. Typical frequency sweeps of a dilute solution made from 5% dextrin (a), concentrated solution made from 5% lambda carrageen (b), and a gel made from 1% agar (c) (Ross-Murphy, 1988).

Xanthan, however, exhibited weak 'gel-like' behavior with low storage modulus values (highest values below 100Pa) and could utilize a more sensitive rheometer apparatus called a concentric cylinder where the bob oscillates (Searle configuration) producing strains as the truncated cone does, Figure A.4. This apparatus ensures less slippage of the geometry and minimal heat distribution between the cup and bob, thus providing a more accurate depiction of the textural behavior of a less viscous substance such as xanthan gum.

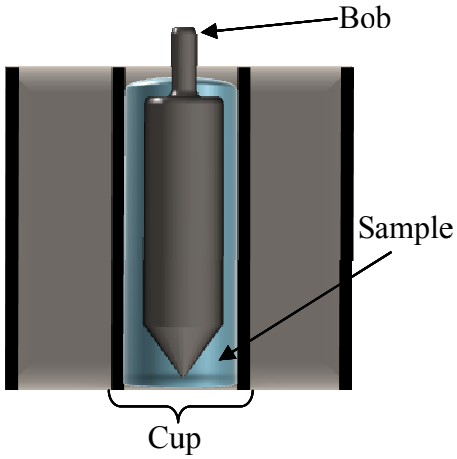

Figure A.4. Cross sectional view of concentric cylinder, or cup and bob, rheometer apparatus.

As previously mentioned, a temperature ramp could also be performed and help understand the samples behavior during temperature changes. This experiment simply involves increasing temperature at some given rate and at some specific angular frequency, measuring the storage and loss moduli. In this experiment, the solvent trap shown in Figure A.1 is vital. The solvent is placed in a well directly above the geometry and enclosed to ensure the solvent does not evaporate during temperature ramping.

A.2 Texture Analyzer

The texture analyzer performs experiments by lowering and raising probe into the sample and measuring the force acting on the probe. In the current dissertation, the 0.5” dia. probe was lowered 20mm into the sample at a rate of 0.5mm/s. The force yielded at 20mm, this was also the maximum, was considered the gel strength of the gums. The probe was then raised at the same rate until it was out of the solution. As the probe was being raised, the force was negative. The absolute value of the area above this negative curve was considered the adhesiveness. Figure A.5 shows an example of a typical gel strength and adhesiveness output.

Figure A.5. Typical texture analyzer output for the samples in the current work, where the maximum peak is the gel strength and the blue shaded area is the adhesiveness of the gel. A 0.5” dia. plastic probe was used with a lowering and raising rate of 0.5 mm/s 20 mm into the sample.

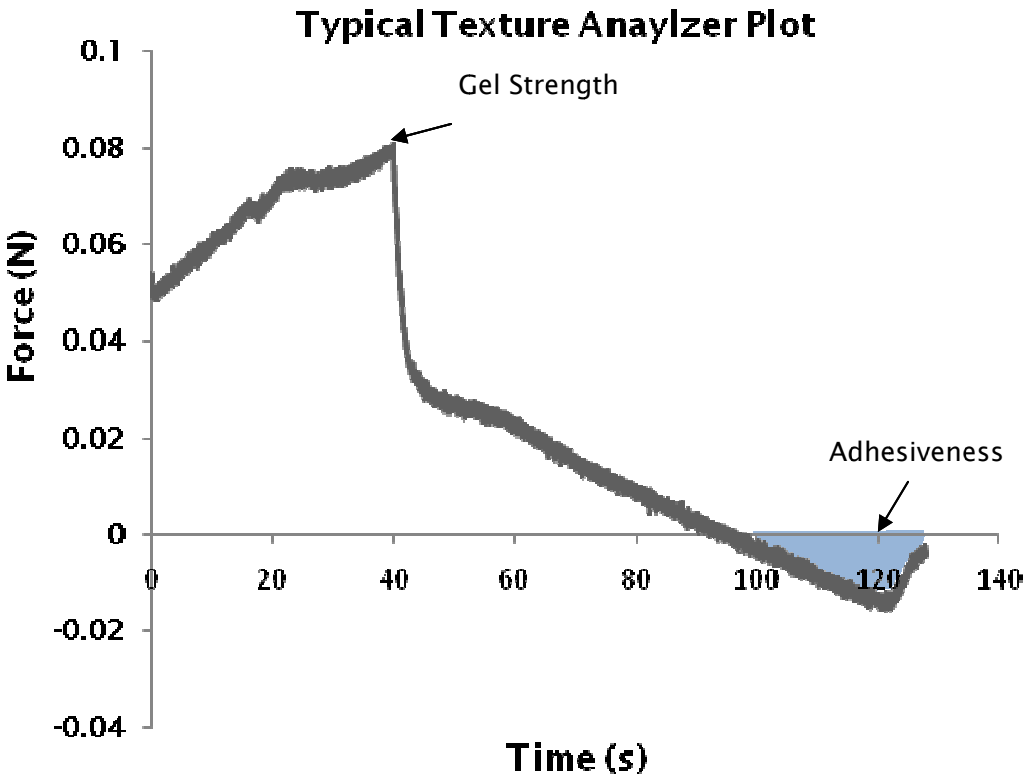

A.3 Ratio Justification

Preliminary studies of various ratios of xanthan to curdlan were performed. Lower modulus values were seen with increased xanthan (while holding the total gum percent at 2%), but lower slopes compared with when more curdlan was added (Table A.1). However, sedimentation of curdlan was observed upon visual inspection, where the initial sample preparation was used (Section 3.2.1) with the samples not under reflux. Under reflux, a stronger gel was produced for curdlan alone, it was thought that adding less than an equal amount of xanthan would eliminate syneresis similar to the 1:1 ratio used throughout the studies, and keep the same rheological properties as curdlan. However, a 1:4 ratio of xanthan to curdlan showed gel particulates in magnetic resonance images in Figure A.6, and a third proton pool in nuclear magnetic resonance relaxometry (Table A.2.), indicating syneresis that was seen during visual observations. Therefore, a ratio of 1:1 underwent further studies.

Table A.1. Comparison of the intercept, a, and slope, b, of the storage modulus ($G' = a\omega^b$) over various ratios of xanthan to curdlan (X:C).

X:C	*a* (Pa s^b)	*b*
1:3	322	0.1465
1:1	56	0.1185
2:1	55	0.1146
5:1	31	0.1539

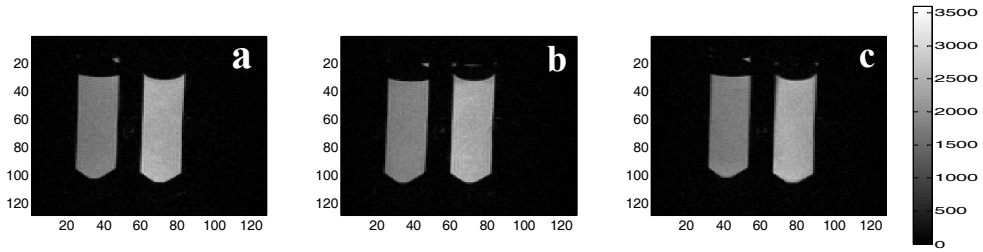

Figure A.6. Representative magnetic resonance images (MRI) of 4:1 xanthan to curdlan prior to freezing (a) after one freeze thaw cycle (b) and after the fifth freeze thaw cycle (c). The scale on the right gives the relationship between signal intensity and grayscale for the images. Axes in the images denote the voxel numbers.

Table A.2. Spin-spin relaxation time[a],T_2 , and relative area of 2.0% xanthan curdlan hydrogel complex (XCHC) with a ration of 1:4 xanthan to curdlan subjected to five freeze-thaw cycles (FTCs) from nuclear magnetic resonance relaxometry.

Xanthan:Curdlan 1:4						
	1st Proton Pool		2nd Proton Pool		3rd Proton Pool	
FTC	T_2 (ms)	Relative Area (%)	T_2 (ms)	Relative Area (%)	T_2 (ms)	Relative Area (%)
0	-	-	248±14.68	21.5±3.58	849±0.00	77.35±3.20
1	120±17.47	6.33±1.71	328±56.29	15.96±1.73	881±36.89	78.33±2.18
5	28±2.99	1.36±0.08	272±18.56	17.52±4.87	865±31.95	80.64±4.34

[a]Each value is the mean ± SD, n=3.

Appendix B: Supplemental Data

Table B.1. The measured pH of HCl or NaOH treated XCHC samples over five freeze-thaw cycles.

	Freeze Thaw Cycles					
pH	0[†]	1	2	3	4	5
2	1.95±0.03	1.90±0.01	1.92±0.02	1.90±0.03	1.90±0.02	1.90±0.03
3	2.88±0.05	2.78±0.03	2.84±0.06	2.75±0.09	2.79±0.03	2.80±0.16
4	3.79±0.21	3.84±0.23	3.83±0.23	3.83±0.23	3.82±0.23	3.80±0.20
5	4.81±0.14	4.74±0.13	4.77±0.12	4.77±0.18	4.79±0.19	4.79±0.19
6	5.63±0.16	5.65±0.10	5.67±0.08	5.55±0.21	5.63±0.07	5.50±0.12
7	6.28±0.18	6.23±0.23	6.28±0.14	6.32±0.18	6.30±0.26	6.16±0.38
8	6.65±0.09	6.61±0.08	6.60±0.10	6.57±0.11	6.64±0.08	6.59±0.21

[†]Values of pH do not match prior to FTCs due to the 24 hr refrigeration period allowing pH to drop. Each sample was initially adjusted to the corresponding pH.

Table B.2. Syneresis of samples treated to achieve pH = 2.

	Syneresis (%)
FTCs	
0	-
1	-
2	2.92
3	24.64
4	32.50
5	41.19

Table B.2. The measured pH of NaCl treated XCHC samples over five freeze-thaw cycles.

	Freeze Thaw Cycles					
NaCl (mM)	0	1	2	3	4	5
5	5.51±0.02	5.51±0.03	5.49±0.01	5.50±0.03	5.50±0.01	5.51±0.00
15	5.26±0.02	5.27±0.03	5.28±0.03	5.31±0.03	5.24±0.03	5.23±0.03
20	5.25±0.01	5.38±0.02	5.33±0.02	5.34±0.05	5.30±0.07	5.31±0.03
75	5.17±0.01	5.16±0.02	5.13±0.03	5.15±0.06	5.12±0.03	5.20±0.05
100	5.13±0.02	5.10±0.02	5.12±0.02	5.12±0.02	5.08±0.01	5.09±0.02
200	4.89±0.08	4.91±0.04	4.98±0.06	4.99±0.02	4.98±0.01	4.95±0.01

Table B.3. Pumpkin pie filling ingredients

Ingredient	Weight
Unsweetened pumpkin puree	141.7 g
Light brown sugar	54.3 g
Ground ginger	0.333 oz
Ground cinnamon	0.25 oz
Salt	0.083 oz
Water	28.8 g
Milk solids non-fat	4.84 g
Heavy cream	56 g
Fresh eggs	50 g
Vanilla extract	0.083 oz

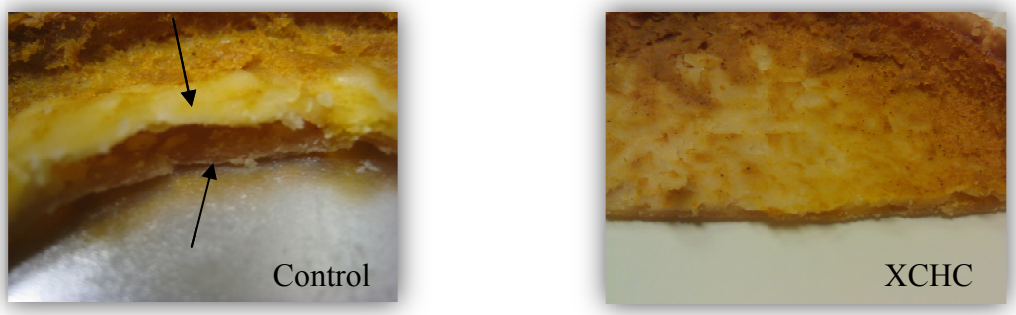

Figure B.1. Crust separation can be seen in the control (on the left) after three freeze-thaw cycles, whereas the crust of the XCHC treated pie filling (on the right) does not show separation after five freeze thaw cycles.

Table B.4. Water activity of the crust and pumpkin pie filling for untreated pumpkin pie (control) and xanthan curdlan hydrogel complex (XCHC) treated pie fillings.

Water Activity		
	Control	
FTC	Crust	Filling
0	0.934±0.019	0.989±0.008
1	0.945±0.007	0.973±0.007
2	0.958±0.014	0.977±0.004
3	0.966±0.002	0.975±0.006
4	0.966±0.007	0.982±0.000
5	0.969±0.008	0.986±0.008
	XCHC	
FTC	Crust	Filling
0	0.951±0.007	0.989±0.001
1	0.948±0.008	0.985±0.005
2	0.953±0.016	0.985±0.004
3	0.958±0.017	0.985±0.003
4	0.985±0.012	0.992±0.005
5	0.975±0.015	0.986±0.012

Appendix C: Statistical Analysis

Tukey's HSD (Honestly Significant Difference) was employed for statistical analysis in order to find significant differences over FTCs. Tukey's HSD requires the calculation of the test statistic *T*, utilizing the equation below:

$$T = q_{\alpha}\sqrt{\frac{s^2}{r}} \quad [1]$$

Where q_{α} is the value obtained from F distribution tables depending on the number of samples with $\alpha = 0.01$, s^2 is the means squared error from analysis of variance, and *r* is the number of replications. The number of replications was the same for all tests at 3. To ascertain whether or not there is a significant difference, the difference between two means must be greater than *T*. Here, the means of the storage modulus at each angular frequency was obtained, thus the following equation was used

$$zSD_x - vSD_y = T - (|z\overline{G'}_x - v\overline{G'}_y|) \quad [2]$$

where *SD* is significant difference between the mean of the storage modulus, $\overline{G'}$, at freeze-thaw cycle *x* or y ($x \neq y$), where *z* and *v* ($z \neq v$) corresponds to pH or NaCl concentrations when applicable. The shaded values in the following table indicate there was a significant difference between the means at its respective angular frequency, ω. The following commands were used to yield necessary information to perform Tukey's HSD using SAS v. 9.2.

```
data Xanthan;
        input FTC $ w @;
        do i=1 to 3;
                input G @;
                output;
        end;
        cards;
run;

proc GLM data=Xanthan;
        class FTC w;
        model G= FTC w FTC*w;
        means FTC FTC*w/tukey;
run;
```

where FTC is freeze-thaw cycle, w is the angular frequency, and G is the storage modulus.

Table C.1. Average storage modulus $(\bar{G}')$ for 2.0% aqueous curdlan gum solutions over 5 FTCs (n=3).

Storage Modules (Pa) Mean for Curdlan						
	Freeze Thaw Cycles					
ω (rad/s)	**0**	**1**	**2**	**3**	**4**	**5**
0.02	1990.0	2304.7	3274.7	2503.0	3846.0	2918.0
0.03	1983.7	2290.0	3243.3	2483.0	3801.3	2892.7
0.03	1979.0	2279.7	3214.0	2466.0	3766.7	2868.3
0.04	1974.7	2269.7	3188.0	2450.3	3732.3	2847.0
0.05	1973.3	2262.3	3166.3	2437.7	3710.7	2828.0
0.06	1974.7	2258.0	3149.7	2425.7	3695.3	2814.7
0.08	1978.3	2258.7	3139.0	2421.0	3688.3	2804.7
0.10	1986.3	2263.0	3135.3	2422.0	3688.0	2800.3
0.13	1997.3	2272.7	3138.0	2428.3	3703.7	2803.3
0.16	2012.3	2286.3	3147.0	2439.7	3724.7	2814.7
0.20	2031.0	2305.0	3164.3	2456.7	3756.3	2833.3
0.25	2053.3	2329.3	3191.7	2479.3	3793.3	2856.7
0.32	2080.3	2358.0	3228.0	2507.3	3839.0	2886.0
0.40	2112.7	2392.0	3269.3	2541.3	3890.7	2920.0
0.50	2147.0	2428.3	3315.7	2577.7	3952.7	2961.7
0.63	2185.0	2468.3	3368.7	2620.3	4019.0	3007.7
0.79	2224.3	2511.0	3425.3	2664.0	4089.7	3059.0
1.00	2266.3	2556.0	3484.3	2712.7	4161.7	3112.3
1.26	2308.7	2601.3	3545.3	2761.0	4237.0	3166.3
1.59	2351.0	2646.7	3606.7	2809.7	4310.3	3219.7
2.00	2394.3	2692.3	3667.7	2859.3	4384.7	3275.3
2.51	2437.7	2738.3	3730.7	2909.7	4460.7	3331.0
3.16	2483.0	2785.7	3793.7	2960.7	4538.0	3389.0
3.98	2527.0	2831.3	3856.3	3011.3	4613.0	3444.3
5.01	2570.7	2877.3	3918.0	3061.7	4689.0	3500.3
6.31	2613.7	2922.0	3979.0	3111.7	4764.7	3555.0
7.94	2656.7	2966.0	4039.3	3161.7	4839.7	3610.3
10.00	2699.3	3009.3	4099.0	3210.7	4914.3	3663.3
12.59	2741.0	3052.3	4157.7	3260.7	4988.3	3716.0
15.85	2783.0	3094.7	4215.3	3310.0	5061.7	3767.3
19.95	2824.7	3135.7	4271.7	3359.0	5134.0	3817.7
25.12	2865.7	3175.7	4326.0	3407.7	5206.0	3867.0
31.62	2905.7	3215.0	4379.7	3455.3	5276.3	3914.7
39.81	2944.7	3252.7	4430.3	3502.7	5345.3	3959.7
50.12	2983.0	3288.7	4479.7	3549.3	5413.7	4003.0
63.10	3019.3	3322.0	4525.3	3594.7	5480.0	4042.7
79.43	3055.7	3353.7	4568.3	3638.7	5543.3	4079.3
100.00	3096.0	3389.7	4619.7	3691.3	5614.3	4123.0

Table C.2. Average storage modulus $(\bar{G}')$ for 2.0% aqueous xanthan gum solutions over 5 FTCs (n=3).

Storage Modules (Pa) Mean for Xanthan						
	Freeze Thaw Cycles					
ω (rad/s)	**0**	**1**	**2**	**3**	**4**	**5**
0.02	60.7	70.5	96.2	99.9	128.9	122.3
0.03	62.0	71.4	97.4	100.9	130.9	123.8
0.03	63.6	72.8	99.3	102.9	133.6	126.1
0.04	65.6	74.6	101.9	105.3	136.8	128.9
0.05	67.9	76.7	104.7	108.4	140.7	132.3
0.06	70.4	79.0	108.1	111.9	144.8	136.2
0.08	73.3	81.9	111.8	115.8	149.3	140.5
0.10	76.3	84.9	115.9	119.9	154.2	144.9
0.13	79.6	88.2	120.2	124.3	159.4	149.8
0.16	83.2	91.8	124.8	129.0	164.9	155.1
0.20	87.0	95.6	129.6	133.9	170.7	160.6
0.25	91.2	99.6	134.6	139.2	176.9	166.5
0.32	95.4	103.7	140.0	144.8	183.3	172.7
0.40	100.0	108.2	145.3	150.5	190.0	179.2
0.50	104.8	112.8	151.1	156.7	197.2	186.0
0.63	109.7	117.7	157.1	163.0	204.6	193.1
0.79	115.1	122.8	163.4	169.6	212.3	200.5
1.00	120.6	128.2	169.8	176.4	220.4	208.1
1.26	126.3	133.7	176.4	183.5	228.5	215.9
1.59	132.2	139.4	183.3	190.8	237.1	224.1
2.00	138.4	145.4	190.4	198.3	245.8	232.4
2.51	144.8	151.6	197.6	206.2	254.8	241.0
3.16	151.5	158.0	205.3	214.2	264.1	250.0
3.98	158.3	164.6	213.1	222.5	273.7	259.2
5.01	165.5	171.5	221.3	231.2	283.7	268.8
6.31	173.1	178.8	229.9	240.3	294.1	278.7
7.94	181.0	186.3	238.8	249.6	304.9	289.0
10.00	189.4	194.3	248.1	259.7	316.2	299.9
12.59	198.4	202.7	258.2	270.3	328.2	311.3
15.85	207.8	211.8	268.9	281.4	341.0	323.6
19.95	218.3	221.7	280.5	293.6	354.7	336.8
25.12	229.8	232.6	293.2	307.0	369.7	351.3
31.62	242.8	244.7	307.6	322.1	386.3	367.2
39.81	257.8	258.7	324.0	339.3	405.3	385.5
50.12	275.6	275.4	343.5	359.4	427.2	406.8
63.10	297.5	295.6	367.2	383.9	453.5	432.5
79.43	325.2	321.1	396.9	414.7	486.0	464.5
100.00	361.5	354.5	435.6	454.5	527.9	505.7

Table C.3. Average storage modulus $(\bar{G}')$ for 2.0% aqueous xanthan curdlan hydrogel complex (XCHC) gum solutions over 5 FTCs (n=3).

Storage Modules (Pa) Mean for XCHC						
	Freeze Thaw Cycles					
ω (rad/s)	**0**	**1**	**2**	**3**	**4**	**5**
0.02	849.0	643.5	674.2	627.9	710.0	602.3
0.03	852.3	651.2	698.4	648.7	720.5	611.0
0.03	902.2	689.7	714.2	735.8	715.9	626.8
0.04	920.2	706.0	733.2	822.3	730.3	645.7
0.05	951.9	722.6	749.0	837.7	747.9	658.6
0.06	975.7	745.1	766.3	1119.9	772.1	676.3
0.08	996.2	761.7	787.3	1032.1	794.2	700.4
0.10	1027.2	782.5	812.1	1096.3	814.3	724.6
0.13	1050.7	804.0	835.5	915.4	838.9	743.3
0.16	1071.0	831.5	859.0	927.8	862.4	766.5
0.20	1095.7	857.8	884.6	919.5	888.8	792.7
0.25	1116.3	881.7	909.9	941.2	913.5	815.6
0.32	1142.7	913.0	936.6	949.2	939.8	840.6
0.40	1169.7	936.3	961.7	976.7	965.4	864.9
0.50	1203.3	959.8	986.7	1014.0	990.7	889.5
0.63	1235.0	990.8	1013.5	1021.6	1019.3	912.2
0.79	1269.3	1014.9	1042.5	1049.6	1046.3	937.6
1.00	1305.3	1042.7	1067.9	1073.4	1071.3	964.7
1.26	1338.0	1070.4	1094.7	1094.8	1100.7	990.0
1.59	1371.0	1097.3	1121.7	1129.0	1128.7	1015.3
2.00	1405.0	1124.2	1149.7	1160.1	1157.0	1042.4
2.51	1439.0	1150.7	1176.3	1177.7	1185.7	1069.7
3.16	1474.0	1179.3	1203.0	1206.3	1214.0	1096.0
3.98	1509.7	1206.7	1230.0	1227.3	1243.0	1122.3
5.01	1544.7	1232.0	1257.3	1258.3	1270.7	1150.3
6.31	1580.7	1259.3	1284.3	1286.7	1299.3	1177.3
7.94	1614.3	1285.0	1311.0	1311.3	1329.0	1205.7
10.00	1648.0	1318.3	1336.3	1334.0	1360.3	1232.0
12.59	1678.0	1347.0	1366.3	1366.3	1389.0	1261.3
15.85	1721.3	1375.0	1395.7	1397.0	1420.0	1290.0
19.95	1754.0	1406.3	1424.3	1428.7	1452.0	1321.0
25.12	1794.3	1437.3	1454.3	1457.0	1483.7	1351.3
31.62	1837.7	1470.3	1487.3	1492.7	1519.3	1387.0
39.81	1876.7	1504.0	1521.3	1542.0	1555.7	1422.3
50.12	1923.3	1540.7	1557.0	1575.7	1594.7	1462.7
63.10	1972.0	1582.0	1597.7	1606.7	1638.3	1505.3
79.43	2027.0	1630.0	1643.0	1669.7	1686.3	1554.7
100.00	2088.7	1685.3	1697.7	454.5	1744.7	1613.0

Table C.4. Average storage modulus $(\bar{G}')$ for 2.0% aqueous xanthan curdlan hydrogel complex (XCHC) gum solutions at pH = 2 over 5 FTCs (n=3).

Storage Modules (Pa) Mean for XCHC at pH = 2						
	Freeze Thaw Cycles					
ω (rad/s)	**0**	**1**	**2**	**3**	**4**	**5**
0.02	323.9	359.4	392.9	435.0	962.8	1566.7
0.03	331.5	363.9	399.2	440.9	968.0	1578.7
0.03	341.9	368.9	406.0	448.7	974.7	1592.3
0.04	351.9	374.7	411.7	458.6	983.2	1610.0
0.05	361.0	380.1	417.8	467.5	995.0	1629.0
0.06	368.8	386.5	425.8	476.7	1010.0	1651.0
0.08	376.7	393.2	433.9	486.0	1027.7	1675.3
0.10	384.4	400.4	442.8	496.0	1046.6	1703.0
0.13	393.0	408.1	452.7	506.8	1068.7	1736.7
0.16	402.7	417.2	463.9	518.3	1093.0	1774.0
0.20	412.9	427.2	475.2	530.5	1120.7	1815.7
0.25	423.6	437.9	487.9	545.0	1150.4	1862.0
0.32	433.6	449.6	501.6	560.2	1183.9	1912.7
0.40	446.5	462.3	516.5	576.6	1220.9	1968.7
0.50	459.1	475.9	532.6	594.0	1258.3	2025.7
0.63	472.9	490.5	549.8	612.4	1299.3	2088.0
0.79	487.5	506.4	567.8	631.7	1342.0	2154.0
1.00	502.7	522.8	586.7	652.0	1386.3	2222.0
1.26	518.7	539.8	606.1	672.9	1430.3	2291.0
1.59	535.1	557.2	625.2	694.2	1475.7	2361.0
2.00	552.2	575.3	644.4	715.2	1520.3	2431.7
2.51	570.0	593.5	664.6	736.3	1565.3	2502.7
3.16	588.3	612.3	684.4	757.6	1610.7	2574.0
3.98	606.6	630.6	704.5	778.6	1654.0	2643.7
5.01	625.2	649.8	724.2	799.6	1697.7	2713.7
6.31	643.9	668.4	743.8	820.4	1741.3	2782.7
7.94	662.9	687.3	763.3	840.9	1783.7	2850.0
10.00	681.9	705.9	782.5	861.3	1825.3	2916.7
12.59	700.9	724.7	801.6	881.8	1866.0	2981.7
15.85	720.0	743.4	820.7	902.1	1906.3	3045.7
19.95	739.1	762.0	840.0	922.5	1945.7	3107.7
25.12	758.5	780.5	859.0	942.7	1984.3	3168.7
31.62	777.8	799.7	877.6	962.8	2022.0	3227.0
39.81	797.3	818.3	896.5	982.8	2059.0	3284.3
50.12	816.8	837.1	915.7	1002.7	2095.3	3340.0
63.10	836.5	855.9	934.8	1022.5	2131.3	3393.0
79.43	856.8	875.3	953.8	1042.3	2167.0	3446.3
100.00	878.4	896.0	976.5	1064.7	2209.7	3504.0

Table C.5. Average storage modulus $(\bar{G}')$ for 2.0% aqueous xanthan curdlan hydrogel complex (XCHC) gum solutions at pH = 3 over 5 FTCs (n=3).

Storage Modules (Pa) Mean for XCHC at pH = 3						
	Freeze Thaw Cycles					
ω (rad/s)	**0**	**1**	**2**	**3**	**4**	**5**
0.02	134.2	106.0	87.8	92.0	91.5	91.8
0.03	136.4	108.3	89.5	91.7	93.0	92.0
0.03	139.1	110.3	90.4	92.5	95.1	93.2
0.04	142.4	112.6	93.4	93.8	97.0	94.7
0.05	145.6	114.3	95.5	95.8	99.3	96.9
0.06	149.3	118.2	97.7	98.0	101.7	99.2
0.08	153.5	121.5	99.8	100.7	104.4	102.0
0.10	157.9	124.8	101.5	103.5	107.4	104.7
0.13	162.8	128.3	106.4	106.5	110.5	107.8
0.16	167.8	132.3	109.6	109.8	113.7	111.2
0.20	173.0	136.3	112.6	113.5	117.5	114.7
0.25	179.0	140.6	117.5	117.3	121.3	118.5
0.32	184.8	145.2	121.4	121.2	125.3	122.5
0.40	190.8	149.9	125.7	125.2	129.3	126.5
0.50	196.7	154.8	130.0	129.4	133.7	130.7
0.63	203.1	159.7	134.3	133.7	138.2	135.0
0.79	209.2	164.9	138.6	138.0	142.6	139.5
1.00	215.8	170.0	143.3	142.4	147.1	144.0
1.26	222.2	175.3	147.8	146.9	151.8	148.5
1.59	228.8	180.5	152.3	151.3	156.3	152.9
2.00	235.3	185.9	156.6	155.7	160.8	157.6
2.51	242.0	191.2	161.5	160.6	165.8	162.2
3.16	248.6	196.6	165.7	165.3	170.5	166.8
3.98	255.2	202.0	170.1	169.8	175.2	171.4
5.01	261.8	207.4	176.4	174.5	180.0	175.9
6.31	268.5	212.7	181.1	179.0	184.6	180.8
7.94	275.2	218.1	185.8	183.7	189.4	185.5
10.00	281.9	223.5	190.6	188.4	194.1	190.2
12.59	288.7	228.9	195.3	193.0	198.8	194.8
15.85	295.4	234.3	200.3	197.8	203.2	199.6
19.95	302.1	239.8	205.2	202.5	208.9	204.4
25.12	309.0	245.3	210.1	207.3	213.8	209.3
31.62	315.9	250.8	215.0	212.0	218.7	214.1
39.81	322.7	256.3	219.8	216.8	223.6	218.8
50.12	329.6	261.7	224.8	221.6	228.5	224.0
63.10	336.4	267.1	229.7	226.4	233.5	228.9
79.43	343.4	272.5	234.7	231.2	238.3	233.9
100.00	351.0	278.4	240.5	236.4	243.4	239.1

Table C.6. Average storage modulus $(\bar{G}')$ for 2.0% aqueous xanthan curdlan hydrogel complex (XCHC) gum solutions at pH = 4 over 5 FTCs (n=3).

Storage Modules (Pa) Mean for XCHC at pH = 4						
	Freeze Thaw Cycles					
ω (rad/s)	**0**	**1**	**2**	**3**	**4**	**5**
0.02	86.1	50.6	46.8	69.8	65.3	63.2
0.03	89.9	49.7	46.8	67.9	60.7	62.4
0.03	90.0	49.6	47.3	66.9	57.3	62.4
0.04	90.6	50.0	48.1	66.6	55.3	62.5
0.05	91.5	50.5	48.9	67.2	55.1	63.3
0.06	92.8	51.2	50.1	68.1	55.4	64.1
0.08	94.3	52.3	51.4	69.6	56.2	65.9
0.10	96.0	53.5	52.8	71.2	57.2	67.4
0.13	98.1	54.9	54.3	73.1	58.4	69.0
0.16	100.8	56.5	56.0	75.3	60.0	71.2
0.20	103.6	58.1	57.9	77.6	61.8	73.5
0.25	106.8	60.1	59.8	80.2	63.7	75.8
0.32	110.2	62.3	62.0	82.9	65.8	78.4
0.40	113.7	64.5	64.2	85.9	68.0	81.0
0.50	117.5	66.8	66.7	89.1	70.5	84.0
0.63	121.6	69.3	69.2	92.2	73.0	86.9
0.79	125.7	71.8	71.7	95.5	75.7	90.1
1.00	130.0	74.5	74.5	99.0	78.4	93.4
1.26	134.3	77.3	77.3	102.7	81.3	96.8
1.59	138.7	80.0	80.2	106.4	84.1	100.2
2.00	143.2	83.1	83.2	110.1	87.1	103.7
2.51	147.8	86.1	86.3	113.9	90.2	107.3
3.16	152.6	89.2	89.4	117.9	93.4	111.1
3.98	157.4	92.3	92.5	122.0	96.6	114.9
5.01	162.3	95.5	95.8	126.0	99.9	118.8
6.31	167.3	98.8	99.2	130.2	103.3	122.6
7.94	172.3	102.2	102.7	134.4	106.7	126.6
10.00	177.4	105.5	106.2	138.8	110.2	130.7
12.59	182.6	109.1	109.7	143.1	113.7	134.8
15.85	187.8	112.6	113.4	147.5	117.3	139.1
19.95	193.1	116.2	117.1	152.0	121.0	143.3
25.12	198.5	119.9	120.8	156.6	124.7	147.6
31.62	204.0	123.7	124.8	161.3	128.5	152.1
39.81	209.6	127.5	128.7	165.9	132.4	156.6
50.12	215.3	131.3	132.7	170.6	136.3	161.2
63.10	221.3	135.2	136.8	175.4	140.3	165.7
79.43	227.3	139.1	141.1	180.2	144.2	170.4
100.00	233.8	143.2	145.6	185.1	148.4	175.3

Table C.7. Average storage modulus $(\bar{G}')$ for 2.0% aqueous xanthan curdlan hydrogel complex (XCHC) gum solutions at pH = 5 over 5 FTCs (n=3).

Storage Modules (Pa) Mean for XCHC at pH = 5						
	Freeze Thaw Cycles					
ω (rad/s)	**0**	**1**	**2**	**3**	**4**	**5**
0.02	51.7	51.7	47.4	61.2	50.1	50.4
0.03	54.0	52.0	48.0	62.1	50.5	50.4
0.03	56.4	52.6	48.7	63.0	51.1	50.8
0.04	58.6	53.5	49.6	64.1	51.9	51.4
0.05	60.5	54.5	50.6	65.2	52.7	52.1
0.06	62.9	55.5	51.7	66.4	53.8	53.0
0.08	64.7	56.7	53.0	67.7	55.0	53.9
0.10	67.4	58.0	54.3	69.0	56.3	55.0
0.13	69.8	59.4	55.9	70.8	57.8	56.2
0.16	72.1	61.1	57.5	72.5	59.4	57.7
0.20	74.9	62.9	59.2	74.5	61.2	59.3
0.25	77.7	64.6	61.2	76.5	63.1	61.1
0.32	80.5	66.2	63.3	78.8	64.9	62.8
0.40	83.4	68.9	65.5	81.2	67.2	64.9
0.50	86.4	71.1	67.7	83.8	69.5	66.6
0.63	89.7	73.5	70.1	86.5	71.8	69.0
0.79	91.7	76.0	72.5	89.3	74.3	71.5
1.00	96.1	78.7	75.1	92.2	76.9	73.9
1.26	99.4	81.3	77.7	95.2	79.4	76.4
1.59	102.7	84.0	80.2	98.2	82.1	78.9
2.00	105.5	86.8	83.0	101.4	84.8	81.5
2.51	109.9	89.5	85.7	104.5	87.6	84.1
3.16	113.5	92.6	88.7	107.9	90.5	86.8
3.98	117.2	95.6	91.6	111.2	93.5	89.7
5.01	120.9	98.6	94.5	114.5	96.4	92.5
6.31	124.7	101.6	97.5	117.9	99.4	95.3
7.94	128.5	104.8	100.5	121.4	102.4	98.2
10.00	132.4	108.0	103.6	124.8	105.5	101.2
12.59	136.3	111.1	106.8	128.4	108.7	104.1
15.85	140.3	114.4	110.0	132.0	111.8	107.1
19.95	144.4	117.7	113.2	135.6	115.0	110.2
25.12	148.5	121.1	116.6	139.3	118.4	113.4
31.62	152.8	124.5	120.0	143.0	121.6	116.5
39.81	157.1	127.9	123.5	146.8	125.1	119.8
50.12	161.5	131.5	127.1	150.6	128.5	123.0
63.10	166.1	135.1	130.8	154.4	131.9	126.4
79.43	170.7	138.6	134.5	158.4	135.5	129.7
100.00	175.3	142.5	138.5	162.4	139.0	133.1

Table C.8. Average storage modulus $(\bar{G}')$ for 2.0% aqueous xanthan curdlan hydrogel complex (XCHC) gum solutions at pH = 6 over 5 FTCs (n=3).

Storage Modules (Pa) Mean for XCHC at pH = 6						
	Freeze Thaw Cycles					
ω (rad/s)	**0**	**1**	**2**	**3**	**4**	**5**
0.02	67.9	59.8	54.1	63.3	60.6	60.7
0.03	68.6	60.8	55.0	64.6	61.0	61.1
0.03	69.4	61.7	56.0	65.9	61.6	61.5
0.04	70.4	62.7	57.1	67.1	64.4	62.2
0.05	71.5	63.7	57.9	68.2	65.3	62.9
0.06	72.9	64.7	58.9	69.5	66.2	63.8
0.08	74.2	65.8	59.9	70.7	67.3	64.7
0.10	75.8	66.9	61.1	72.0	68.7	66.0
0.13	77.6	68.3	62.3	73.6	69.9	67.3
0.16	79.4	69.8	63.7	75.1	71.5	68.8
0.20	81.3	71.4	65.3	77.0	73.1	70.5
0.25	83.0	73.2	66.9	78.8	74.9	72.2
0.32	85.6	75.0	68.6	80.8	77.0	74.1
0.40	88.3	77.1	70.5	82.9	79.0	76.0
0.50	90.9	79.2	72.5	85.2	81.1	78.2
0.63	93.4	81.4	74.6	87.5	83.5	80.4
0.79	96.1	83.6	76.7	90.0	85.8	82.7
1.00	98.8	86.0	79.0	92.5	88.3	85.1
1.26	101.6	88.4	81.3	95.1	90.8	87.5
1.59	104.4	90.9	83.6	97.7	93.3	90.0
2.00	107.3	93.3	86.0	100.3	95.8	92.5
2.51	110.1	95.9	88.4	103.1	98.5	95.0
3.16	113.2	98.5	90.9	105.9	101.2	97.6
3.98	116.2	101.1	93.4	108.7	103.8	100.2
5.01	119.2	103.8	95.9	111.5	106.5	102.9
6.31	122.3	106.4	98.5	114.4	109.3	105.7
7.94	125.6	109.2	101.1	117.3	112.1	108.4
10.00	128.8	112.0	103.7	120.3	114.9	111.2
12.59	132.1	114.9	106.4	123.2	117.8	114.0
15.85	135.5	117.8	109.2	126.3	120.7	117.0
19.95	139.0	120.8	112.1	129.4	123.8	120.0
25.12	142.6	123.8	115.0	132.6	126.8	123.1
31.62	146.3	127.0	118.0	135.9	130.0	126.3
39.81	150.2	130.2	121.1	139.3	133.2	129.7
50.12	154.2	133.6	124.4	142.9	136.6	133.2
63.10	158.3	137.0	127.8	146.6	140.1	136.9
79.43	162.7	140.7	131.4	150.5	143.8	140.7
100.00	167.3	144.3	135.3	154.3	147.5	144.7

Table C.9. Average storage modulus $(\bar{G}')$ for 2.0% aqueous xanthan curdlan hydrogel complex (XCHC) gum solutions at pH = 7 over 5 FTCs (n=3).

Storage Modules (Pa) Mean for XCHC at pH = 7						
	Freeze Thaw Cycles					
ω (rad/s)	**0**	**1**	**2**	**3**	**4**	**5**
0.02	73.6	70.9	74.7	64.1	67.5	66.1
0.03	75.1	72.4	75.7	65.1	68.4	66.6
0.03	76.6	74.0	76.6	66.5	69.5	67.3
0.04	77.7	75.3	78.2	67.5	70.4	68.1
0.05	79.5	76.6	79.6	68.7	71.4	70.4
0.06	80.9	77.9	81.5	70.0	72.9	71.4
0.08	82.8	79.4	83.1	71.7	74.3	72.6
0.10	84.9	81.0	85.0	73.5	75.5	73.8
0.13	87.3	82.4	86.9	75.3	77.3	75.2
0.16	89.7	84.1	89.1	77.3	79.0	76.8
0.20	92.1	86.1	91.3	79.3	80.9	78.7
0.25	94.7	88.2	93.6	81.4	83.0	80.7
0.32	97.4	90.4	96.1	83.7	85.3	82.8
0.40	100.2	92.8	98.8	86.1	87.7	85.1
0.50	102.9	95.3	101.5	88.5	90.2	87.4
0.63	106.2	97.8	104.4	91.1	92.7	89.9
0.79	109.1	100.5	107.3	93.8	95.4	92.4
1.00	112.5	103.7	110.3	96.5	98.2	95.1
1.26	115.6	106.4	113.4	99.4	101.0	97.8
1.59	118.9	109.3	116.4	102.2	103.8	100.5
2.00	122.2	112.3	119.6	105.1	106.7	103.2
2.51	125.6	115.3	122.7	108.0	109.6	106.1
3.16	129.0	118.3	126.0	111.0	112.5	109.0
3.98	132.4	121.4	129.0	114.0	115.4	111.8
5.01	135.8	124.5	132.7	117.0	118.4	114.7
6.31	139.2	127.5	136.1	120.1	121.4	117.7
7.94	142.8	130.7	139.5	123.2	124.5	120.6
10.00	146.4	133.8	142.9	126.4	127.6	123.7
12.59	149.9	136.9	146.4	129.6	130.8	126.7
15.85	153.6	140.2	149.9	132.9	134.1	129.9
19.95	157.4	143.5	153.5	136.2	137.4	133.0
25.12	161.2	146.8	157.2	139.6	140.7	136.3
31.62	165.1	150.2	161.0	143.1	144.2	139.6
39.81	169.1	153.6	164.7	146.6	147.8	143.1
50.12	173.2	157.1	168.6	150.3	151.4	146.6
63.10	177.5	160.7	172.7	154.2	155.2	150.4
79.43	182.0	164.4	176.7	158.2	159.1	154.3
100.00	186.8	168.2	181.1	162.6	163.3	158.5

Table C.10. Average storage modulus $(\overline{G'})$ for 2.0% aqueous xanthan curdlan hydrogel complex (XCHC) gum solutions at pH = 8 over 5 FTCs (n=3).

Storage Modules (Pa) Mean for XCHC at pH = 8						
	Freeze Thaw Cycles					
ω (rad/s)	**0**	**1**	**2**	**3**	**4**	**5**
0.02	80.1	64.8	57.7	44.1	63.4	59.4
0.03	80.5	66.4	58.0	45.6	65.4	60.3
0.03	81.2	67.6	58.7	47.0	66.6	61.2
0.04	82.0	68.9	59.2	48.4	67.6	61.7
0.05	84.2	70.1	60.2	49.7	69.0	62.6
0.06	86.1	71.3	60.9	51.1	70.3	63.6
0.08	88.4	72.7	62.3	52.7	71.9	64.5
0.10	90.4	74.3	63.6	54.1	73.5	65.7
0.13	92.4	75.9	65.2	55.8	75.1	67.0
0.16	94.5	77.8	66.6	57.5	76.9	68.6
0.20	96.7	79.8	68.5	59.2	78.8	70.1
0.25	99.2	81.9	70.3	61.0	80.8	71.8
0.32	101.8	84.2	72.3	62.9	83.1	73.6
0.40	104.5	86.5	74.2	64.8	85.5	75.5
0.50	107.3	88.9	76.6	66.8	87.8	77.6
0.63	110.1	91.4	78.7	68.9	90.3	79.7
0.79	113.0	94.0	80.9	71.1	92.8	81.9
1.00	116.0	96.7	83.4	73.2	95.5	84.3
1.26	119.2	99.4	85.7	75.5	98.1	86.6
1.59	122.2	102.0	88.2	77.6	100.7	89.0
2.00	125.4	104.9	90.7	80.0	103.5	91.4
2.51	128.6	107.7	93.1	82.2	106.3	93.9
3.16	131.9	110.6	95.8	84.7	109.1	96.4
3.98	135.2	113.6	98.3	87.1	111.9	98.9
5.01	138.6	116.6	100.9	89.5	114.8	101.5
6.31	142.0	119.6	103.5	91.9	117.6	104.0
7.94	145.5	122.6	106.1	94.4	120.6	106.6
10.00	149.1	125.7	108.8	96.9	123.5	109.2
12.59	152.7	128.9	111.6	99.5	126.4	111.9
15.85	156.4	132.2	114.4	102.1	129.4	114.6
19.95	160.1	135.5	117.2	104.8	132.5	117.4
25.12	164.2	138.9	120.1	107.5	135.6	120.3
31.62	168.1	142.5	123.1	110.3	138.9	123.2
39.81	172.4	146.1	126.2	113.3	142.2	126.2
50.12	176.7	150.0	129.3	116.3	145.6	129.4
63.10	181.2	153.9	132.7	119.4	149.2	132.6
79.43	185.9	158.1	136.1	122.8	152.7	136.1
100.00	190.6	162.4	139.8	126.3	156.3	139.8

Table C.11. Average storage modulus $(\overline{G'})$ for 2.0% aqueous xanthan curdlan hydrogel complex (XCHC) gum solutions with 5 mM NaCl over 5 FTCs (n=3).

Storage Modules (Pa) Mean for XCHC with 5 mM NaCl						
	Freeze Thaw Cycles					
ω (rad/s)	**0**	**1**	**2**	**3**	**4**	**5**
0.02	79.0	66.5	87.6	87.3	78.9	94.1
0.03	77.3	64.4	83.9	86.6	77.4	90.8
0.03	76.9	63.4	82.0	87.4	76.0	88.4
0.04	76.4	63.2	82.5	88.4	75.6	87.3
0.05	77.1	63.7	83.5	89.8	76.3	86.5
0.06	78.1	64.8	84.9	90.9	77.1	86.4
0.08	78.9	66.1	86.8	93.7	78.6	86.9
0.10	81.0	67.6	88.9	96.9	80.4	87.5
0.13	81.5	69.3	91.1	99.5	82.0	88.5
0.16	85.2	71.3	93.8	102.4	84.1	89.7
0.20	87.6	73.2	96.3	105.3	86.2	91.2
0.25	90.0	75.5	99.2	108.3	88.5	92.8
0.32	92.7	77.7	102.0	111.4	90.9	94.8
0.40	95.4	80.2	105.1	114.6	93.3	96.8
0.50	98.2	82.5	108.2	117.8	95.9	99.1
0.63	101.0	85.0	111.3	121.0	98.7	101.7
0.79	104.0	87.5	114.6	124.4	101.5	104.1
1.00	106.9	90.1	117.9	127.9	104.4	106.8
1.26	110.0	92.8	121.2	131.3	107.4	109.5
1.59	112.9	95.4	124.5	134.8	110.3	112.3
2.00	116.0	98.2	127.9	138.4	113.3	115.0
2.51	119.1	101.0	131.3	141.9	116.4	117.8
3.16	122.3	103.8	134.8	145.6	119.5	120.7
3.98	125.4	106.6	138.2	149.2	122.6	123.5
5.01	128.6	109.4	141.7	152.9	125.8	126.4
6.31	131.8	112.3	145.2	156.6	129.0	129.3
7.94	135.2	115.2	148.7	160.4	132.3	132.2
10.00	138.5	118.1	152.3	164.2	135.6	135.2
12.59	141.9	121.1	155.8	167.9	138.9	138.1
15.85	145.2	124.2	159.4	172.2	142.3	141.1
19.95	148.7	127.2	163.0	176.4	145.7	144.1
25.12	152.1	130.3	166.7	180.5	149.1	147.0
31.62	155.6	133.4	170.3	184.6	152.6	150.1
39.81	159.2	136.6	174.0	188.8	156.2	153.2
50.12	162.8	139.9	177.6	193.0	159.8	156.3
63.10	166.6	143.2	181.3	197.4	163.4	159.4
79.43	170.3	146.5	185.0	201.7	166.9	162.5
100.00	174.0	149.8	188.6	206.4	170.2	165.6

Table C.12. Average storage modulus $(\overline{G'})$ for 2.0% aqueous xanthan curdlan hydrogel complex (XCHC) gum solutions with 15 mM NaCl over 5 FTCs (n=3).

Storage Modules (Pa) Mean for XCHC with 15 mM NaCl						
	Freeze Thaw Cycles					
ω (rad/s)	**0**	**1**	**2**	**3**	**4**	**5**
0.02	117.9	99.5	124.1	109.3	91.8	90.5
0.03	116.0	97.9	121.3	106.7	89.9	97.5
0.03	116.4	97.5	120.3	106.4	90.1	97.6
0.04	117.4	98.2	119.9	106.5	90.6	98.1
0.05	119.7	99.3	120.9	107.2	92.3	100.1
0.06	122.2	100.9	122.6	108.8	94.2	102.4
0.08	124.8	102.8	124.9	110.4	95.8	103.6
0.10	128.0	105.1	127.1	113.3	98.1	106.8
0.13	131.5	107.6	130.3	116.1	100.5	110.1
0.16	135.1	110.1	133.7	119.5	103.7	113.3
0.20	138.8	113.1	137.2	123.1	106.8	116.6
0.25	142.9	116.5	141.0	126.8	110.5	119.8
0.32	147.0	119.9	145.2	130.6	113.8	123.4
0.40	151.2	123.4	149.3	134.5	117.3	127.4
0.50	155.4	127.0	153.7	138.4	119.5	131.6
0.63	160.0	130.6	158.3	142.5	124.6	135.6
0.79	164.5	134.6	162.8	146.8	128.9	140.0
1.00	169.0	138.5	167.4	151.0	132.8	143.4
1.26	173.7	142.6	172.2	155.1	136.8	148.8
1.59	178.3	146.5	176.9	159.6	140.7	153.1
2.00	182.9	150.7	181.7	164.1	144.8	157.6
2.51	187.7	154.8	186.5	168.5	148.8	162.0
3.16	192.5	159.0	191.5	172.9	153.1	166.4
3.98	197.3	163.1	196.3	177.4	157.2	170.8
5.01	202.1	167.4	201.2	181.9	161.4	175.2
6.31	207.0	171.6	206.0	186.4	165.6	179.8
7.94	211.8	175.8	210.9	190.9	169.8	184.4
10.00	216.8	180.0	215.9	195.5	174.0	189.0
12.59	221.8	184.3	220.9	200.0	178.4	193.5
15.85	226.8	188.7	225.9	204.6	182.7	198.1
19.95	231.8	193.0	230.8	209.2	187.2	202.7
25.12	237.0	197.4	236.0	213.9	191.6	207.1
31.62	242.1	201.8	241.1	218.5	196.0	211.9
39.81	247.3	206.2	246.3	223.3	200.5	216.8
50.12	252.7	210.6	251.5	228.1	205.0	221.1
63.10	258.0	215.1	256.7	232.9	209.6	226.4
79.43	263.5	219.6	262.1	237.8	214.5	231.0
100.00	269.3	223.7	267.7	242.8	219.2	235.6

Table C.13. Average storage modulus $(\overline{G'})$ for 2.0% aqueous xanthan curdlan hydrogel complex (XCHC) gum solutions with 20 mM NaCl over 5 FTCs (n=3).

Storage Modules (Pa) Mean for XCHC with 20 mM NaCl						
	Freeze Thaw Cycles					
ω (rad/s)	**0**	**1**	**2**	**3**	**4**	**5**
0.02	89.0	122.4	102.9	83.4	95.7	98.7
0.03	99.4	120.9	101.4	82.3	94.5	94.0
0.03	100.9	121.3	101.0	84.6	94.5	96.3
0.04	102.1	122.1	101.5	87.0	96.5	96.2
0.05	103.6	123.4	102.9	88.9	99.3	97.2
0.06	105.7	125.1	104.7	91.1	102.1	98.7
0.08	108.4	127.0	106.8	93.3	105.5	100.7
0.10	111.4	129.1	109.1	95.6	108.4	103.0
0.13	114.3	131.7	111.6	98.1	111.5	105.6
0.16	117.5	134.7	114.3	100.6	114.6	108.3
0.20	120.7	137.9	117.2	103.4	117.8	111.3
0.25	124.3	141.4	120.1	106.2	121.0	114.4
0.32	128.0	144.9	123.3	109.2	124.4	117.6
0.40	131.7	148.6	126.5	112.0	127.8	120.9
0.50	135.4	152.4	129.7	115.1	131.2	124.3
0.63	139.3	156.2	133.2	118.3	134.7	127.7
0.79	143.1	160.2	136.7	121.6	138.3	131.2
1.00	147.1	164.2	140.1	124.9	142.0	134.9
1.26	151.0	168.2	143.8	128.1	145.6	138.5
1.59	155.1	172.3	147.4	131.4	149.3	141.7
2.00	159.2	176.3	151.0	134.8	153.1	145.9
2.51	163.3	180.5	154.6	138.2	156.8	149.6
3.16	167.4	184.6	158.3	141.6	160.6	153.3
3.98	171.5	188.8	161.9	145.0	164.3	157.0
5.01	175.7	192.9	165.6	148.5	168.1	161.0
6.31	179.9	197.1	169.3	151.9	171.9	164.8
7.94	184.0	201.4	173.0	155.4	175.7	168.6
10.00	188.2	205.6	176.7	158.9	179.6	172.4
12.59	192.5	209.9	180.3	162.4	183.4	176.2
15.85	196.7	214.2	184.1	165.9	187.3	180.0
19.95	201.1	218.5	187.8	169.4	191.3	183.9
25.12	205.4	222.8	191.5	173.0	195.3	187.8
31.62	209.9	227.2	195.3	176.6	199.3	191.6
39.81	214.2	231.6	199.1	180.3	203.3	195.6
50.12	218.7	236.1	202.9	184.1	207.4	199.5
63.10	223.3	240.6	206.8	188.0	211.6	203.5
79.43	227.8	245.2	210.7	237.8	215.9	207.6
100.00	232.6	250.1	215.0	242.8	220.6	211.7

Table C.14. Average storage modulus $(\overline{G'})$ for 2.0% aqueous xanthan curdlan hydrogel complex (XCHC) gum solutions with 75 mM NaCl over 5 FTCs (n=3).

Storage Modules (Pa) Mean for XCHC with 75 mM NaCl						
	Freeze Thaw Cycles					
ω (rad/s)	**0**	**1**	**2**	**3**	**4**	**5**
0.02	111.0	110.7	100.7	117.4	137.1	131.8
0.03	109.8	110.0	100.5	114.7	133.9	131.0
0.03	109.0	110.4	101.2	112.3	131.7	131.2
0.04	109.4	111.1	102.3	112.0	130.6	132.3
0.05	111.1	112.1	103.9	112.4	130.1	134.0
0.06	113.6	113.3	105.8	113.6	130.2	136.1
0.08	116.5	115.4	108.0	115.6	131.0	138.8
0.10	119.3	117.7	110.5	117.9	132.4	141.9
0.13	122.5	120.1	113.1	120.7	134.4	145.1
0.16	125.9	122.5	115.9	123.9	136.6	148.5
0.20	129.3	125.1	118.7	127.0	139.4	152.2
0.25	132.8	128.0	121.8	130.6	142.5	155.9
0.32	136.5	130.9	124.9	134.2	146.0	159.9
0.40	139.9	134.0	128.1	137.8	149.5	163.9
0.50	143.6	137.5	131.5	141.3	153.1	168.0
0.63	147.3	141.1	134.8	144.9	157.0	172.2
0.79	151.0	144.6	138.3	148.6	160.9	176.4
1.00	154.8	148.2	141.9	152.3	164.7	180.8
1.26	158.7	152.0	145.4	156.3	168.8	185.0
1.59	162.5	155.7	148.9	160.1	172.8	189.4
2.00	166.2	159.4	152.5	163.9	176.7	193.8
2.51	170.1	163.1	156.0	167.8	180.8	198.2
3.16	173.9	166.9	159.6	171.6	184.9	202.5
3.98	177.7	170.7	163.3	175.4	188.9	207.0
5.01	181.6	174.6	166.9	179.4	193.0	211.3
6.31	185.5	178.3	170.5	183.3	197.0	215.7
7.94	189.4	182.1	174.1	187.2	201.0	220.2
10.00	193.3	186.0	177.8	191.0	205.0	224.6
12.59	197.2	189.8	181.4	194.9	209.1	229.1
15.85	201.1	193.6	185.0	198.9	213.2	233.6
19.95	205.2	197.4	188.7	202.9	217.3	238.1
25.12	209.1	201.3	192.4	206.9	221.5	242.6
31.62	213.2	205.3	196.1	211.0	225.5	247.2
39.81	217.2	209.2	200.0	215.1	229.7	251.7
50.12	221.4	213.1	203.7	219.4	233.8	256.4
63.10	225.7	217.3	207.6	223.8	238.0	261.2
79.43	229.9	221.4	211.6	228.3	242.2	265.9
100.00	234.6	225.9	215.9	233.0	246.8	270.8

Table C.15. Average storage modulus $(\overline{G'})$ for 2.0% aqueous xanthan curdlan hydrogel complex (XCHC) gum solutions with 100 mM NaCl over 5 FTCs (n=3).

Storage Modules (Pa) Mean for XCHC with 100 mM NaCl						
	Freeze Thaw Cycles					
ω (rad/s)	**0**	**1**	**2**	**3**	**4**	**5**
0.02	117.7	120.5	111.7	137.8	143.3	137.4
0.03	116.5	121.1	113.1	134.7	140.9	135.5
0.03	116.4	122.3	114.8	132.4	139.8	135.3
0.04	117.0	124.0	116.9	132.9	139.9	135.5
0.05	118.2	125.7	119.6	134.4	140.7	136.0
0.06	119.9	127.8	122.4	137.1	141.9	136.8
0.08	121.9	130.3	125.4	140.0	143.6	138.2
0.10	124.5	133.1	128.7	143.2	145.8	139.6
0.13	127.2	136.2	131.9	146.7	148.4	141.3
0.16	130.1	139.8	135.5	150.5	151.2	143.1
0.20	133.4	143.6	138.9	154.6	154.5	144.9
0.25	136.8	147.5	142.6	158.7	158.2	148.5
0.32	140.3	151.6	146.3	162.9	162.4	152.3
0.40	144.0	155.7	150.1	167.1	166.5	156.2
0.50	147.7	159.9	154.2	171.3	170.5	160.2
0.63	151.5	164.3	158.4	175.7	174.9	164.5
0.79	155.4	168.7	162.5	180.1	179.2	168.6
1.00	159.4	173.1	166.7	184.3	183.6	173.0
1.26	163.5	177.6	171.1	174.3	188.0	177.3
1.59	167.5	182.2	175.4	178.5	192.4	181.7
2.00	171.6	186.7	179.6	182.8	196.8	186.1
2.51	175.7	191.3	184.0	187.1	201.3	190.5
3.16	179.8	195.9	188.3	191.5	205.7	194.9
3.98	183.9	200.4	192.6	195.8	210.1	199.3
5.01	188.0	205.1	197.0	200.2	214.7	203.7
6.31	192.2	209.7	201.4	204.6	219.1	208.1
7.94	196.3	214.3	205.8	208.9	223.6	212.6
10.00	200.5	218.9	210.2	213.4	228.0	217.0
12.59	204.8	223.6	214.6	217.8	232.6	221.4
15.85	209.0	228.3	219.1	222.3	237.1	225.7
19.95	213.4	233.1	223.5	226.7	241.7	230.3
25.12	217.8	237.9	228.0	231.2	246.3	235.6
31.62	222.3	242.7	232.6	235.7	251.0	240.2
39.81	226.7	247.7	237.1	240.3	255.7	244.8
50.12	231.2	252.8	241.7	244.9	260.4	249.5
63.10	236.0	257.9	246.4	249.6	265.3	254.3
79.43	240.8	263.2	251.2	254.2	270.3	259.1
100.00	246.0	268.9	215.9	258.9	275.8	264.2

Table C.16. Average storage modulus $(\overline{G'})$ for 2.0% aqueous xanthan curdlan hydrogel complex (XCHC) gum solutions with 200 mM NaCl over 5 FTCs (n=3).

Storage Modules (Pa) Mean for XCHC with 200 mM NaCl						
	Freeze Thaw Cycles					
ω (rad/s)	**0**	**1**	**2**	**3**	**4**	**5**
0.02	97.7	93.8	97.4	104.1	101.9	121.9
0.03	97.2	92.8	96.1	102.6	101.5	122.5
0.03	96.5	93.3	95.5	103.3	102.4	124.0
0.04	95.7	94.1	95.3	105.1	103.8	125.1
0.05	97.4	95.0	95.9	107.4	106.0	127.1
0.06	100.6	96.3	96.7	110.1	108.9	129.4
0.08	104.5	98.6	98.1	112.7	111.6	132.6
0.10	108.1	101.7	100.1	115.6	115.1	135.9
0.13	111.9	105.0	102.3	118.5	117.1	139.6
0.16	115.8	108.4	104.8	121.8	121.6	143.6
0.20	119.7	111.8	107.5	125.2	124.9	147.8
0.25	123.7	115.4	110.3	128.8	128.2	152.3
0.32	127.4	118.9	113.3	132.6	131.9	156.7
0.40	132.0	122.6	116.6	136.4	135.6	161.3
0.50	136.1	126.3	119.9	140.4	139.5	166.0
0.63	140.4	130.1	123.3	144.5	143.4	170.7
0.79	144.5	133.9	126.8	148.6	147.3	175.6
1.00	148.9	137.8	130.4	152.7	151.2	180.5
1.26	153.2	141.6	134.0	157.0	155.7	185.4
1.59	157.4	145.6	137.7	161.4	159.8	190.2
2.00	161.8	149.5	141.4	165.3	163.9	195.1
2.51	166.2	153.5	145.0	169.9	168.0	199.9
3.16	170.5	157.4	148.7	174.1	172.1	204.7
3.98	174.8	161.4	152.4	178.2	176.2	209.5
5.01	179.2	165.4	156.1	182.4	180.4	214.3
6.31	183.5	169.3	159.8	186.9	184.5	219.7
7.94	187.9	173.4	163.6	191.2	188.5	224.7
10.00	192.3	177.3	167.4	195.4	192.4	229.5
12.59	196.8	181.4	171.1	199.7	196.8	234.5
15.85	201.2	185.5	174.9	204.0	201.2	239.4
19.95	205.7	189.6	178.9	208.4	205.4	244.4
25.12	210.2	193.8	182.8	212.7	209.8	249.5
31.62	214.8	198.2	186.7	217.1	214.1	254.6
39.81	219.5	202.5	191.0	221.5	218.5	259.8
50.12	224.2	206.9	195.2	226.0	222.9	265.0
63.10	229.1	211.6	199.4	230.6	227.5	270.5
79.43	234.1	216.4	203.9	235.5	232.2	275.9
100.00	239.8	221.8	208.8	240.8	237.3	282.0

References

Adhikari B, Howes T, Bhandari BR, Truong V. 2001. Stickiness in foods: a review of mechanisms and tests methods. Int J Food Prop 4(1): p 1-33.

Annable P, Williams PA, Nishinari K. 1994. Interaction in xanthan-glucomannan mixtures and the influence of electrolyte. Macromolecules 27, 4204-4211.

Arbuckle WS. 1986. Effects of emulsifiers on protein-fat interactions in ice-cream mix during ageing. I. Quantitative analyses. In: Ice Cream, Avi Publishing, pp. 84-94.

Beranbaum RL. 1998. “The Pie and Pastry Bible.” New York: Simon & Schuster.

Bernstein MA, King KF, Zhou XJ. 2004. Handbook of MRI Pulse Sequences. Burlington, MA USA: Elsevier Academic Press.

Chaisawang M and Suphantharika M. 2006. Pasting and rheological properties of native and anionic tapioca starches as modified by guar gum and xanthan gum. Food Hydrocolloid 20: 641-649.

Champion S. "The effect of microcrystalline cellulose on the organoleptic properties of ice cream," Gums and Stabilisers for the Food Industry 8. Eds. G.O. Phillips, P.A. Williams, and

Chen C, Wang R, Sun G, Fang H, Ma D, Yi S. 2010. Effects of high pressure level and holding time on properties of duck muscle gels containing 1% curdlan. InnovFood Sci Emerg 11:538-542.

Choi H and Yoo B. 2008. Rheology of mixed systems of sweet potato starch and galactomannans. Starch 60:263-269.

Coviello T and Burchard W. 1992. Criteria for the point of gelation in reversibly gelling systems according to dynamic light scattering and oscillatory rheology. Macromolecules 25, 1011-1012.

Dea ICM, Morris ER, Rees DA, Welsh EJ, Barnes HA, Price J. 1977. Associations of like and unlike polysaccharides: Mechanism and specificity in galactomannans, interacting bacterial polysaccharides, and related systems. Carbohyd Res 57 249-272.

Dickenson E. 2008. Hydrocolloids as emulsifiers and emulsion stabilizers. Food Hydrocolloid 23 1473-1482.

Dolz M, Hernandez MJ, Delegido J. 2002. Kinetic interpretation of influence of sodium chloride concentration and temperature on xanthan gum dispersion flow model. J Appl Polym Sci 83: 332-339.

FDA. 1996. 21 CFR 172: Food additives permitted for direct addition to food for human consumption: Curdlan. Federal Regulations 61: 65941–65942.

Fernández PP, Martino MN, Zaritzky NE, Guignon B, Sanz PD. 2007. Effects of locust bean, xanthan and guar gums on the ice crystals of sucrose solution frozen at high pressure. Food Hydrocolloid 21: 507-515.

Freeland M. 2002. Formulation tips on Hydrocolloids. Prepared Foods, 171 (6) 69.

French and KH. Gardner pp. 385-410. American Chemical Society, Washington, DC. 53

Fulton WS and Atkins EDT. 1980. The gelling mechanism and relationship to molecular structure of microbial polysaccharide curdlan. Fiber Diffraction Methods. Eds. A.D.

Funami T, Funami M, Yada H, Nakao Y. (1999a). Rheological and thermal studies on gelling characteristics of curdlan. Food Hydrocolloid 13: 317–324.

Funami T, Funami M, Yada H, Nakao Y. (1999b). Gelation mechanism of curdlan by dynamic viscoelasticity measurements. J Food Sci 64: 129–132.

Gagnon MA, Lafleur M. 2007. From curdlan powder to the triple helix gel structure: an attenuated total reflection-infrared study of the gelation process. Appl Spectrosc 61:374–378.

Giannouli P and Morris ER. 2003. Cryogelation of xanthan. Food Hydrocolloid 17:495–501.

Gil AM, Belton PS, Hills BP. 1996. Applications of NMR to Food Science. In: Webb GA, editor. Annual reports on NMR spectroscopy. Vol 32. San Diego: Academic Press Inc. p 1-43.

Glicksman M. Food Hydrocolloids. Vol. 3. Boca Raton: CRC Press, Inc. 1986

Goff HD, Caldwell KB, Stanley DW. 1993. The influence of polysaccharides on the glass transition in frozen sucrose solutions and ice cream. J Dairy Sci 76:1268-1277.

Goff HD. "Hydrocolloid applications in frozen foods: An end-user's view point." Gums and Stabilisers for the Food Industry 13. Eds. G.O. Phillips and P.A. Williams. Cambridge: Royal Society of Chemistry. 2006 pp. 403-412.

Goycoola FM, Morris ER, Gidley M. 1995. Viscosity of galactomannans at alkaline and neutral pH: Evidence of 'hyperentanglement" in solution. Carbohyd Polym 27: 69-71.

Graham H. Food Colloids. Westport: The AVI Publishing Company, Inc. 1977.

Granz AJ. 1977. Cellulose Hydrocolloids. Food Colloids. Ed. H. Graham. Westport: The AVI Publishing Company, Inc. pp 382-417.

Harada T and Harada A. 1996. Curdlan and succinoglycan. Polysaccharides in Medical Applications. Ed. S. Dumitriu pp. 21-58, CRC Press, Boca Raton, FL.

Harada T, Masada M, Fujimari K. And Maeda, I. 1966. Production of a firm, resilient gel-forming polysaccharide by a mutant of Alcaligenes faecalis var. myxogenes 10C3. Agric Biol Chem 30: 196–198.

Harada T, Okuyama K, Konno A, Koreeda A, Harada A. 1994. Effect of heating on formation of curdlan gels. Carbohyd Polym 24, 101–106.

Hatakeyama T, Ueda C, Hatakeyama H. 2006. Structural change of water by gelation of curdlan suspension. J ThermAnal Calorim 85(3): 661-668.

Higiro J, Herald TJ, Alavi S. 2006. Rheological study of xanthan and locust bean gum interaction in dilute solution. Food Res Int 39: 165-175.

Hirashima M, Takaya T, Nishinari K. 1997. DSC and rheological studies on aqueous dispersions of curdlan. Thermochimica Acta 306: 109-114.

Hoefler AC. Hydrocolloids. St. Paul: Eagan Press, 2004

Hosseinzadeh H. 2009. A new salt-resistant superabsorbent hydrogel based on kappa-carrageenan. e-Polymers 128: 1-13.

Hsu SY and Chung HY. 2000. Interactions of konjac, agar, curdlan gum, κ-carrageenan and reheating treatment in emulsified meatballs. J Food Eng 44: 199-204.

IBISWorld Inc. 2011. Frozen Food Production in the U.S.: 31141.

Iijima H and Takeo K. 2000. Microcrystalline cellulose: an overview In: Handbook of Hydrocolloids. Eds. G.O. Phillips and P.A. Williams. Boca Raton: CRC Press LLC.

Ikeda S, Nitta Y, Kim BS, Temsiripong T, Pongsawatmanit R, Nishinari K. 2004. Single-phase mixed gels of xyloglucan and gellan. Food Hydrocolloid 18: 669-675.

Imeson AP. "Carrageenan." Handbook of Hydrocolloids. Handbook of Hydrocolloids. Eds. G.O. Phillips and P.A. Williams. Boca Raton: CRC Press LLC. 2000, pp. 87-102.

Imeson AP and Humphreys W. 1997. "Microcrystalline cellulose," Thickening and gelling agents for food. Ed. A.P. Imeson. Suffolk: St Edmunsbury Press pp. 180-197.

Jezequal V. 1998. Curdlan: A new functional beta-glucan. Cereal Food World 43(5): 361-364.

Kanzawa Y, Koreeda A, Harada A, Harada T. 1989. Electron Microscopy of the gel-forming ability of polysaccharide food additives. Agr Biol Chem Tokyo 53(4): 979-986.

Kerr WL and Wicker L. 2000. NMR proton relaxation measurements of water associated with high methoxy and low methoxy pectins. Carbohyd Polym 42: 133-141.

Khouryieh HA, Herald TJ, Aramouni F, Alavi S. 2006. Influence of mixing temperature on xanthan conformation and interaction of xanthan-guar gum in dilute aqueous solutions. Food Res Int 39: 964-973.

Kim B-S, Takemasa M, Nishinari K. 2006. Synergistic interaction of xyloglucan and xanthan investigated by rheology, Differential Scanning Calorimetry, and NMR. Biomacromolecules 7: 1223-1230.

Konno A. and Harada T. 1991. Thermal properties of curdlan in aqueous suspension and curdlan gel. Food Hydrocolloid 5: 427–434.

Lazaridou A, Biliaderis CG, Izydorczyk MS. 2000. Structural characteristics and rheological properties of locust bean galactomannans: a comparison of samples from different carob tree populations. J Sci Food Agr 81: 68-75.

Lee MH, Baek MH, Cha DS, Park HJ, Lim ST. 2002. Freeze-thaw stabilization of sweet potato starch gel by polysaccharide gums. Food Hydrocolloid 16: 345-352.

Lin H-Y, Tsai J-C, Lai L-S. 2009. Effect of salts on the rheology of hydrocolloids from mulberry (*Morus alba* L.) leaves in concentrated domain. Food Hydrocolloid 23: 2331-2338.

Lo CT, Ramsden L. 2000. Effects of xanthan and galactomannan on the freeze/thaw properties of starch gels. Nahrung 44: 211–214.

Lo YM, Robbins KL, Argin-Soysal S, Sadar LN. 2003. Viscoelastic effects on the diffusion properties of curdlan gels. J Food Sci 68: 2057-2063.

Lopes Da Silva JA, Rao MA, Fu JT. 1998. Rheology of structure development and loss during gelation and melting. Phase/State Transitions in Foods. Eds. M.A. Rao and R.W. Hartel pp. 111-157. Marcel Dekker, New York.

Lozinsky V, Damshkaln LG, Brown R, Norton IT. 2002. Study of cryostructuation of polymer systems. XXI. Cryotropic gel formation of the water-maltodextrin systems. J Appl Polym Sci 83: 1658-1667.

Lund BM. 2000. Freezing. In: Lund BM, Baird-Parker TC, Gould GW, editors. The microbiological safety and quality of food. Vol. 1. Gaithersburg: Aspen Publishers. p 122-145.

Lüsse S, and Arnold K. 1998. Water binding polysaccharides—NMR and ESR Studies. Macromolecules 31: 6891-6897.

Maeda HS, Masada M, Harada T. 1967. Properties of gels formed by heat treatment of curdlan, a bacterial beta-1,3 glucan. Agric Biol Chem 31: 1184-1188.

Makri EA Doxastakis GI. 2006. Study of emulsions stabilized with Phaseolus vulgaris or Phaseolus coocineus with the addition of Arabic gum, locust bean gum and xanthan gum. Food Hydrocolloid 20: 1141-1152.

Mandala IG, Sawas TP, Kostaropoulos AE. 2004. Xanthan and locust bean gum influence on the rheology and structure of a white model-sauce. J Food Eng 64: 335-342.

Marchessault RH Deslandes Y. 1978. Fine structure of (1→3)-β-D-glucans: Curdlan and paramylon. Carbohyd Res 75: 231–242.

Marshall RT, Goff HD, Hartel RW. Ice Cream. 6th ed. New York: Kluwer Academic/Plenum Publishers, 2003.

Martin DR, Ablett S, Darke A, Sutton RL, Sahagian M. 1999. Diffusion of aqueous sugar solutions as affected by locust bean gum studied by NMR. J Food Sci 64(1): 46-49.

McCleary B. 1979. Enzymic hydrolysis, fine structure, and gelling interaction properties of galactomannans. Carbohyd Res 71: 205-230.

Mcintosh M, Stone BA, Stanisich VA. 2005. Curdlan and other bacterial (1→3)-β-D-glucans. Appl Microbiol Biot 68: 163-173.

Medina-Torres L, Brito-De La Fuente E, Gómez-Aldapa CA, Aragonpiña A, Toro-Vazquez JF. 2006. Structural characteristics of gels formed by mixtures of

carrageenan and mucilage gum from Opuntia ficus indica. Carbohyd Polym 63: 299-309.

Mikkonen KS, Tenkanen M, Cooke P, Xu C, Rita H, Willfo S, Holmbom B, Hicks KB, Yadav MP. 2009.Mannans as stabilizers of oil-in-water beverage emulsions. LWT-Food Sci Technol 42: 849-855.

Mintel International Group Ltd. 2009. Ice cream and frozen novelties.

Morris ER, Cutler AN, Ross-Murphy SB, Rees DA, Price J. 1981. Concentration and shear rate dependence of viscosity in random coil polysaccharide solutions. Carbohyd Polymer, 1: 5-21.

Na K, Park KH, Kim SW, Bae YH. 2000. Self-assembled hydrogel nanoparticles from curdlan derivatives: characterization, anti-cancer drug release and interaction with a hepatoma cell line (HepG2). J Control Release 69: 225-236.

Nakao Y. 1997. Properties and food applications of curdlan. Agro Food Ind Hi Tec January/February 12–15.

Nakao Y, Konno A, Taguchi T, Tawada T, Kasai H, Toda J, Terasaki M. 1991. Curdlan: Properties and application to foods. J Food Sci 56: 769-772.

Newman RH and Hemmingson JA. 1998. Interactions between locust bean gum and cellulose characterized by ^{13}C N.M.R. spectroscopy. Carbohyd Polym 36: 167-172.

Nishinari K. 2007. Rheological and related studies on industrially important polysaccharides and proteins. J Cent South Univ T 14: 498-504.

Okobira T, Miyoshi K, Uezu K, Sakurai K, Shinkai S. 2008. Molecular Dynamics Studies of Side Chain Effect on the β-1,3-D-Glucan Triple Helix in Aqueous Solution. Biomacromolecules 9: 783-788.

Oztop MH, Rosenberg M, Rosenberg Y, McCarthy KL, McCarthy MJ. 2010. Magnetic resonance imaging (MRI) and relaxation spectrum analysis as methods to investigate swelling in whey protein gels. J Food Sci 75(8): E508-E515.

Pai V, Srinivasarao M, Khan SA. 2002. Evolution of microstructure and rheology in mixed polysaccharide systems. Macromolecules 35: 1699-1707.

Paradossi G, Chiessi E, Barbiroli A, Fessas D. 2002. Xanthan and glucomannan mixtures: Synergistic interactions and gelation. Biomacromolecules 3: 498-504.

Parker SP. 1984. McGraw-Hill Dictionary of Science and Engineering.

Pederson J. 1979. The selection of hydrocolloids to meet functional requirements. In: Blanshard JMV, Mitchell JR, editors. Polysaccharides in Food. London: Butterworths. p 219–227.

Pinotti A, Garcia MA, Martino MN, Zaritzky NE. 2007. Study on microstructure and physical properties of composite films based on chitosan and methylcellulose. Food Hydrocolloid 21: 66-72.

Pongsawatmanit R, Temsiripong T, Suwonsichon T. 2007. Thermal and rheological properties of tapioca starch and xyloglucan mixtures in the presence of sucrose. Food Res Int 40: 239-248.

Puliga SL, Handa S, Gumadi SN, Doble M. 2010. Enhancement and scale-up of beta-(1,3) glucan production by *Agrobacterium* sp. Int J Food Eng 6: Art 6.

Rao SJ, Prasad MS, Rao GV. 1993. Effect of xanthan gum on the quality of bread. J Food Sci Technol 4(30): 265-268.

Rao VSR, Qasba PK, Balaji PV, Chandrasekaran R. Conformation of carbohydrates. Amsterdam: Overseas Publishers Association, 1998.

Richter S, Boyko V, Matzker R, Schröter K. 2004. A thermoreversible gelling system: Mixtures of xanthan gum and locust-bean gum. Macromol Rapid Comm 25: 1504-1509.

Richter S, Brand T, Berger S. Comparative monitoring of the gelation process of a thermoreversible gelling system made of xanthan gum and locust bean gum by dynamic light scattering and 1H NMR Spectroscopy. MacromolRapid Comm 26: 548-553.

Rocks JK. 1971. Xanthan gum. Food Technol 25(5): 476-483.

Rochefort WE and Middleman S. 1987. Rheology of xanthan gum: salt, temperature, and strain effects in oscillatory and steady shear experiments. J Rheol 319(4): 337-369.

Rodd AB, Dunstan DE, Boger DV, Schmidt J, Burchard W. 2001 Heterodyne and nonergodic approach to dynamic light scattering of polymer gels: Aqueous xanthan in the presence of metal ions (aluminum(III)). Macromolecules 34(10): 3339-3352.

Ross-Murphy SB. 1988. Small deformation measurements. In: Blanshard JMB, Mitchel JR, editors. Food Structure – Its Creation and Evaluation. Butterworths, London. p 387-400.

Sadar LN. 2004. Rheological and textural characteristics of copolymerized hydrocolloidal solutions containing curdlan gum. M.S. thesis. University of Maryland, College Park, MD.

Saito H, Miyata E, Sasaki Y. 1978. A 13C nuclear magnetic resonance study of gel-forming (1→3)-β-Dglucans: Molecular-weight dependence of helical conformation and of the presence of junction zones for association of primary molecules. Macromolecules 11: 1244–1251.

Sanchez C, Zuniga-Lopez R, Schmitt C, Despond S. Hardy J. 2000. Microstructure of acid-induced skim milk-locust bean gum-xanthan gels. Int Dairy J 10: 199-212.

Sanderson GR. 1996. Gums and their use in food systems. Food Technol-Chicago 50: 81-84.

Sandolo C, Matricardi P, Alhaique F, Coviello T. 2008. Effect of temperature and cross-linking density on rheology of chemical cross-linked guar gum at the gel point. Food Hydrocolloid 23: 210-220.

Selomulyo VO and Zhou W. 2007. Frozen bread dough: Effects of freezing storage and dough improvers. J Cereal Sci 45: 1-17.

Seviour RJ, McNeil B, Fazenda ML, Harvey LM. 2011. Operating bioreactors for microbial exopolysaccharide production. Crit Rev Biotechnol 32: 170-185.

Sikor M, Badrie N, Deisingh AK, Kowalski S. 2008. Sauces and dressings: A review of properties and applications. Crit Rev Food Sci 48: 50-77.

Steffe JF. 1996. Rheological Methods in Food Process Engineering. 2nd ed. East Lansing: Freeman Press. p 294-349.

Sun Y, Liu Y, Li Y, Lv M, Li P, Xu H, Wang L. 2011. Preparation and characterization of novel curdlan/chitosan blending membranes for antibacterial applications. Carbohyd Polym 84: 952-959.

Sworn G. 2000. Xanthan Gum. In: Phillips GO, Williams PA, editors. Handbook of Hydrocolloids. Boca Raton: CRC Press LLC. p 103–115.

Tada T, Matsumoto T, Masuda T. 1999. Dynamic viscoelasticity and small-angle X-ray scattering studies on the gelation mechanism and network structure of curdlan gels. Carbohyd Polym 39: 53–59.

Takigami S, Shimada M, Williams PA, Phillips GO. 1993. E.S.R. study of the conformation transition of spin-labeled xanthan gum in aqueous solution. Int J Biol Macromol15: 367-371.

Taylor Nelson Sofres (TNS), A Kantor Group Company. 2008. December 2008 UK Market Report.

Tojo E and Prado J. 2003. A simple ^{1}H NMR method for the quantification of carrageenans in blends. Carbohyd Polym 53: 325-329.

Towle GA. "Stabilisation of chilled and frozen foods," Gums and Stabilisers for the Food Industry 8. Eds. G.O. Phillips, P.A. Williams, and D.J. Wedlock. New York: Oxford University Press, Inc. 1996.

Vittadini E, Dickinson LC, Chinachoti P. 2002. NMR water mobility in xanthan and locust bean gum mixtures: possible explanation of microbial response. Carbohyd Polym 49: 261-269.

Wang F, Wang Y-J, Sun Z. 2002a. Conformational role of xanthan in its interaction with guar gum. J Food Sci 67(9): 3289-3294.

Wang F, Wang Y-J, Sun Z. 2002b. Conformational role of xanthan in its interaction with locust bean gum. J Food Sci 67(7): 2609-2614.

Wang MJ, Chen CG, Sun GJ, Wang W, Fang HM. 2010. Effects of curdlan on the color, syneresis, cooking qualities, and textural properties of potato starch noodles. Starch 62: 429-434.

Wedlock DJ. New York: Oxford University Press, Inc. 1982 pp. 361-366.

Weil JA, Bolton JR, Wertz JE. Electron paramagnetic resonance: elementary and practical applications. New Jersey: John Wiley & Sons, Inc. 2007.

West TP. 2009. Elevated curdlan production by a mutant of *Agrobacterium* sp. ATCC 31749. J Basic Microb 49: 589-592.

Westra JG. 1989. Rheology of carboxymethyl cellulose with xanthan gum properties. Macromolecules 22(1): 367-370.

Whitcomb PJ and Macosko CW. 1978. Rheology of Xanthan Gum. J Rheol 22(5): 493-505.

Whitney SEC, Brigham JE, Darke AH, Reid JSG, Gidley MJ. 1998. Structural aspects of the interaction of mannan-based polysaccharides with bacterial cellulose. Carbohyd Res 307: 299-309.

Wielinga WC and Maehall AG. "Galactomannans." Handbook of Hydrocolloids. Eds. G.O. Phillips and P.A. Williams. Boca Raton: CRC Press LLC. 2000, pp. 137-154.

Williams PD, Sadar LN, Lo YM. 2009. Texture stability of hydrogel complex containing curdlan gum over multiple freeze-thaw cycles. J Food Process Pres 33: 126–139.

Yaşar F, Toğrul H, Arslan N. 2007. Flow properties of cellulose and carboxymethyl cellulose from orange peel. J Food Eng 81: 187-199.

Yu LJ, Wu JR, Liu J, Zhan XB, Zheng ZY, Lin CC. 2011. Enhanced curdlan production *Agrobacterium* sp ATCC 31749 by addition of low-polyphosphates. Biotechnol Bioproc E 16: 34-41.

Zeira A and Nussinovitch A. 2004. Mechanical Properties of weak locust bean gum (LBG) Gels under controlled rapid freeze-thawing. J Texture Stud 34: 561-573.